

2008

Utilization of Aptamers as Affinity Probes in Polymeric Microdevices for Disease Management and the Production of a Recombinant Membrane Protein

Anne Obubuafo

Louisiana State University and Agricultural and Mechanical College, ankwor@yahoo.com

Follow this and additional works at: https://digitalcommons.lsu.edu/gradschool_dissertations

 Part of the [Chemistry Commons](#)

Recommended Citation

Obubuafo, Anne, "Utilization of Aptamers as Affinity Probes in Polymeric Microdevices for Disease Management and the Production of a Recombinant Membrane Protein" (2008). *LSU Doctoral Dissertations*. 3805.
https://digitalcommons.lsu.edu/gradschool_dissertations/3805

This Dissertation is brought to you for free and open access by the Graduate School at LSU Digital Commons. It has been accepted for inclusion in LSU Doctoral Dissertations by an authorized graduate school editor of LSU Digital Commons. For more information, please contact gradetd@lsu.edu.

**UTILIZATION OF APTAMERS AS AFFINITY PROBES IN
POLYMERIC MICRODEVICES FOR DISEASE
MANAGEMENT AND THE PRODUCTION OF A
RECOMBINANT MEMBRANE PROTEIN**

A Dissertation
Submitted to the Graduate Faculty of the
Louisiana State University and
Agricultural and Mechanical College
In partial fulfillment of the
requirements for the degree of
Doctor of Philosophy
in
The Department of Chemistry

by
Anne Obubuafo
B.Sc., Kwame Nkrumah University of Science and Technology, 1995
M.S., Wright State University, 2001
August 2008

Dedication

This work is dedicated to all my loved ones, especially to my son Francis Kofi Asseye Adom who is my source of inspiration and motivation. To Mom and Dad for your undying love, guidance and toils and to you, Joyce, the most loving and self-less sister one could ever have.

Acknowledgements

My sincerest thanks go to my advisor, Dr. Steven A. Soper for his guidance throughout my studies and efforts in getting me this far. Thanks also to Dr. David Spivak for his guidance, support and help with research. To the rest of my graduate committee, Dr. Jayne Garno, Dr. Steven Watkins and Dr. Robb Brumfield I would like to express my sincerest gratitude for the time taken by each one of you in reading through my dissertation and your help despite the busy schedules you all have.

My thanks to the Department of Chemistry for the opportunity granted me to undertake graduate studies in Chemistry at LSU; especially to Ms. Sherri Wilkes for all your help and patience in handling my paperwork and lending an ear when I needed to talk. I'll never forget the pleasantness and warmth you greeted me with when I first came to the department. Thanks to all my colleagues and Post Docs in the Soper research group for the interesting experience of working with them. Thanks to Dr. Subramanian Balamurugan and Timothy Jensen for all the help with research. It was a pleasure working with both of you.

To my family and friends I would like to express my thanks for all the support during my studies. Thanks to Joyce for sacrificing your time and always being there for Francis and I, especially at those very critical times. I'll never be able to thank you enough and I know the Lord will richly bless you. Thanks to my parents, Mr. and Mrs. Obubuafo for your belief in me and encouragement. To my sister, Elizabeth, brothers David and Jonathan, husband Kafui, Dr. and Mrs. Asigbe, Tanti Maggie and my cousins Dzifa and Kafui, and the Ongors thanks for your support and encouragement. Thanks also to my friends Catherine Situma, Ligia da Silva, Paul Okagbare, Janet Manono, Ms.

Terri Johnson and all whose names I haven't mentioned for all your support. To you, Francis, I couldn't have asked for a more understanding child. Thanks for giving me a new purpose in life and for the late nights spent waiting for mommy to finish studying.

My utmost gratitude goes to the Almighty God, my ultimate source of strength and inspiration, who made all this possible and is constantly watching over me and guiding me unscathed through trying times. *But they that wait upon the Lord shall renew their strength; they shall mount up with wings as eagles; they shall run, and not be weary; and they shall walk and not faint (Isaiah 40:31).* God bless you all!!

Table of Contents

Dedication	ii
Acknowledgements	iii
List of Tables	viii
List of Figures	ix
Abstract	xiv
Chapter 1 Aptamers: A Class of Affinity Compounds with Potential Applications in Therapeutics and Disease Diagnosis	1
1.1 Introduction	1
1.2 The Aptamer Generation Process	3
1.2.1 The SELEX Library	3
1.2.2 Aptamer Selection Targets.....	7
1.2.3 Selection Process	10
1.2.4 Amplification, Elution and Characterization of Aptamers	13
1.3 Challenges Associated with Aptamers	14
1.4 Applications of Aptamers	15
1.4.1 Therapeutic and <i>In Vivo</i> Diagnostic Applications	15
1.4.2 <i>In vitro</i> Diagnostic Applications.....	15
1.5 References	20
Chapter 2 Poly(Methyl Methacrylate) Microchip Affinity Capillary Gel Electrophoresis of Aptamer-Protein Complexes for the Analysis of Thrombin in Plasma*	24
2.1 Introduction	24
2.2 Experimental	28
2.2.1 Reagents and Materials	28
2.2.2 Thrombin Labeling Procedure	29
2.2.3 Optimization of Aptamer Assay Conditions.....	30
2.2.4 Microchip CE.....	30
2.2.5 Standard Curve Generation.....	32
2.2.6 Analysis of Plasma Samples	32
2.3 Results and Discussion	33
2.3.1 Optimization of Aptamer Assay Conditions.....	33
2.3.2 Microchip CZE	33
2.3.4 Standard Curve Generation.....	39
2.3.5 Analysis of Plasma Samples	40
2.4 Conclusion	43
2.5 References	43

Chapter 3. Investigating the Expression of Recombinant EpCAM in Bacteria and Mammalian Cells and the Development of a Selective Tandem IMAC/ Electro Elution Purification Protocol for Histidine-Tagged Recombinant Proteins in Mammalian Cells	48
3.1 Introduction	48
3.2 Experimental	52
3.2.1 Cell Lines	52
3.2.2 Reagents and Materials	52
3.2.3 Production of EpCAM cDNA from Total RNA of Breast Cancer Cells and Generation of EpCAM/Vector Constructs	54
3.2.4 Bacteria Expression of rEpCAM	56
3.2.5 Expression of C-Terminus Histidine-Tagged Recombinant EpCAM in Mammalian Cells	56
3.2.6 Purification of Recombinant EpCAM	56
3.2.7 Optimization of mMetal Affinity Purification Protocol for Recombinant EpCAM	57
3.2.8 Gel Electrophoresis and Western Blot Analysis	58
3.2.9 Electro Elution of rEpCAM from SDS-PAGE Gels	58
3.3 Results and Discussion	59
3.3.1 Insertion of RT-PCR Amplified EpCAM cDNA into the Vectors	59
3.3.2 Bacterial Expression Studies	62
3.3.3 Mammalian Expression of rEpCAM	66
3.3.4 Extraction and Affinity Purification of rEpCAM from Mammalian Cells	69
3.4 Conclusion	75
3.5 References	76
Chapter 4 Immobilization of Aptamers onto Poly(Methyl Methacrylate) Polymer, PMMA, Substrates for Aptamer Sandwich Assay Development and Screening Low Levels of Protein Biomarkers	79
4.1 Introduction	79
4.2.1 Reagents and Materials	84
4.2.2 Methylmesoporphyrin IX (NMM) Fluorescence Enhancement Test G-Quartet Structure Formation of Immobilized Thrombin Aptamers	85
4.2.3 Aptamer Sandwich Assay for Thrombin by Laser Scanning Confocal Microscopy (LSCM)	86
4.2.4 Sandwich Assays for Thrombin and PDGF-BB Analyzed Using a Home-Built Near-IR Array Scanner	87
4.2.5 Optimization of Conditions for EDC/NHS Immobilization of Aptamers onto PMMA	88
4.2.6 Sandwich Assays for Thrombin and PDGF Using Optimized Immobilization Conditions	89
4.3 Results and Discussion	89
4.3.1 NMM Fluorescence Test for Evaluating G-Quartet Structure Formation of Immobilized Thrombin Aptamers	89
4.3.2 HD1-HD22 Sandwich Assay for Thrombin Detection	92
4.3.3 Optimization of the Aptamer Immobilization Protocol	96

4.3.4 Sandwich Assay Development Using Optimized EDC/NHS Immobilization Conditions	100
4.4 Conclusion	102
4.5 References	102
Chapter 5 Utilization of an Aptamer Pair in Single Molecule FRET Determination of Low Levels of Thrombin	105
5.1 Introduction	105
5.2 Experimental	108
5.2.1 Reagents and Materials	108
5.2.2 Ensemble FRET Experiments	109
5.2.3 smFRET Analysis of Thrombin/Aptamer Complexes	110
5.2.4 Instrumentation for smFRET Determinations	110
5.2.5 smFRET data analysis	111
5.3 Results	112
5.3.1 Effects of an Ethylene Glycol Spacer on the FRET Response of Annealed Cy3 and Cy5 Labeled Complementary Oligonucleotide	112
5.3.2 Ensemble FRET Assays of the Aptamer Beacons for Analysis of Thrombin and Prothrombin	112
5.3.3 smFRET Analysis of Thrombin-Aptamer Assays	114
5.4 Conclusion	117
5.5 References	118
Chapter 6 Conclusions, Current and Future Developments	120
6.1 Conclusions	120
6.2 Current Work	121
6.3 Future Developments	122
6.4 References	124
Appendix: Letter of Permission	125
Vita	127

List of Tables

- Table 1.1** Examples of targets used for aptamer selection, the types of aptamers generated and their dissociation constants..... **4**
- Table 2.1** Microchip CGE and microchip CZE electrophoretic properties of thrombin, its aptamers and complexes formed in buffer or plasma. Symbols and abbreviations in this Table: Migration time, asymmetry factor (AF), resolution (Rs) and apparent electrophoretic mobility (μ_{app}) and electrophoretic mobility (μ_{ep}). The negative sign on μ_{app} , EOF or μ_{ep} represents directional movement from cathode to anode..... **36**
- Table 3.1:** The mammalian cell solubilizing efficiency of four mild detergents in comparison to SDS in terms of total protein content of lysate produced used in mammalian cell lysis..... **69**
- Table 4. 1:** Sequences of DNA aptamers of thrombin (A-D), PDGF (E and F) used in sandwich assay development and the aptamer (G), a DNA variant of the prostate specific antigen aptamer, used for optimizing the EDC/NHS immobilization protocol on PMMA. Abbreviations used in the table are: AmMC6 = primary amine modification with a six carbon linker, iSp9 and iSp18 represent the internal spacers triethylene glycol and hexaethylene glycol respectively. The internal spacer, iSp18, was used to further extend immobilized aptamers from the surface to reduce steric effects and improve interaction of the aptamers with their targets..... **86**

List of Figures

- Figure 1.1:** *In vitro* selection of target-specific aptamers using SELEX. The cyclic selection process uses a synthetic oligonucleotide library made up of either ssDNA or RNA molecules that are incubated with the target. Following removal of the non-bound fraction of the library, the bound DNA/RNA sequences are eluted from the target and amplified and this pool subjected to the appropriate number of cycles. The final pool of oligonucleotides is cloned and sequenced. Each cycle will produce aptamers with higher specificity and binding strength to the selected target. 6
- Figure 1.2** Possible modifications carried out on nucleotides in generating libraries for SELEX. Modifications on the ribose sugar create nuclease resistant oligonucleotides while the bases can be modified depending on the required function. (Adapted from Jayasena, 1999)¹ 8
- Figure 1.3** The quartet structure formed by guanine molecules in thrombin aptamers: (A) the quadruplex stabilized by potassium ions and; (B) a diagram depicting the three-dimensional non-canonical structure adopted by the thrombin aptamers when binding to the exosites. 9
- Figure 1.4** A schematic of the cell-SELEX process involving counter-SELEX using negative control cells to eliminate non-specifically interacting aptamers during the selection process. The aptamer enrichment steps for the target cells involve utilization of the unbound pool of aptamers from the counter-SELEX process. (Adapted from Shangguan *et al.* (2006))⁴⁰ 12
- Figure 1. 5** Schematic of the thrombin detecting aptamer beacon designed to produce a FRET signal when both aptamers bind to thrombin. (Adapted from Heyduk and Heyduk 2005)⁶⁹ 18
- Figure 2. 1:** Microchip CE traces of (A) Alexa Fluor 633-labeled thrombin run by microchip CZE in TG buffer at pH 8.4, E = 300 V/cm, and (B) HD1, HD22 and thrombin (all were labeled with Alexa Fluor 633) individually analyzed by microchip CGE in TG buffer (pH 8.8) with 2% LPA and E = 300 V/cm. Peaks appearing before the thrombin peak at less than 40 s in the CGE electropherogram were due to residual dye from purification of labeled thrombin. The detection was accomplished using laser induced fluorescence with a He-Neon laser (5 mW of laser power). For the microchip CGE case, the PMMA walls were conditioned with MHEC prior to the electrophoretic separation. All separations were performed in PMMA chips. 35
- Figure 2.2:** Electrophoresis traces of mixtures of 75, 250 and 500 nM unlabeled thrombin incubated with Alexa Fluor 647 labeled (A) HD1 and (B) HD22 showing the corresponding increases in complex peak areas with increasing thrombin concentrations (top to bottom). The electrophoresis run buffer consisted of TG buffer at pH 8.8 with 2% LPA gel with the microchip CGE performed using a field

strength of 300 V/cm. Electrophoresis conditions were similar to those described in Figure 2.1B. 38

Figure 2.3: Variation of the amount of affinity complex produced with increasing unlabeled thrombin concentration for assays with HD1 (red circle plot) and HD22 (black square plot), both labeled with Alexa Fluor 647, in terms of average normalized complex peak areas obtained for the analyses carried out using three different PMMA microchips. The assays were performed using PMMA microchip CGE with LIF detection..... 40

Figure 2. 4: Representative microchip CGE traces for HD22 assays in TG buffer (pH 8.8 E = 300V/ cm) for (A) 100 nM prothrombin analysis in buffer and (B) 25% rabbit plasma, (C) 10% and (D) 25% human plasma samples. Plasma samples were desalted and buffer exchanged into CGE buffer without LPA prior to dilution and microchip CGE analysis. 42

Figure 3.1 A schematic of the molecular cloning process. RNA extracted from an over-expressing source of the protein biomarker is reverse transcribed to the cDNA of the target. After PCR amplification the cDNA insert is enzymatically incorporated into the vector with subsequent transformation of bacteria with the recombinant vector. The recombinant vector containing the gene of interest is amplified by culturing the transformed bacteria in the presence of antibiotic and purified for transfection of eukaryotic hosts or transformation of bacteria for protein expression. 49

Figure 3. 2 Agarose gel electrophoresis of restriction enzyme digests of the three recombinant plasmids produced for rEpCAM expression. Given below the image are the calculated fragment sizes expected for each restriction enzyme digestion..... 60

Figure 3. 3: Growth curves of Tuner (DE3)pLac bacteria transformed with pTriEx 4 Neo/ EpCAM-V5-His6 and a control plasmid. The graphs show the rate of growth of the un-induced bacteria from initial media inoculation through the stationary phase. 63

Figure 3. 4: Optical density measurements of un-induced and IPTG induced transformed bacteria cells, showing the effect of the recombinant pTriEx/ EpCAM plasmid on the growth of the cells (Ep Tuner) at various IPTG concentrations. Control cells (Ctl Tuner) were induced at 0 and 1000 μ M IPTG levels to determine the effect of the inducer on cell growth. 64

Figure 3. 5: The effect of temperature on A) protein over-expression in IPTG induce cells determined by electrophoresis with Gelcode Blue staining and B) the growth of the bacteria cells under different temperature conditions as determined by OD measurements..... 65

Figure 3. 6: Western blots of rEpCAM expression in three different mammalian cells. In A) lysates from Cos 7, BHK and Hep2 cells obtained 5 days after transfection were

mixed in native sample buffer and immediately separated by SDS-PAGE on 10% tris-HCl gel prior to electrotransfer to nitrocellulose for western blotting using antiEpCAM and anti-V5 primary antibodies. In B and C, the lysates from stable transfectants were reduced with dithiothreitol and heat denatured prior to SDS-PAGE separation and western blot analysis using anti-V5 antibody. Image C also shows loss of rEpCAM expression by BHK and Hep2 cells after sub-culturing for between 4 to 5 passages. 67

Figure 3. 7: Optimization of IMAC purification protocol for batch purification of rEpCAM from Cos 7 lysate using 0.09% NP40 in TBS. The Western blot image shows elution of rEpCAM at imidazole concentrations as low as 25 mM. 72

Figure 3. 8: A western blot (above) and gel images of fractions from a two-stage IMAC purification of rEpCAM from Cos 7 lysate showing the presence of rEpCAM in addition to non-EpCAM protein contaminants present in the elution fractions. Symbols used for the fractions collected are : L-lystae (1), U-unbound (2), w-wash (3, 4, 11, 12), E-eluates (5, 6,; 13, 14), B-resin (7, 15), S-EpCAM standard, P-positope (8), E2-ultrafiltered eluate (9), EU- unbound eluate (10), M-markers. 74

Figure 3. 9: Western blots of electro elution fractions of IMAC purified rEpCAM. Western blots were carried out with anti-EpCAM and ant-V5 primary antibodies to determine retention of native structure of the protein. 75

Figure 4. 1: A) Schematic of the UV-modification and EDC/NHS coupling process used in immobilizing aptamers onto PMMA, (B) Depiction of the NMM fluorescence enhancement assay showing intercalation of the dye to the G-quartet structure of the aptamer resulting in fluorescence enhancement. (C) The results of the fluorescence enhancement assays for HD1 and HD22 immobilized covalently onto PMMA chips. The aptamer chips were either heat treated at 80 °C in buffer and cooled prior to immersion in NMM solution (h) or placed in the solution without heat treatment (c) with un-functionalized PMMA as the control. Fluorescence emission was obtained at 610nm with excitation at 400 nm. (D) Schematic depicting the aptamer sandwich assay performed for thrombin and PDGF proteins on a PMMA substrate with immobilized aptamers. 91

Figure 4. 2: LSCM analysis of thrombin aptamer sandwich assay on PMMA UV modified through a TEM grid showing A) an image of HD22 functionalized chip treated with 10 nM thrombin assayed with 2.5 µM Cy5-HD1 with the detector set at PMT voltage of 700 V and B) a graphical representation of the chip obtained using ImageQuant analysis. The line drawn across the image in (A) represents the sampling section obtained for the profile shown in (B). Chips were incubated overnight at 4 °C prior to scanning. 93

Figure 4. 3: ImageQuant analysis of LSCM images acquired for thrombin aptamer assays performed on PMMA that was UV-modified through a TEM grid. The bar graph shows intensity differences of the LSCM images of HD22 functionalized and

unmodified regions of the PMMA chips generated for different thrombin concentrations, BSA and the control samples. The blank is an HD22 immobilized chip treated with Cy5-HD1. A chip treated with 10 mg/ mL BSA was used in testing specificity of the assay for thrombin. Images were obtained at a fixed PMT voltage of 700 V..... 94

Figure 4. 4: Near-IR fluorescence images of 1:1 serial dilutions of thrombin (0, 0.125, 0.25, 0.5, 1.0, 2.0 and 4 μ M) and PDGF-BB (0, 0.058, 0.115, 0.231, 0.462, 0.925 and 1.85) were mixed with 3 μ M Cy5.5-labeled aptamer (aptamer D and F in table 1) and spotted on an HD22 and PDGF-functionalized PMMA slides respectively. The slides were incubated overnight at 4 °C prior to scanning. The scan rate was 500 μ m/s over a scan area of 18 x 20 mm. In (A) thrombin samples are represented as T1-T7 and PDGF-BB samples are represented as P1 – P6 in increasing order of protein concentration. 97

Figure 4.5: A) Images of a one-step EDC/NHS coupling reaction for various concentrations of immobilized Cy5.5 labeled aptamer (G) onto UV-modified PMMA with different incubations times of I) 30 min and II) 5 h in pH 6.7 MES buffer and III) 30 min and IV) 80 min in pH 7.2 HEPES buffer, and B) plots of fluorescence intensity of the spots showing the effect of pH and EDC concentration on the coverage density of the labeled aptamer. The MES buffer contained EDC at 50 mM while in the HEPES buffer EDC concentration was increased to 200 mM with a fixed 40 mM NHS concentration in both buffers. Imaging conditions are the same as those given in Figure 4.4. 99

Figure 4.6: Sandwich assay intensity profiles of A) various PDGF-BB concentrations ranging from 0 - 500 nM combined with 500 nM Cy5.5-PDGF aptamer and B) thrombin at concentrations between 31 nM and 2000 nM with a fixed concentration of 1000 nM for the Cy5.5-HD1 reporting aptamer. The assays were incubated at 37 °C for approximately 1 h before scanning using the near-IR imager. 101

Figure 5.1: Diagram of the smFRET instrument set-up showing a 532 laser for excitation of the fluorophores and a system of dichroic mirrors and filters, and an avalanche diode detector for detection Cy5 fluorescence emission. 111

Figure 5.2: FRET and fluorescence emission spectra for annealed complementary seven-oligonucleotide sequences and the Cy5-labeled sequences in TBS buffer at pH 7.7. Excitation was carried out at 532 nm and the fluorescence emission spectra obtained for Cy5 emission. Both oligonucleotide sequences were synthesized with the FRET dyes attached with (represented by a prime (')) or without an ethylene glycol internal spacer between the dye and the sequence to determine the best linker combination for maximum FRET response. 113

Figure 5.3: Variation in ensemble FRET response for aptamer beacon assays with increasing concentration of thrombin or prothrombin in TBS at pH 8.5. The HD1 and HD22 beacon concentrations were fixed at 250 nM. 114

Figure 5.4: Computer generated readouts of the assays showing the rate of photon count with time obtained on the Cy5 fluorescence detector for A) buffer only, B) 30 pM Cy5-HD22 beacon in buffer, C) 30 pM HD1-Cy3/Cy5-HD22 mixture in buffer and D) 30 pM HD1-Cy3/Cy5-HD22 with 6 pM thrombin. Samples were prepared in buffer at pH 8.5, incubated at room temperature at a higher concentration and diluted to 30 pM aptamer beacon concentration prior to analysis on the smFRET system. **116**

Figure 5. 5: Plots of photon burst data obtained for smFRET analysis of the aptamer assay showing the frequency of molecular events obtained at different count rate thresholds for Cy5-HD22, both aptamer beacons without thrombin and the assay with thrombin at 6 pM concentration..... **117**

Figure 6. 1: Diagrammatic representation of the layout of a simple polymeric microdevice for immobilization and purification of histidine-tagged proteins with subsequent electrophoretic separation of complexes formed with nucleic acid strands in a degenerate library for aptamer selection. Reservoir A contains nanoposts functionalized with tetradentate chelating groups for immobilized metal affinity purification in channel AB with channel CD as the separation channel..... **123**

Abstract

Aptamers have emerged as potential affinity agents that rival or complement antibodies in developing diagnostic assays for disease detection. We have demonstrated the use of PMMA microfluidic devices for conducting rapid affinity microchip CGE of a target protein using aptamers as the affinity probes with an electrophoresis development time of <2 min. Migration times were reproducible for thrombin complexes and free aptamers in CGE buffer with device-to-device RSD variations below 10%. By removing salts from plasma and adding an unlabeled random sequence oligonucleotide to the plasma, thrombin was detected in plasma. This method can be easily adapted to high-throughput parallel screening of plasma samples in multi-channel polymeric microdevices.

The expression of rEpCAM in bacteria and mammalian cells was investigated with results showing successful expression in the mammalian systems, while protein expression in the bacteria was inhibited. Higher and prolonged expression levels were obtained in Cos 7 cells as compared to BHK and Hep2 cells due to episomal expression in Cos 7 cells. By combining a one-step IMAC procedure with electrophoresis and electro elution a more selective approach to obtaining electrophoretically pure rEpCAM was achieved.

We developed dual-aptamer sandwich assays for thrombin and PDGF-BB targets on PMMA substrate using UV modification with a one-step EDC/NHS coupling reaction. Results indicate that the use of high EDC concentrations lead to faster immobilization and increased coverage density with a shorter sandwich assay development time. The

assays were sensitive for both proteins and showed linearity in fluorescence response to changing protein concentration.

Single molecule detection methods provide high sensitivity techniques in which aptamers can find use. We have demonstrated the use of two aptamers in a FRET-based assay for the detection of low levels of thrombin. Sensitivity and reliability of the aptamer smFRET assay depends on complex formation and stability. Due to the dissociation constants of the aptamers, single molecule events detected were below the calculated value for a 6 pM concentration of thrombin. Future work will involve adjusting the single molecule system by the use of pinholes to enable analysis of higher sample concentrations.

Chapter 1 Aptamers: A Class of Affinity Compounds with Potential Applications in Therapeutics and Disease Diagnosis

1.1 Introduction

Affinity agents, such as antibodies, are the central component in many bioanalytical techniques. This is due to their high level of specificity and selectivity for the recognition of targets embedded in complex sample matrices. Antibodies are proteinaceous materials and are generated *in vivo* through induction of an immune response in animal hosts or by hybridoma technology.^{1, 2} Their use in the development of bioanalytical techniques suffers from certain disadvantages however, including their protracted method of production, the need for relatively large targets to induce an immune response in the host, cross reactivity of antibodies with structurally similar analytes and instability of their tertiary protein structures leading to short shelf-life. Alternatives to antibodies have been studied which include peptides and nucleic acid aptamers. The latter group of newly developed affinity agents, aptamers, hold promise as viable alternatives to antibodies in many bioanalytical methods requiring an affinity agent.¹

Aptamer-based molecular recognition applications are rapidly developing into a field that is projected to be competitive with antibody-based biosensors, immunoassays, and other analytical formats currently in use.³ Aptamers (derived from the Latin words *aptus*-to fit and *meros*-particle)⁴ are artificial receptors, primarily DNA or RNA sequences between 15 to 60 bases in length, which are generated *in vitro* toward target molecules ranging in size from 100 daltons^{5, 6} to as large as whole cells.^{7, 8} They are short single-stranded sequences with specific and complex three-dimensional structures comprised of stems, loops, bulges, hairpins, triplex or quadruplex motifs.⁹ The high affinity displayed by aptamers to a variety of molecules can be attributed to their ability to incorporate small molecules into their three-dimensional nucleic acid structure, or to integrate into the structure of larger molecules such as proteins, using

noncovalent interactions. These interactions include but are not limited to stacking of aromatic rings, electrostatic and/or van der Waals interactions, hydrogen bonding, or from a combination of these effects.^{10, 11} Aptamers can also adopt an induced-fit mechanism when binding to their targets in solution. Many aptamers exhibit binding affinities similar to monoclonal antibodies with dissociation constants (K_D) in the nanomolar to micromolar range for small molecules and picomolar to nanomolar range for larger targets such as proteins.⁹

Table 1.1 provides a literature survey of aptamers that have been developed for selected targets and the dissociation constants. These targets range from as small as divalent metal cations (zinc and nickel) or organic molecules such as malachite green, ethanolamine and theophylline, to large targets such as enzymes, antibodies and leukemia cells (see Table 1.1). Also, aptamers can distinguish between chiral molecules through the design of the aptamers for recognition of a specific stereoisomer. In a study by Michaud *et al* (2003) a DNA aptamer capable of recognizing the D-enantiomer of an oligopeptide, arginine-vasopressin, was used as a stationary phase for liquid chromatographic separation of the L and D stereoisomers of the oligopeptide, in which the D form was retained by the column while the L form eluted in the void volume.¹²

Aptamers can be an attractive alternative to antibodies in a variety of research applications due to their potential as molecular recognition elements with certain advantages over their antibody counterparts.¹³ Unlike antibodies, aptamers have the benefits of being chemically and thermally stable, can be selected toward a wider range of targets (see Table 1.1) and are generated by *in vitro* solid phase synthesis techniques without the constraints of *in vivo* generation required for antibodies.¹³

The selection process allows generation of aptamers towards specific regions of the target whereas the antibody generation process is subject to the immune system of the animal it is produced in, which means researchers have very little control over the exact epitope an antibody

can be raised against.¹³ Surface immobilized aptamers can be easily regenerated for repeated use in devices without undergoing denaturation as is observed with antibodies.³ Also, the smaller size, ease of modification and single stranded structure of nucleic acid aptamers allow their immobilization on surfaces in a more highly ordered form compared to antibodies, making them more appropriate for techniques requiring immobilization of affinity agents onto solid support. The production of aptamers by solid phase synthesis also enables chemical modifications to be made during production, such as incorporation of functional groups or structural alterations, to increase stability of the molecule without affecting function.¹ The *in vitro* selection process of aptamer generation makes it advantageous for quick aptamer selection toward newly discovered biomarkers even under conditions similar to those used in assays for which the aptamers are being developed.^{9, 14}

1.2 The Aptamer Generation Process

The aptamer selection technique, dubbed **S**ystematic **E**volution of **L**igands by **E**xponential enrichment (SELEX), is an iterative method in which combinatorial elements (i.e. different sequences of DNA or RNA) are incubated with a target for selection of library elements that bind tightly to the target.^{15, 16} The unbound fraction is partitioned off and the bound fraction, once eluted from the target, amplified by PCR for another round of selection. The process is repeated until an enriched pool of tightly binding oligonucleotides is obtained. The pool of oligonucleotides is cloned and analyzed via sequencing to determine the nucleotide content of the newly generated aptamers (see Figure 1.1). Each step of the SELEX process is of great importance in order to produce aptamers with very high specificity or low K_D values.¹⁷

1.2.1 The SELEX Library

The combinatorial library is usually made up of ribonucleic acids¹⁸ or deoxyribonucleic acids (DNA) and consists of random synthetic sequences of 20 – 80 nucleotides flanked by

Table 1.1 Examples of targets used for aptamer selection, the types of aptamers generated and their dissociation constants.

Targets	Type of aptamer	K _d	References
Zn ²⁺	RNA	1.2 mmol/L	Ciesiolka et al. (1995) ¹⁹
Ni ²⁺	RNA	0.8–29 mmol/L	Hofmann et al. (1997) ²⁰
Ethanolamine	DNA	6–19 nmol/L	Mann et al. (2005) ⁶
Theophylline	RNA	100 nmol/L	Jenison et al. (1994) ²¹
Malachite green	RNA	1 mmol/L	Grate and Wilson (2001) ²²
Organic dyes	DNA	33–46 mmol/L	Ellington and Szostak (1992) ²³
Ricin toxin	DNA	58–105 nmol/L	Tang et al. (2006) ²⁴
L-tyrosinamide	DNA	45 mmol/L	Vianini et al. (2001) ²⁵
a-Thrombin	DNA	200 nmol/L	Bock et al. (1992) ²⁶
	RNA	<1–4 nmol/L	White et al. (2001) ²⁷
Bovine thrombin	RNA	164–240 nmol/L	Liu et al. (2003) ²⁸
Immunglobulin E	DNA	23–39 nmol/L	Mendonsa and Bowser (2004) ²⁹
PDGF	DNA	0.1 nmol/L	Green et al. (1996) ³⁰
VEGF	RNA	0.1–2 nmol/L	Jellinek et al. (1994) ³¹
TTF1	DNA	3.3–67 nmol/L	Murphy et al. (2003) ³²
HGF	DNA	19–25 nmol/L	Saito and Tomida (2005) ³³
L-Selectin	DNA	1.8–5.5 nmol/L	Hicke et al. (1996) ³⁴
Taq DNA polymerase	DNA	0.04–9 nmol/L	Dang and Jayasena (1996) ³⁵
Prion protein (PrPc)	RNA	0.1–1.7 nmol/L	Proske et al. (2002) ³⁶
Hepatitis C virus RdRp	DNA	1.3/23.5 nmol/L	Jones et al. (2006) ³⁷
Tumour marker MUC1	DNA	0.1–34 nmol/L	Ferreira et al. (2006) ³⁸
U251 glioblastoma cells/tenascin-C	RNA	5 nmol/L	Hicke et al. (2001) ³⁹
Leukemia cells CCRF-CEM	DNA	0.8–229 nmol/L	Shangguan et al. (2006) ⁴⁰

predetermined sequences at the 5' and 3' ends for polymerase chain reaction (PCR) amplification of DNA, transcription or reverse transcription followed by PCR (RT-PCR) when RNAs are used as the recognition element.⁹ The complexity of the library depends intimately on the number of nucleotides in the random region. For example, the theoretical number of unique sequences for a library containing “n” nucleotides will be 4^n , thus a thirty random nucleotide sequence would have 4^{30} ($\sim 1.2 \times 10^{18}$) unique sequences.^{15, 41} However, most libraries are generated to contain between 10^{13} to 10^{15} individual sequences.¹³ The oligonucleotide libraries used for aptamer selection can be directly utilized in the SELEX process, with some researchers preferring to PCR amplify and purify the library prior to the start of SELEX to eliminate damaged DNA or un-amplifiable sequences that may interfere with the selection process.⁴² The use of RNA libraries, however, requires the design of forward primers and oligonucleotide 5' regions with a T7 promoter sequence for conversion of DNAs to RNAs before the selection step. Amplification of the bound RNA oligonucleotides occurs by RT-PCR and transcription of the cDNA back to RNA for subsequent selection steps.⁹

Important considerations in library design to ensure success in aptamer selection include the length of the random sequence, which affects the amplification process.⁴³ It has been observed that long sequences of approximately 80 to 100 bases provide high structural complexity during the binding process compared to shorter oligonucleotide strands of about 20 to 40 bases, especially for targets not known to bind nucleic acids naturally.^{3, 9, 42} However, long oligonucleotide strands with 80 bases or more tend to produce lower yields of full length products and generate by-products during the PCR amplification process.⁴³ Truncated versions of the oligonucleotide strands occur as the number of PCR cycles increases above 20 when the PCR product concentration is increased to between 20- 50 nM and serve as templates from which single stranded/ double stranded DNA (ss-dsDNA) by-products are produced. Variations in the

melting temperatures due to guanine and cytosine compositional differences also cause some members of the library not to be amplified if the strands are not sufficiently unfolded to allow primer binding.⁴³

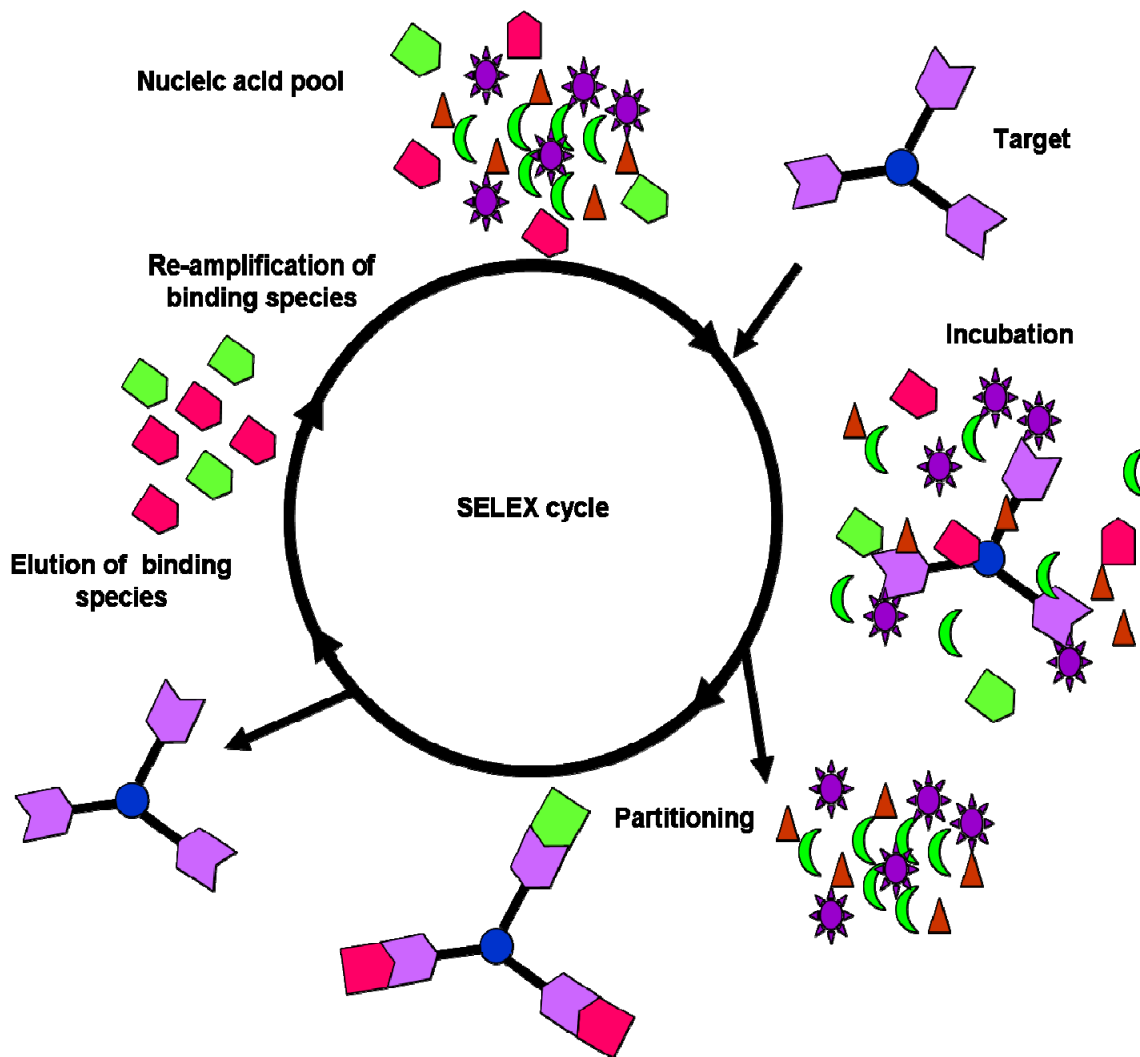


Figure 1.1: *In vitro* selection of target-specific aptamers using SELEX. The cyclic selection process uses a synthetic oligonucleotide library made up of either ssDNA or RNA molecules that are incubated with the target. Following removal of the non-bound fraction of the library, the bound DNA/RNA sequences are eluted from the target and amplified and this pool subjected to the appropriate number of cycles. The final pool of oligonucleotides is cloned and sequenced. Each cycle will produce aptamers with higher specificity and binding strength to the selected target.

Thus, to circumvent these problems researchers PCR amplify the starting library and purify the resulting amplicons prior to initiation of the SELEX process.⁹

Because oligonucleotides are composed of only 4 different nucleotide bases, this limits the possible randomized combinations available in producing these libraries compared to the alternative synthetic recognition element, peptoids, which are generated from a pool of 20 different amino acids. However, chemical modifications can be introduced into the DNA/RNA sequences to increase library complexity and also provide conformational stability and/or confer nuclease resistance characteristics. Typical modifications include replacement of the 2'-hydroxyl group on the ribose of pyrimidine nucleotides with a primary amine, introduction of a fluoride or methoxy group to create nuclease resistant RNA (see Figure 1.2).^{44,45} Another means of stabilizing nucleic acid aptamers is to use stereoisomers of the target in the selection process with subsequent synthesis of the mirror image of the generated aptamer, referred to as spiegelmers.⁴⁶ By substituting D-ribose with L-ribose the nuclease resistance of RNA aptamers can be increased as well.⁴⁷ Alternatively, the phosphate backbone can be altered by replacing non-binding oxygen with a sulfur group to increase nuclease resistance.⁴⁸ Carbon positions 5 and 8 on the pyrimidine and purine bases, respectively, can also be modified with amino acid groups to generate aptamers capable of tightly binding anionic targets.⁹ Modified nucleotides, such as 5-bromouracyl and 5-iodouracyl, have been incorporated into aptamer sequences to allow photo-crosslinking of aptamers to targets.⁴⁹ With modifications to nucleotide bases, the complexity of a combinatorial library can be further increased to extend the range of target diversity to which aptamers can be generated.⁹

1.2.2 Aptamer Selection Targets

Since its inception in 1990, SELEX has been applied to different classes of targets ranging from small molecules such as divalent cations,²⁰ ethanolamine,⁶ and antibiotics⁵⁰ to large complex targets such as proteins,^{26, 29} mixtures of targets (found as aggregates or on cell surfaces) and whole cells.^{3, 13, 40} Aptamers can be generated toward targets that are naturally

associated with nucleic acids such as nucleotides, cofactors and DNA binding proteins and for targets not naturally associated with nucleic acids (organic dyes and growth factors).^{4, 23, 30, 51}

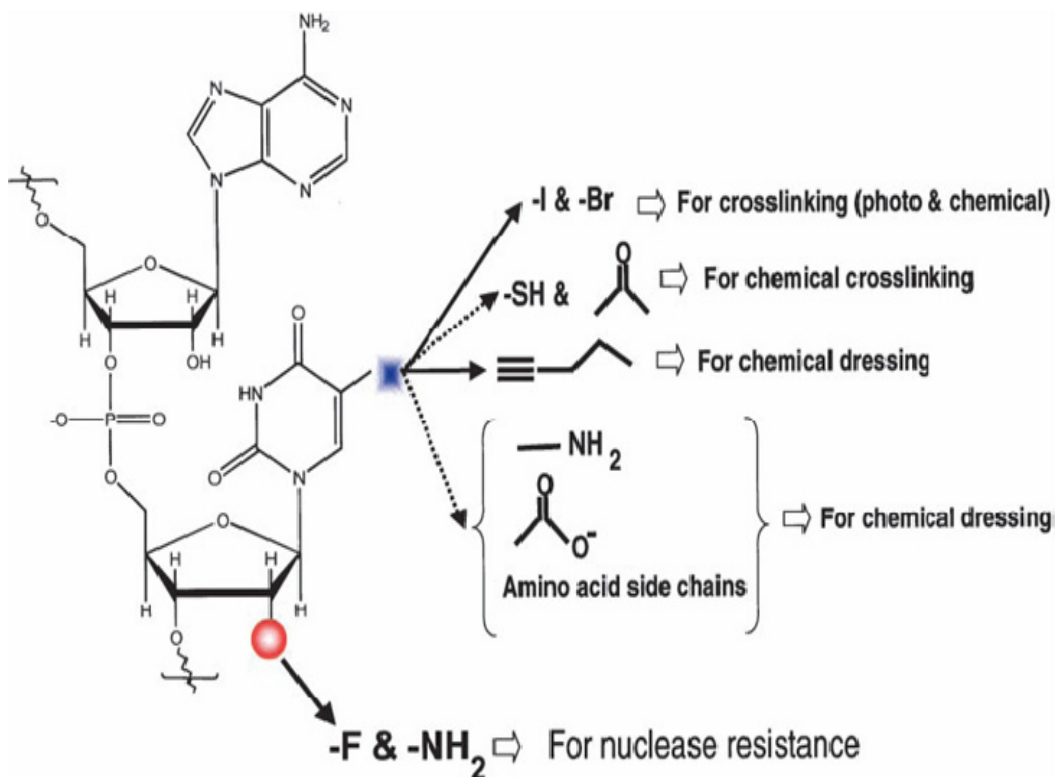


Figure 1.2 Possible modifications carried out on nucleotides in generating libraries for SELEX. Modifications on the ribose sugar create nuclease resistant oligonucleotides while the bases can be modified depending on the required function. (Adapted from Jayasena, 1999)¹

A large percentage of aptamer selections carried out to-date have been directed toward protein or peptide targets, both free and extra-cellular domain of membrane bound proteins, due to the large multi-functional surfaces possessed by proteins making them excellent targets for aptamer selection.^{26, 34} The wide variety of targets used in aptamer selection gives an indication of the wide-range applicability of these recognition elements to virtually any target. However, in order to generate highly specific and tightly binding aptamers for a given target certain

requirements need to be met. For example the target should be present at sufficient enough levels and of very high purity to prevent enrichment of non-specifically interacting oligonucleotides.⁹

Characteristics that enhance aptamer selection include possession of positively charged groups (e.g. primary amines), presence of hydrogen bond donors and acceptors and planar structures (as found in aromatic groups). These allow the aptamers to bind to the target through a combination of interactive forces such as shape complementarity, aromatic structure and nucleotide stacking interactions, electrostatic and hydrogen bonding interactions.^{10, 11, 52}

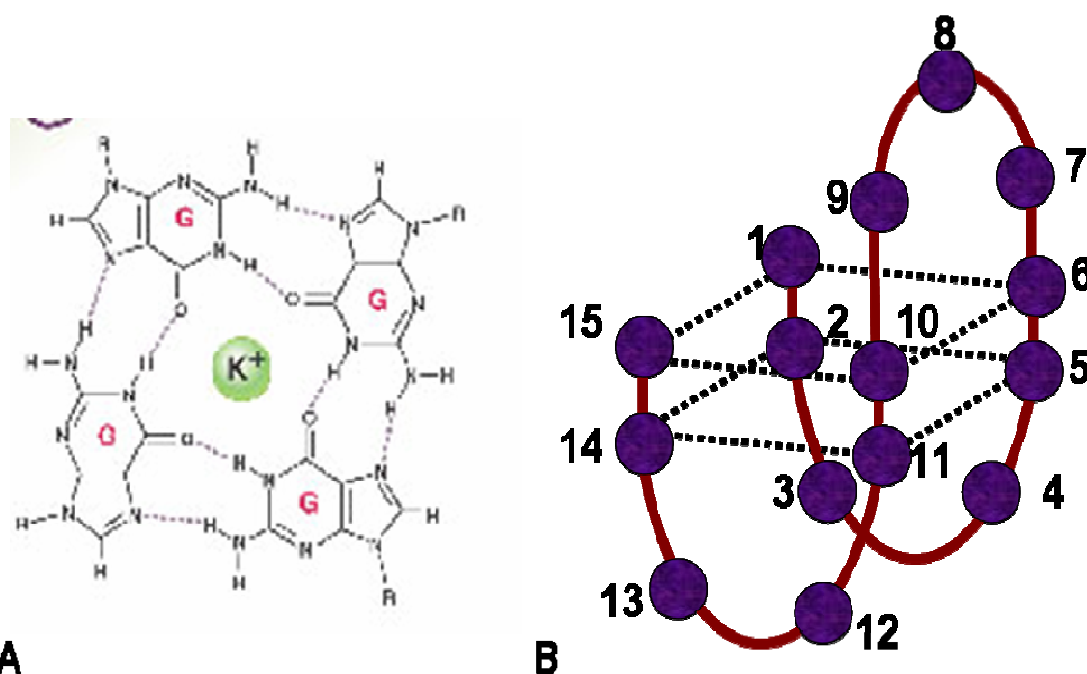


Figure 1.3 The quartet structure formed by guanine molecules in thrombin aptamers: (A) the quadruplex stabilized by potassium ions and; (B) a diagram depicting the three-dimensional non-canonical structure adopted by the thrombin aptamers when binding to the exosites.

Another interesting feature of aptamers is their ability, in the presence of their targets and on formation of the binding complex, to undergo adaptive conformational changes. Three-dimensional structure formation enables an aptamer to encapsulate small targets while for higher molecular weight targets different surface sub-structures on the target may be involved in the aptamer binding process.^{9, 11} For example, the thrombin aptamers, HD1 and HD22, bind to its cationic exosites through the formation of a G-quartet structure (see Figure 1.3).

Highly anionic or hydrophobic targets are less likely to serve as good targets for aptamer selection due to molecular repulsion and electrostatic considerations. To minimize these effects, modifications can be made to the combinatorial library to create cationic or hydrophobic functional groups in these strands to enhance their affinity toward these targets. Protein biomarkers serve as good targets for aptamer selection due to the multifunctional surface groups that allow oligonucleotides to bind easily. Current advances in protein engineering allow for the rapid generation of proteins or segments of proteins engineered with fusion tags³² that can be used as targets for affinity selection processes and biochemical interaction processes. Aptamer selection against some protein biomarkers are thus carried out with recombinant proteins as targets. For example, an N-terminus hexahistidine-tagged recombinant of a thyroid transcription factor was immobilized onto magnetic metal chelating resins and used as a target for SELEX with the derived aptamer characterized by surface plasmon resonance, enzyme linked assays, western blot and affinity purification.³²

1.2.3 Selection Process

The basic concepts of SELEX developed by Kramer *et al.*⁵³ were independently utilized by two groups^{4, 17} in the early 1990s to develop the general approach for aptamer generation from a random oligonucleotide library.⁵⁴ Since then, numerous variations to the original Tuerk and Gold SELEX method (1990) have been developed. This has given rise to different names for the SELEX process depending on the factors used for the aptamer selection. For example, counter-SELEX involves affinity elution of bound aptamers with structural analogs to eliminate aptamers that bind closely-related compounds.¹ Cell-SELEX involves selection of aptamers against whole-cell targets as was originally done for the generation of the Tenasin C aptamer.⁵⁵ An example of the cell-SELEX process was recently demonstrated in a study by Shannguan *et al* (2006) to generate aptamers for cancer diagnosis. Aptamers were derived toward a lymphoblastic

leukemia cell-line (CCRF-CEM) through a counter-SELEX process involving the use of human Burkitt's lymphoma cell line (Ramos) as the negative target.⁴⁰ Figure 1.4 shows the cell-SELEX process. During the selection process, the unbound fraction of the combinatorial library from the counter-SELEX process using Ramos cells was used in the selection of high affinity aptamers toward the CCRF-CEM target. The aptamers were used in flow cytometry studies to determine their ability to bind specifically to membrane proteins on the surfaces of the leukemia cells.⁴⁰

Direct interaction of a target with a combinatorial library for a given time period with subsequent removal of the unbound oligonucleotides forms the selection step of the SELEX process. This process is application-oriented and does not require in-depth knowledge of the characteristics of the target. Various methods exist for enhancing the incubation and partitioning of the bound and unbound fractions of the library during each selection round. These comprise methods that do or do not require target immobilization. Target immobilization typically involves column chromatography in which targets, such as proteins and dye molecules, are immobilized through affinity interaction or by cross-linking them to support matrices.^{4, 32} This is the most conventional method for target immobilization, but requires large amounts of sample to allow efficient loading onto the columns.^{56, 57} However, by using magnetic beads and affinity immobilization, smaller sample sizes can be used and in parallel format for high throughput screening of different targets in both manual and automated formats, which also enables elimination of several intermediate steps such as centrifugation and filtration.⁵⁴

Selection methods requiring no target immobilization include membrane filtration, capillary electrophoresis (CE-SELEX), Surface Plasmon Resonance, centrifugation, and flow cytometry.⁵⁴ Membrane filtration selection utilizes nitrocellulose membranes with various molecular weight cut-offs to separate unbound oligonucleotides from nucleic acid-target complexes after pre-incubation of a combinatorial library with the target of interest (usually a

protein). After washing to remove unbound oligonucleotides the bound oligonucleotides are eluted and amplified for the next round of SELEX.

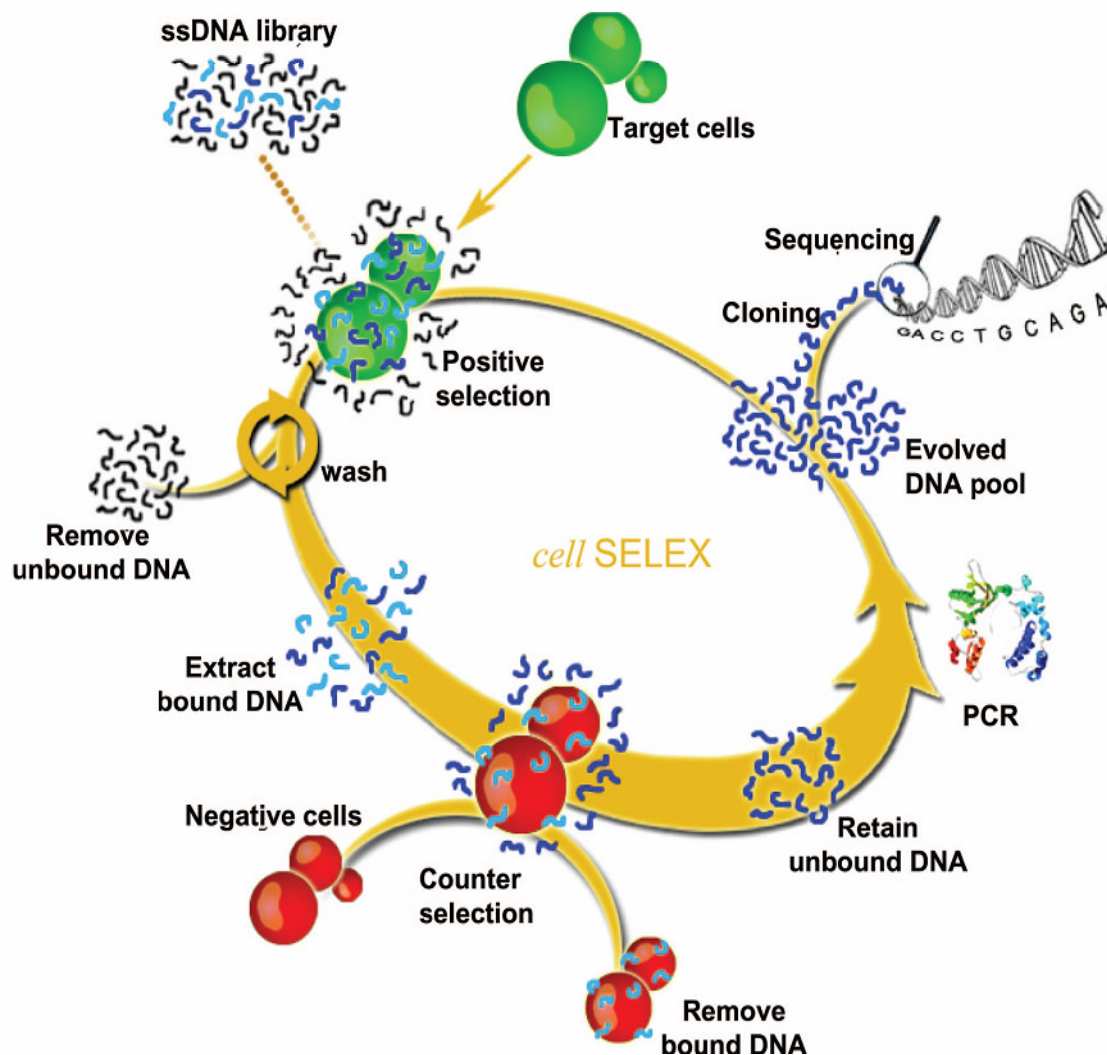


Figure 1.4 A schematic of the cell-SELEX process involving counter-SELEX using negative control cells to eliminate non-specifically interacting aptamers during the selection process. The aptamer enrichment steps for the target cells involve utilization of the unbound pool of aptamers from the counter-SELEX process. (Adapted from Shangguan *et al.* (2006))⁴⁰

Another technique demonstrated by Mosing *et al.* (2005) and Tang *et al.* (2006) is selection using capillary electrophoresis (CE-SELEX).^{24, 58} This technique enables faster generation of aptamers in as few as four rounds. For example, in the studies carried out by Tang

and co-workers, aptamers were derived against ricin using two *in vitro* techniques, affinity chromatography and CE-SELEX. In this study, 10 pM ricin was incubated with the ssDNA pool for 30 min and separated by CE. Their results showed that the rate of oligonucleotide enrichment increased to 60.2% after two rounds of SELEX compared to 38.5% obtained by conventional SELEX, making CE-SELEX a faster process for aptamer selection against targets.²⁴ The CE-SELEX method has also been employed in aptamer selection processes for producing high affinity aptamers against human immunoglobulin E (IgE),²⁹ and HIV reverse transcriptase.⁵⁸

1.2.4 Amplification, Elution and Characterization of Aptamers

One major advantage of aptamer selection is the ease of amplification of the bound oligonucleotides using biosynthetic processes, such as, PCR (DNAs) and RT-PCR (RNAs). In the enrichment and identification steps associated with SELEX, bound oligonucleotides need to be amplified due to the complexity of the starting library. Although a high concentration of starting library can be used, the concentrations of the binding sequences will initially be very low due to the large number of diverse sequences present, requiring amplification and enrichment in subsequent processes to increase the amount of high affinity sequences in each round. The amplification process can be carried out using modified primers to aid in purification and detection of the aptamers. DNA aptamers only require PCR amplification using Taq polymerase, while the RNA aptamers require RT-PCR and subsequent transcription.⁴² Thus, RNA aptamer SELEX requires the use of primers with a T7 promotor sequence.

For subsequent rounds of selection, the amplified DNA must be in single-stranded form and unfortunately, PCR generates double-stranded products. As such, techniques must be used to generate the prerequisite single-stranded form. Reverse primers functionalized with biotin can be designed to help with immobilization of amplified double stranded DNA (dsDNA) through

avidin/biotin interaction with subsequent release of the single stranded DNA (ssDNA) after denaturing the immobilized dsDNA.³² Other techniques for generating the single stranded construct include asymmetric PCR in which an excess of one primer is used to generate more of one type of ssDNA, usually the binding strand.⁵⁹

Elution strategies for releasing bound aptamers from their targets include heat treatment, addition of urea, sodium dodecyl sulfate (SDS) or ethylene diamine tetra acetic acid (EDTA) to disrupt complexation. The use of competitive binders has also been reported in the elution step to displace a bound target. Selection rounds range between 4 to 20 cycles after which the amplified sequences are cloned and sequenced to characterize the binding oligonucleotide strands.¹³ The number of different aptamers obtained depends on the target and stringency of the selection process and ranges between 1 and 10⁶. To characterize the aptamers, software programs have been developed, such as CLUSTAL W, to help align sequences to determine homology and mfold for secondary structural conformation determination.⁹

1.3 Challenges Associated with Aptamers

In spite of the promising research on aptamers and their generation, there are a few disadvantages associated with them. One of the main disadvantages is that this technology is a relatively new area compared to antibodies which have been very widely studied, and as such, not many high affinity aptamers are commercially available.⁹ Also, not all targets are suitable for aptamer selection due to the absence of the necessary structural motifs present in the target that provide molecular interactions for binding to aptamers. For example, anionic and hydrophobic targets are not suitable for aptamer selection unless modifications are made to the bases (see Section 1.2.2). Although aptamers can be selected toward a wide range of targets, research has indicated that aptamers with micromolar to millimolar dissociation constants are primarily derived for smaller targets (see Table 1.1), which implies lower affinities when

compared to antibodies.⁹ Thus more information is required on the interactions involved in generation of high affinity aptamers and developing a standard protocol for generating aptamers.⁹ For example, in terms of standardizing a protocol for aptamer arrays, Collet et al. (2005) observed that a single buffer systems could not be used to allow different aptamers to bind efficiently to corresponding targets.⁶⁰ Also, modifications to aptamers to confer nuclease resistance also add to the cost of the aptamers produced.

1.4 Applications of Aptamers

1.4.1 Therapeutic and *In Vivo* Diagnostic Applications

Aptamers can be adapted to a variety of therapeutic and *in vivo* diagnostic applications where affinity agents are required. In the area of therapeutics, aptamers are rapidly catching up with antibodies.⁶¹ The first Food and Drug Administration⁶² approved aptamer for therapeutic function is the vascular endothelial growth factor aptamer which has been approved for treatment of macular degeneration.^{61, 63} In the area of *in vivo* diagnostics, aptamers are in general more suitable than antibodies for conducting *in vivo* imaging for disease detection due to the smaller size of aptamers compared to antibodies, which provides a faster clearance rate in the body for agents that may be toxic. Aptamers also have lower immunogenicity and can be modified to extend their half-life in the blood.⁹

1.4.2 *In vitro* Diagnostic Applications

In vitro diagnostics (IVD) has been an area of considerable innovation and scientific advancement over the past decade in an attempt to provide medical professionals with tools to enable the acquisition of obtain objective information about disease states in order to effectively and rapidly treat patients.^{5, 64} Some of the most significant promises come from the utilization of validated biomarkers to predict a patient's likelihood of responding to a medicine or avoiding certain side effects.⁵ With the yearly growth in the market value of IVD, substantial amounts of

resources are being invested into diagnostic research aimed at identifying and validating new biomarkers and the detection science involved in IVD tests.^{64, 65}

IVD tests can generally be classified as medical tests conducted in a controlled environment, such as a test tube, outside of a living organism. The FDA's definition of IVD products are those reagents, instruments and systems intended for use in diagnosis of disease or other conditions, including a determination of the state of health, in order to cure, mitigate, treat, or prevent disease or its sequelae (chronic condition).^{62, 65} These include analytical and bioanalytical techniques used in clinical laboratories like mass spectrometry, immunoassays and electrophoresis;⁶⁶ and point-of-care (POC) devices, such as biosensors based on several different transduction modalities such as acoustic, optical and electrochemical detection.⁶⁴

A new IVD classification category was introduced by the FDA in 1996 as a modification to its regulatory oversight in the area of IVDs. This category called the analyte-specific reagents (ASRs) include antibodies, both monoclonal and polyclonal, specific receptor proteins, nucleic acid sequences and similar reagents which, through specific binding or chemical reaction with substances in a specimen, are intended for use in a diagnostic application for identification and quantification of an individual chemical substance or ligand in biological specimens.⁶⁵ This new category was based on the recognition by the FDA that ASRs are the active ingredients of in-house tests, which when used in combination with general purpose reagents and laboratory instruments, could be the basis for new assays, which could benefit public health.

Antibodies are currently the most widely available agents used in affinity-based diagnostic techniques that can use biosensors, arrays or bioseparations as the functional platform for the diagnostic. However, aptamers are rapidly penetrating this area.⁶⁷ Because of their robustness compared to antibodies in terms of their ability to withstand extreme pH, temperature

and regeneration conditions that induce denaturing, they may be more suited for creating affinity-based assays using the afore mentioned techniques.⁶⁸

Biosensors are devices that couple a biological recognition element with a physical transducer to allow for the detection of a target. Commonly used transducers are optical, electrochemical or mass sensitive devices that generate light, current or frequency signals for quantitative or semi-quantitative information.¹³ Using aptamers as recognition elements, several biosensors have been developed to analyze a variety of targets in real samples. In a study by Heyduk et al. (2005), a fluorescence-based sensor was developed for the detection of thrombin in complex matrices using fluorescence resonance energy transfer (FRET) as the readout modality. Using aptamers that recognized two different epitopes on thrombin, each aptamer was designed attached via a long linker to a short complementary seven-base sequence to which a donor or acceptor dye was conjugated (see Figure 1.5).⁶⁹ In the presence of the target, the aptamers bind to different epitopes on thrombin causing the dye-labeled complementary oligonucleotide sequences to anneal generating a FRET response. Other biosensor formats have involved the interaction of aptamers developed against HIV-Tat and tubulin proteins with transduction accomplished via surface plasmon resonance, in which thiol functionalized aptamers were immobilized onto glass slides for capturing the target molecules.^{70, 71}

Microarrays consist of recognition probes covalently immobilized onto a solid support, such as glass. The recognition elements typically used for microarrays are oligonucleotide probes for targeting DNAs/RNAs, or antibodies, for targeting proteins. However, aptamers can be used for microarrays as well. In a study to optimize the conditions for producing aptamer microarrays, biotin functionalized aptamers were used as capture elements on streptavidin-coated microarray glass slides.^{60, 72}

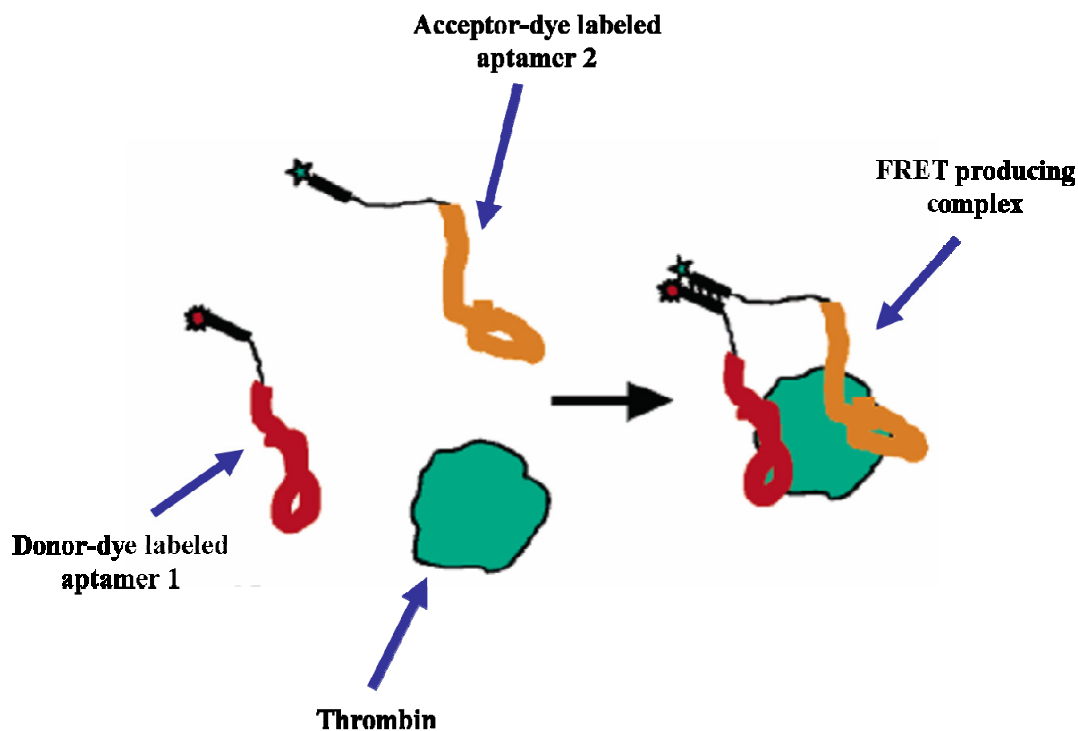


Figure 1. 5 Schematic of the thrombin detecting aptamer beacon designed to produce a FRET signal when both aptamers bind to thrombin. (Adapted from Heyduk and Heyduk 2005)⁶⁹

Conditions for effectively generating the microarrays such as pH and buffer composition were considered. The researchers found that phosphate buffered saline containing 5 mM MgCl₂ could be used in assays of different targets even though it was not the buffer used in the SELEX process for some of the aptamers.⁷² They also demonstrated that aptamer microarrays can be developed on streptavidin-coated glass slides using automated systems for the detection of labeled protein in cell lysate.⁶⁰

In the separation sciences aptamers have been used in affinity chromatography (AC),⁷³ affinity probe capillary electrophoresis (ACE), and capillary electrochromatography (CEC).¹³ In AC studies using aptamers in place of antibodies, a biotinylated aptamer of adenosine immobilized on streptavidin beads was used for the separation of adenosine from its analogues, cyclic-AMP, NAD⁺, AMP and ADP. It was observed that the column could selectively retain and separate ATP and its analogs.⁷⁴ CEC studies using immobilized thrombin aptamer were

carried out to separate non-target analytes such as binary mixtures of amino acids (D-tryptophan/D-tyrosine and D and L-tryptophan) and polycyclic aromatic hydrocarbons.⁷⁵ Most separation studies performed using aptamers have been ACE-based to determine the interaction of aptamers with their targets. The ease of labeling aptamers during synthesis allows generation of fluorescently-tagged aptamers for detection of analytes of interest or for real-time monitoring of targets in clinical samples.⁷⁶ In a competitive assay a fluorescently labeled DNA aptamer was used for quantifying human immunoglobulin E by ACE.⁷⁷

The goal of this research was to demonstrate the attributes of aptamers in various bioanalytical assays using a polymer-based microfluidic format and to evaluate the immobilization of aptamers for affinity-based methods using polymeric substrates. For example, in Chapter 2, the use of dye-labeled thrombin aptamers for the detection of thrombin in plasma by PMMA microchip capillary gel electrophoresis will be discussed. Aptamers have been used in affinity-based sandwich assays for electrochemical detection in biosensors. In Chapter 4, I will discuss the application of aptamers in dual-aptamer sandwich assays on PMMA substrate using fluorescence detection.

Recombinant DNA technology provides a means of producing relatively high amounts of low abundant biomarkers, such as membrane-bound proteins. This enables the creation of recombinant proteins in high purity and reasonable amounts that make them appropriate for the SELEX process to generate aptamers against these targets, which may serve as biomarkers for *in vitro* diagnostics. I will also show in this dissertation the cloning and expression of a hexahistidine tagged recombinant of the epithelial cell adhesion molecule (EpCAM), which is a membrane protein over-expressed in epithelial cells originating from adenocarcinomas.⁷⁸ I will demonstrate in Chapter 3, an extensive technique toward the production of this membrane-bound recombinant and its purification to greater than 99% purity through the use of immobilized metal

affinity chromatography with electro elution. This purified recombinant protein can thus be used as a target for SELEX to generate aptamers against the native protein, which currently do not exist (see Table 1.1).

1.5 References

- (1) Jayasena, S. D. *Clin. Chem.* **1999**, *45*, 1628-1650.
- (2) Kolher, G.; Milstein, C. *Nature* **1975**, *256*, 496-497.
- (3) Klussmann, S., Ed. *The Aptamer Handbook: Functional Oligonucleotides and Their Applications* Wiley-VCH: Weinheim, 2006.
- (4) Ellington, A. D.; Szostak, J. W. *Nature* **1990**, *346*, 818– 822.
- (5) Gottlieb, S.; Woodcock, J. *Nat. Biotechnol.* **2006**, *24*, 927-929.
- (6) Mann, D.; Reinemann, C.; Stoltenburg, R.; Strehlitz, B. *Biochem. Biophys. Res. Commun.* **2005**, *338*, 1928-1934.
- (7) Lee, Y. J.; Lee, S. W. *J. Microbiol. Biotechnol.* **2006**, *16*, 1149-1153.
- (8) Homann, M.; Goringe, H. U. *Nucleic Acids Res.* **1999**, *27*, 2006-2014.
- (9) Stoltenburg, R.; Reinemann, C.; Strehlitz, B. *Biomol. Eng* **2007**, *24*, 381-403.
- (10) Patel, D. J.; Suri, A. K.; Jiang, F.; Jiang, L. C.; Fan, P.; Kumar, R. A.; Nonin, S. *J. Mol. Biol.* **1997**, *272*, 645-664.
- (11) Hermann, T.; Patel, D. J. *Science* **2000**, *287*, 820-825.
- (12) Michaud, M.; Jourdan, E.; Villet, A.; Ravel, A.; Grosset, C.; Peyrin, E. *J. Am. Chem. Soc.* **2003**, *125*, 8672-8679.
- (13) Luzi, E.; Minunni, M.; Tombelli, S.; Mascini, M. *TrAC, Trends Anal. Chem.* **2003**, *22*, 810-818.
- (14) Mukhopadhyay, R. *Anal. Chem.* **2005**, *77*, 114a-118a.
- (15) Gold, L. *J. Biol. Chem.* **1995**, *270*, 13581-13584.
- (16) Gold, L.; Polisky, B.; Uhlenbeck, O.; Yarus, M. *Annu. Rev. Biochem.* **1995**, *64*, 763–797.
- (17) Tuerk, C.; Gold, L. *Science* **1990**, *249*, 505-510.
- (18) Moreno, M.; Rincon, E.; Pineiro, D.; Fernandez, G.; Domingo, A.; Jimenez-Ruiz, A.; Salinas, M.; Gonzalez, V. M. *Biochem. Biophys. Res. Commun.* **2003**, *308*, 214–218.
- (19) Ciesiolka, J.; Gorski, J.; Yarus, M. *RNA* **1995**, *1*, 538–550.

- (20) Hofmann, H. P.; Limmer, S.; Hornung, V.; Sprinzl, M. *Rna-a Publication of the Rna Society* **1997**, *3*, 1289-1300.
- (21) Jenison, R. D.; Gill, S. C.; Pardi, A.; Polisky, B. *Science* **1994**, *263*, 1425–1429.
- (22) Grate, D.; Wilson, C. *Bioorg. Med. Chem.* **2001**, *9*, 2565–2570.
- (23) Ellington, A. D.; Szostak, J. W. *Nature* **1992**, *355*, 850– 852.
- (24) Tang, J. J.; Xie, J. W.; Shao, N. S.; Yan, Y. *Electrophoresis* **2006**, *27*, 1303-1311.
- (25) Vianini, E.; Palumbo, M.; Gatto, B. *Bioorg. Med. Chem.* **2001**, *9*, 2543–2548.
- (26) Bock, L. C.; Griffin, L. C.; Latham, J. A.; Vermaas, E. H.; Toole, J. J. *Nature* **1992**, *355*, 564–566.
- (27) White, R.; Rusconi, C.; Scardino, E.; Wolberg, A.; Lawson, J.; Hoffman, M.; Sullenger, B. A. . *Mol. Ther.* **2001**, *4*, 567–574.
- (28) Liu, X. M.; Zhang, D. J.; Cao, G. J.; Yang, G.; Ding, H. M.; Liu, G.; Fan, M.; Shen, B. F.; Shao, N. S. . *J. Mol. Recognit.* **2003**, *16*, 23–27.
- (29) Mendonsa, S. D.; Bowser, M. T. *Anal. Chem.* **2004**, *76*, 5387-5392.
- (30) Green, L. S.; Jellinek, D.; Jenison, R.; Ostman, A.; Heldin, C. H.; Janjic, N. *Biochemistry* **1996**, *35*, 14413-14424.
- (31) Jellinek, D.; Green, L. S.; Bell, C.; Janjic, N. *Biochemistry* **1994**, *33*, 10450–10456.
- (32) Murphy, M. B.; Fuller, S. T.; Richardson, P. M.; Doyle, S. A. *Nucleic Acids Res.* **2003**, *31*.
- (33) Saito, T.; Tomida, M. *DNA Cell Biol.* **2005**, *24*, 624–633.
- (34) Hicke, B. J.; Watson, S. R.; Koenig, A.; Lynott, C. K.; Bargatze, R. F.; Chang, Y. F.; Ringquist, S.; Moon-McDermott, L.; Jennings, S.; Fitzwater, T.; Han, H. L.; Varki, N.; Albinana, I.; Willis, M. C.; Varki, A.; Parma, D. *J. Clin. Invest.* **1996**, *98*.
- (35) Dang, C.; Jayasena, S. D. *J. Mol. Biol.* **1996**, *264*, 268–278.
- (36) Proske, D.; Gilch, S.; Wopfner, F.; Schatzl, H. M.; Winnacker, E. L.; Famulok, M. *Chem. Biochemistry* **2002**, *3*, 717–725.
- (37) Jones, L. A.; Clancy, L. E.; Rawlinson, W. D.; White, P. A. *Antimicrobial Agents* **2006**, 3019–3027.
- (38) Ferreira, C. S. M.; Matthews, C. S.; Missailidis, S. *Tumor Biol.* **2006**, *27*, 289–301.
- (39) Hicke, B. J.; Marion, C.; Chang, Y. F.; Gould, T.; Lynott, C. K.; Parma, D.; Schmidt, P. G.; Warren, S. *J. Biol. Chem.* **2001**, *276*, 48644-48654.

- (40) Shangguan, D.; Li, Y.; Tang, Z. W.; Cao, Z. H. C.; Chen, H. W.; Mallikaratchy, P.; Sefah, K.; Yang, C. Y. J.; Tan, W. H. *Proc. Natl. Acad. Sci. U. S. A* **2006**, *103*, 11838-11843.
- (41) Switzer, C. Y.; Moroney, S. E.; Benner, S. A. *Biochemistry* **1993**, *32*, 10489-10496.
- (42) Marshall, K. A.; Ellington, A. D. *Methods Enzymol.* **2000**, *318*, 193-214.
- (43) Musheev, M. U.; Krylov, S. N. *Anal. Chim. Acta* **2006**, *564*, 91-96.
- (44) Pieken, W. A.; Olsen, D. B.; Benseler, F.; Aurup, H.; Eckstein, F. *Science* **1991**, *253*, 314-317.
- (45) Heidenreich, O.; Eckstein, F. *Biol. Chem. Hoppe-Seyler* **1991**, *372*, 673-673.
- (46) Eulberg, D.; Klusmann, S. *Chembiochem* **2003**, *4*, 979-983.
- (47) Klusmann, S.; Nolte, A.; Bald, R.; Erdmann, V. A.; Furste, J. P. *Nat. Biotechnol.* **1996**, *14*, 1112-1115.
- (48) Andreola, M. L.; Calmels, C.; Michel, J.; Toulme, J. J.; Litvak, S. *Eur. J. Biochem.* **2000**, *267*, 5032-5040.
- (49) Golden, M. C.; Collins, B. D.; Willis, M. C.; Koch, T. H. *J. Biotechnol* **2000**, *81*, 167-178.
- (50) Kwon, M.; Chun, S. M.; Jeong, S.; Yu, J. *Mol. Cells* **2001**, *11*, 303-311.
- (51) Lorsch, J. R.; Szostak, J. W. *Biochemistry* **1994**, *33*, 973-982.
- (52) Patel, D. J. *Curr. Opin. Chem. Biol.* **1997**, *1*, 32-46.
- (53) Kramer F. R.; Mills D.R.; Cole P.E.; Nishihara T.; S., S. *J. Mol. Biol.* **1974**, *89*, 719-736.
- (54) Gopinath, S. C. B. *Anal. Bioanal. Chem.* **2007**, *387*, 171-182.
- (55) Daniels, D. A.; Chen, H.; Hicke, B. J.; Swiderek, K. M.; Gold, L.; . *Proc. Natl. Acad. Sci. U. S. A* **2003**, *100* 15416-15421.
- (56) Liu, J. J.; Stormo, G. D. *Nucleic Acids Res.* **2005**, *33*, -.
- (57) Tombelli, S.; Minunni, A.; Mascini, A. *Biosensors & Bioelectronics* **2005**, *20*, 2424-2434.
- (58) Mosing, R. K.; Mendonsa, S. D.; Bowser, M. T. *Anal. Chem.* **2005**, *77*, 6107-6112.
- (59) Wu, L. H.; Curran, J. F. *Nucleic Acids Res.* **1999**, *27*, 1512-1516.
- (60) Collett, J. R.; Cho, E. J.; Ellington, A. D. *Methods* **2005**, *37*, 4-15.
- (61) Nimjee, S. M.; Rusconi, C. P.; Sullenger, B. A. *Annu. Rev. Med.* **2005**, *56*, 555-+.

- (62) FDA In 21; DHHS, Ed., 2007; Vol. 8.
- (63) Tucker, C. E.; Chen, L. S.; Judkins, M. B.; Farmer, J. A.; Gill, S. C.; Drolet, D. W. *J. Chromatogr., B: Anal. Technol. Biomed. Life Sci.* **1999**, *732*, 203-212.
- (64) Black, K. M.; Vats, N. *Analyst* **2007**, *132*, 1183-1185.
- (65) Gutman, S. *Clin. Chem.* **1999**, *45*, 746-749.
- (66) Heath, J. R.; Davis, M. E. *Annu. Rev. Med.* **2008**, *59*, 251-265.
- (67) Clark, S. L.; Remcho, V. T. *Electrophoresis* **2002**, *23*, 1335-1340.
- (68) Drabovich, A. P.; Berezovski, M.; Okhonin, V.; Sergey N. Krylov, S. N. *Anal. Chem.* **2006**, *78*, 3171-3178.
- (69) Heyduk, E.; Heyduk, T. *Anal. Chem.* **2005**, *77*, 1147-1156.
- (70) Kawakami, J.; Imanaka, H.; Yokota, Y.; Sugimoto, N. *J. Inorg. Biochem.* **2000**, *82*, 197-206.
- (71) Fukusaki, E.; Hasunuma, T.; Kajiyama, S.; Okazawa, A.; Itoh, T. J.; Kobayashi, A. *Biorg. Med. Chem. Lett.* **2001**, *11*, 2927-2930.
- (72) Cho, E. J.; Collett, J. R.; Szafranska, A. E.; Ellington, A. D. *Anal. Chim. Acta* **2006**, *564*, 82-90.
- (73) Tuerk, C.; Macdougall, S.; Gold, L. *Proc. Natl. Acad. Sci. U. S. A* **1992**, *89*, 6988-6992.
- (74) Deng, Q.; German, I.; Buchanan, D.; Kennedy, R. T. *Anal. Chem.* **2001**, *73*, 5415-5421.
- (75) Kotia, R. B.; Li, L. J.; MCGOWN, L. B. *Anal. Chem.* **2000**, *72*, 827-831.
- (76) Fischer, N.; Tarasow, T. M.; Tok, J. B. H. *Curr. Opin. Chem. Biol.* **2007**, *11*, 316-328.
- (77) German, I.; Buchanan, D. D.; Kennedy, R. T. *Anal. Chem.* **1998**, *70*, 4540-4545.
- (78) Seligson, D. B.; Pantuck, A. J.; Liu, X. L.; Huang, Y. D.; Horvath, S.; Bui, M. H. T.; Han, K. R.; Correa, A. J. L.; Eeva, M.; Tze, S.; Beldegrun, A. S.; Figlin, R. A. *Clinical Cancer Research* **2004**, *10*, 2659-2669.

Chapter 2 Poly(Methyl Methacrylate) Microchip Affinity Capillary Gel Electrophoresis of Aptamer-Protein Complexes for the Analysis of Thrombin in Plasma*

2.1 Introduction

Thrombin is a multi-functional serine protease that plays procoagulation and anticoagulation roles in hemostasis. As a procoagulant, thrombin activates factors V, VII and XI through a feedback mechanism and converts fibrinogen to fibrin during clot formation.^{1,2} Thrombin also regulates coagulation by binding to thrombomodulin to activate protein C.² Because of its importance in the maintenance of hemostatic balance, its level of generation in the blood can be greatly affected by the onset and progression of certain diseases.

In diseases marked by hypocoagulation, such as hemophilia A and B, which are characterized by the generation of low levels of factors VIII and IX, respectively,³ clotting time is prolonged leading to excessive bleeding due to lower levels of generated thrombin. The role of thrombin and prothrombin in proteolysis of microtubule associated tau protein in the brain has been studied as well and hypothesized to be important in the development of alzheimer's disease and Parkinsonism dementia of Guam.⁴ Hypercoagulation in thromboembolic diseases⁵⁻¹⁰, such as acute coronary syndromes in which intracoronary thrombus formation occurs in disrupted atherosclerotic plaque, is characterized by elevated levels of thrombin.

The aforementioned conditions and the need for tight regulation and reporting on thrombin levels in plasma creates the need for monitoring thrombin using a simple, robust but highly sensitive assay.¹¹⁻¹³ These assays can also be used for determining the effectiveness of therapeutic treatments, such as administering therapeutic drugs for the treatment of hemophilia¹⁴,¹⁵ or the use of heparins as anticoagulants after surgery or in thromboembolic disease treatment.^{16, 17}

Thrombin is responsible for its own non-linear generation, which occurs in two phases. The first phase results in nanomolar (*i.e.*, 10-30 nM) amounts of thrombin¹⁸ and represents the time within which clot formation occurs.² The second phase, the propagation phase, occurs with 96% of thrombin generated and is usually overlooked in some techniques for determining disorders in hemostasis. Average thrombin generation profiles reported for normal individuals show maximum thrombin levels between 200 nM and 800 nM.^{12, 18}

Current methods available for analyzing thrombin in blood include: Clotting-based assays¹⁹, which depend on the time it takes for fibrin formation; monitoring enzymatic activity of generated thrombin using a synthetic chromogenic^{20, 21} or fluorogenic substrate;²²⁻²⁴ immunoassays;^{25, 26} or capillary electrophoresis (CE) of hydrolytic products of thrombin's action on fibrinogen.²⁷ In clotting-based techniques, the time required for clot formation to occur in a sample is determined and compared to a clotting standard curve generated using different concentrations of thrombin. This technique addresses the initiation phase of thrombin generation since only 10 nM of thrombin is required for clot formation. Although clotting-based techniques are useful in identifying congenital abnormalities associated with hemophilia A, B and C and for evaluation of oral anticoagulant therapies, they overlook the propagation phase of thrombin generation.^{2, 5} The propagation phase provides information on the level of depression of thrombin generation and is most important in hemorrhagic syndromes.

Immunoassays for thrombin include enzyme-linked immunosorbent assays (ELISA) and western blotting for detecting thrombin-antithrombin III complex, fibrinopeptide A, prothrombin and factors such as factor V and platelet factor 4.^{22, 25} These antibody-based assays are typically very time consuming requiring assay turn-around-times as long as 24 h or more.

Thrombin assays based on enzymatic activity are very popular approaches for continuously monitoring the thrombin generation cycle using synthetic chromophore or fluorophore

conjugated oligopeptides as performed in the endogenous thrombin potential (EPT) test.^{15, 20, 24} This approach can be used in a microtitre plate format for large sample number processing and also with platelet-rich or poor samples through activation of coagulation by adding human replicated recombinant tissue factor in the presence of synthetic phospholipids.^{9, 23} Chromogenic assays require the utilization of defibrinated plasma samples in the analysis due to increased interference from the resulting turbidity when fibrinogen is added to the assay. Fluorogenic assays are more sensitive and allow for the use of smaller sample sizes compared to their chromogenic counterparts, however, there is no direct linear correlation between the fluorescence signal and thrombin activity.²⁸

Another technique for monitoring thrombin levels is capillary electrophoresis (CE) of fibrinopeptides with ultraviolet absorption detection.²⁷ CE provides highly efficient separations of a wide range of analytes in short development times due to the ability to use high electric field strengths without degrading separation performance. The capability of this technique to separate and simultaneously concentrate an analyte in a mixture for identification and quantification makes CE a valuable technique for the analysis of low levels of potential disease biomarkers.²⁹ In addition, CE can be used for real-time sample analysis due to its short development times³⁰. Various formats have been developed for CE including affinity capillary electrophoresis (ACE), which combines high affinity probes, such as antibodies or aptamers, with their respective binding partners.^{31, 32} ACE coupled to laser-induced fluorescence³³ detection enables the analysis of trace levels of analytes with high specificity.^{34, 35}

The affinity probe of choice for competitive and non-competitive formats of ACE separations has traditionally been antibodies due to their high specificity.³⁶ In the competitive format, the antigen or antibody is incorporated into the running buffer to maintain complexes formed at equilibrium. The non-competitive format, also known as non-equilibrium CE, is run without

addition of the affinity probe to the CE running buffer such that the equilibrium mixture of affinity probe and its target are analyzed under non-equilibrium conditions.^{37, 38} To permit LIF detection, the affinity probe can be fluorescently labeled to simplify the implementation of the assay. Unfortunately, most labeling chemistries for antibody-based affinity probes lead to non-uniformity in the number of dyes attached to the antibody,³⁶ with subsequent generation of multiple peaks during electrophoresis and difficulties with quantitation.

The development of aptamers as potential affinity probes can eliminate the problem associated with multiple labeling due to the ease and uniformity of dye incorporation during solid phase synthesis of the aptamers.^{31, 39} Aptamers are synthetic single-stranded oligonucleotides, obtained using random nucleotide libraries through Systematic Evolution of Ligands by Exponential enrichment (SELEX), with high binding specificity for their cognizant targets.⁴⁰ They are structurally more stable when compared to antibodies,³⁹ making them attractive alternatives to antibody-based probes for ACE.

Two DNA aptamers, HD1 and HD22, bind with high affinity to thrombin's exosites I and II, respectively, and have been used in various applications for thrombin analysis.^{40,41} ACE utilizing aptamers as affinity probes have been carried out using conventional capillary zone electrophoresis, CZE,⁴² for studying protein-DNA interactions and in some cases for quantifying this target.^{42, 43} Thrombin and its interaction with anti-thrombin III was studied by ACE with real-time monitoring of protein-protein interactions using fluorescently labeled HD1 aptamer.⁴³ In this study, protein-protein interactions were analyzed using CZE by adding polyethylene glycol (2%) to the running buffer in order to stabilize the aptamer-thrombin complex. In another study, Berezovski *et al.*³⁸ analyzed thrombin-HD1 complexes by non-equilibrium CZE to determine binding constants and unknown thrombin concentrations using calculated dissociation constants and dissociated peak areas from the electropherograms.³⁸

Implementation of various CE formats in microfluidic devices have been proposed for a number of applications and offers some attractive attributes, such as simplicity in its implementation, short development times for the electrophoresis, integration of front-end sample processing steps to the separation platform and potential real-time analysis capabilities. The use of polymers as the substrate material for microchip CE is particularly attractive due to the flexibility in the choice of micromanufacturing the devices, the ability to produce chips in a high production mode and at low-cost and the favorable optical properties of many polymeric material, such as poly(methyl methacrylate), PMMA.⁴⁴ In our laboratory, work has been reported on the effective utilization of polymeric microchips for many types of bio-separations.⁴⁵

In this report, we will discuss the use of microchip electrophoresis using PMMA substrates for the high resolution and rapid analysis of thrombin in plasma. Microchip CZE and microchip capillary gel electrophoresis⁴ were evaluated as possible modes to analyze thrombin using aptamers as affinity probes under non-equilibrium conditions. Characterization of the electrophoretic properties of thrombin in the presence of its DNA aptamers, HD1 and HD22, that were fluorescently labeled were compared to select and optimize the separation best suited for ACE analysis in terms of separation speed, resolving power and electrophoretic reproducibility.

2.2 Experimental

2.2.1 Reagents and Materials

Human alpha thrombin (MW=37,600 Da), thrombin inhibitor (FPRCK), prothrombin and human plasma were obtained from Haematologic Technologies Inc. (Essex Junction, VT). Poly(ethylene glycol), PEG, propionic acid disulfide was obtained from PolyPure (Oslo, Norway). Alexa Fluor 633 maleimide fluorescent dye was obtained from Invitrogen (Carlsbad, CA). Immobilized Tris (2-carboxyethyl) phosphine (TCEP) used in disulphide bond reduction was purchased from Pierce (Rockford, IA). Acrylamide (99%), N, N, N', N'-tetra-

methylethylenediamine (TEMED) and ammonium persulfate (APS) for linear polyacrylamide (LPA) preparation and Micro Bio-Spin® 6 chromatography columns were obtained from BioRad Laboratories (Hercules, CA). Alexa Fluor 647 labeled thrombin specific aptamers, HD1 and HD22, and unlabeled poly deoxythymidine (poly-dT), (5'Alexa 647 N/sp9/TTT GGT TGG TGT GGT TGG; 5'Alexa647 N/sp9/TAG TCC GTG GTA GGG CAG GTT GG GG TGA CT; and TTT TTT TTT TTT TTT TTT), were obtained from Integrated DNA Technologies (Coralville, IA). Rabbit blood citrate (Colorado Serum Co., Denver, CA) was used as a plasma source. Methyl hydroxyl ethyl cellulose (MHEC), Tris(hydroxyamino) methane (Tris) and glycine were from Sigma-Aldrich (St. Louis, MO). Nanopure water was obtained from a Barnstead Ultrapure water system (Barnstead/Thermolyne, Dubuque, IA) and was used in all buffer preparations and rinsing steps. PMMA sheets (4 mm thickness for microchip substrate and 0.125 mm thick cover slips) were obtained from GoodFellow (Berwyn, PA).

2.2.2 Thrombin Labeling Procedure

Human alpha thrombin was site-specifically labeled with Alexa Fluor 633 using peptidyl chloromethyl ketone inhibitor (FPRCK) as follows: An 87.3 μL aliquot of a 546 μM PEG ($n = 7$) acid disulphide was added to 113.7 μL of 100 mM MES (pH 6.0) containing 10 mg/mL 1-ethyl-3-[3-dimethylaminopropyl] carbodiimide, EDC, and 12 mg/mL N-hydroxysulfosuccinimide, NHS, and allowed to react for 15 min at room temperature. The PEG succinimidyl ester disulfide mixture was reacted with 9.5 μmol of FPRCK for 1.5 h at room temperature. A 30 μL aliquot of the crosslinker-inhibitor conjugate was treated with immobilized TCEP for 30 min to reduce the disulphide linkages and 200 μL containing 1 mg of Alexa Fluor 633 maleimide dye was added. This was allowed to react for 2 h at room temperature with excess ethylene diamine (0.1 μL) added to terminate the reaction. The dye-labeled inhibitor was filtered by centrifugation into a solution containing 1 mg of thrombin in HEPES buffer (pH 7.4). This was allowed to

react overnight at 4°C with shaking. Alexa Fluor 633-labeled thrombin was purified using desalting columns and analyzed by denaturing polyacrylamide gel electrophoresis. Labeled-thrombin used in the CE experiments was exchanged into the appropriate CE buffer using Micro Bio-Spin® 6 columns prior to the electrophoresis.

Buffers used for the electrophoresis and aptamer assays contained Tris (25 mM) and Glycine (19 mM) as the major constituents and adjusted to the required ionic strength and pH. Other components, such as methyl hydroxy ethylcellulose (MHEC) and LPA were added when needed. Linear polyacrylamides (LPAs) were synthesized by reacting 800 mg of acrylamide with 38 mg of APS and 12 μ L TEMED in a total volume of 20 mL of Tris-Glycine (TG) buffer. The reaction mixture was degassed by sonication for 10 min and incubated for 2 h at 60°C. The LPA produced was precipitated with 100% ethanol at 2.5 times its volume, centrifuged and the precipitate dried and re-suspended in twice its initial volume using a TG buffer.

2.2.3 Optimization of Aptamer Assay Conditions

Binding assays were prepared by incubating unlabeled thrombin with Alexa Fluor 647-labeled HD1 or HD22 aptamers in a TG or other CE running buffer. Incubation time was 1 h at room temperature but later reduced to 10 min when it was observed that binding saturation was achieved at the shorter incubation time. Fixed concentrations of aptamer (500 nM) were incubated with thrombin ranging from 10 nM to 500 nM concentrations for the CE analyses.

2.2.4 Microchip CE

Microchip CE was performed in single channel “simple T” PMMA microfluidic devices with all separations performed at room temperature. The devices were hot-embossed into 4 mm thick PMMA wafers using a micro-milled brass mold master.⁴⁶ All channels were 50 μ m wide and 50 μ m deep. A 10 mm injection cross was bisected 5 mm from one end of a 50 mm separation channel. Holes of 2 mm diameter were drilled at the ends of the channels to provide reservoirs

for the separation buffer, sample and waste. A 0.125 mm thick PMMA cover slip was thermally annealed to each embossed microchip at 107°C for 25 min after cleaning by sonication in detergent and nanopure water for 6 min followed by drying at 70°C for 30 min. In each series of experiments, three different PMMA microchips were selected to test assay reproducibility.

All buffers used for the microchip CE studies were filtered and degassed by sonication for 10 min prior to use. Microchip CZE (reverse mode – injection end cathodic and detection end anodic) of dye-labeled thrombin was performed using a 25 mM TG (pH 8.4) running buffer. Microchip CGE was accomplished with a TG buffer containing 0.01% MHEC (used to suppress the EOF and reduce non-specific adsorption) and LPA prepared with 2% acrylamide and buffered at pH 8.8. The microchips were rinsed for 2 min with 0.2 M NaOH followed by a nanopure water rinse for the initial use of a microchip device. For microchip CGE, the channel surfaces were pre-conditioned with 5 mg/mL MHEC in deionized water for 10 min and rinsed with TG buffer without LPA before filling the device with the CGE running buffer containing LPA. Microchip CGE was carried out in a reverse mode of operation (injection end cathodic and detection end anodic).

The electrophoresis equipment used in this work, consisting of four independently controlled high-voltage power supplies and a laser-induced fluorescence³³ detection system, was assembled in-house and has been reported previously.⁴⁵ Prior to injection, a positive voltage (0.2 kV) was applied to the sample reservoir for ~20 s while allowing the other three reservoirs to float. Sample was then injected by applying a positive voltage (0.3 kV) to the sample waste reservoir for the required length of time to allow sample to migrate into and fill the fixed volume injector. Separation was achieved by applying 1.5 kV to the separation waste reservoir (anode) and maintaining the sample and sample waste reservoirs at 11% and 10% of the applied voltage applied to the separation waste reservoir, respectively, and grounding the separation buffer

reservoir (cathode). Detection was carried out 2.3 cm from the injection point (effective separation length, $L_{\text{eff}} = 2.3$ cm) using LIF with an excitation wavelength of 632.8 nm supplied by a He-Neon laser. Individual samples of dye-labeled aptamers, HD1 and HD22, were diluted in the electrophoresis run buffer to a final concentration of 500 nM, while dye-labeled thrombin was buffer exchanged into TG buffer and diluted to 2 μM with either the microchip CZE or microchip CGE running buffer.

2.2.5 Standard Curve Generation

A fixed concentration of aptamer (500 nM) was pre-incubated with various concentrations of thrombin (10 – 500 nM) for 10 min at room temperature in the electrophoresis run buffer and analyzed by microchip CGE. Electropherogram peak areas for data analysis were integrated using Microcal Origin software (OriginLab Corp., Northampton, MA). The thrombin/aptamer complex electrophoretic peak areas were normalized by dividing the complex peak area by the combined peak areas of free aptamer and complex. These values were used in plotting standard curves. The equilibrium complex concentration at each thrombin level was obtained by multiplying the peak area fractions by the initial aptamer concentrations and plotted against the initial thrombin concentrations.

2.2.6 Analysis of Plasma Samples

Rabbit plasma was obtained by centrifuging citrated rabbit blood at 2500x for 20 min and decanting the plasma into clean tubes for storage at -20°C . Human and rabbit plasma, thawed and centrifuged, were diluted to 10, 25 and 50% in the electrophoresis run buffer and spiked with dye-labeled HD22 to a final concentration of 500 nM. Each sample was incubated at room temperature for 10 min with the aptamer solution (500 nM) and analyzed by microchip CGE. Prior to assay preparation, the plasma was either used without pretreatment or buffer exchanged into TG buffer containing 0.01% w/v MHEC. Later, unlabeled poly-dT was added to the diluted

plasma samples at a 3 μM final concentration to reduce non-specific interactions between dye-labeled HD22 and plasma components.

2.3 Results and Discussion

2.3.1 Optimization of Aptamer Assay Conditions

Various incubation times used for aptamer binding to thrombin in these non-equilibrium-based assays were evaluated and ranged between 10 min to 1 h. Metrics used to optimize the incubation time included the amount of complex formed and the resolution between the complex and free aptamer electrophoretic bands. Formation of the G quartet structure is facilitated by the presence of potassium cations and has been reported to enhance binding of HD1 and HD22 aptamers to thrombin.⁴⁷⁻⁴⁹ Addition of KCl salt up to 5 μM to the electrophoresis buffer resulted in a substantial increase in the current level, potentially leading to excessive Joule heating, which could affect electrophoresis performance in terms of plate numbers. Thus, in this study the incubation of the aptamers with thrombin was carried out in the absence of K^+ ions. The initial incubation time of aptamers with thrombin evaluated was 1 h and the electrophoretic peak area of the complex band was determined. However, it was found that a 10 min incubation time was adequate to maximize the number of thrombin/aptamer complexes based on the electrophoretic peak area of the complex. The average complex peak areas obtained for HD22 assays of 50 nM thrombin incubated at room temperature was 0.19 ± 0.03 for times ranging from 30 min to 1 h, while the 10 min incubation time gave an average peak area value of 0.20 ± 0.03 .

2.3.2 Microchip CZE

Most CE-based affinity assays reported to-date using aptamers as the affinity probe have employed free-solution capillary electrophoresis. There have been only a few reports in the literature using affinity capillary gel electrophoresis,⁵⁰⁻⁵² which can potentially provide higher resolution and efficiencies compared to CZE as well as stabilizing the aptamer/thrombin

complex when run under non-equilibrium conditions. Thus, in this study we were interested in comparing the performance of microchip CZE and microchip CGE for the analysis of thrombin using PMMA microdevices with aptamers as the affinity probes.

To understand the electrophoretic behavior of thrombin using PMMA as the electrophoresis substrate, dye-labeled thrombin was first analyzed by microchip CZE without the affinity probes. Figure 2.1a shows a representative electropherogram for the CZE/LIF analysis of dye-labeled thrombin only. At pH 8.4, the dye-labeled thrombin possessed a migration time of ~5 min ($L_{\text{eff}} = 2.5$ cm). Subsequent injections on the same device without pre-conditioning the separation channel resulted in no observable thrombin peak or a very broad peak appearing at ~1,000 s. The lack of reproducibility between CZE runs was most likely due to alterations in the electroosmotic flow (EOF) of the PMMA device due to adsorption artifacts. EOF determinations at pH 8.4 for unmodified PMMA devices and the electrophoretic mobility of the dye-labeled thrombin indicated that they were very similar in magnitude (see Table 2.1), thus leading to longer and irreproducible migration times for thrombin during microchip CZE, especially with slight changes in the magnitude of the EOF due to adsorption to the device wall. In fact, slight increases in the EOF can cause migration toward the cathode and as such, the thrombin would not be seen by the LIF detection point, which is located at the anodic end of the separation channel (reverse mode for electrophoresis).

We also found that attempts to reduce EOF and adsorption by dynamically coat the PMMA separation channel using MHEC or covalently coating amine terminated polyethylene glycol through EDC coupling in ultraviolet light activated PMMA channels for CZE did not dramatically improve the migration time reproducibility for the dye-labeled thrombin (data not shown). Thus, MHEC coating of microchannel walls was selected as the coating method of choice.

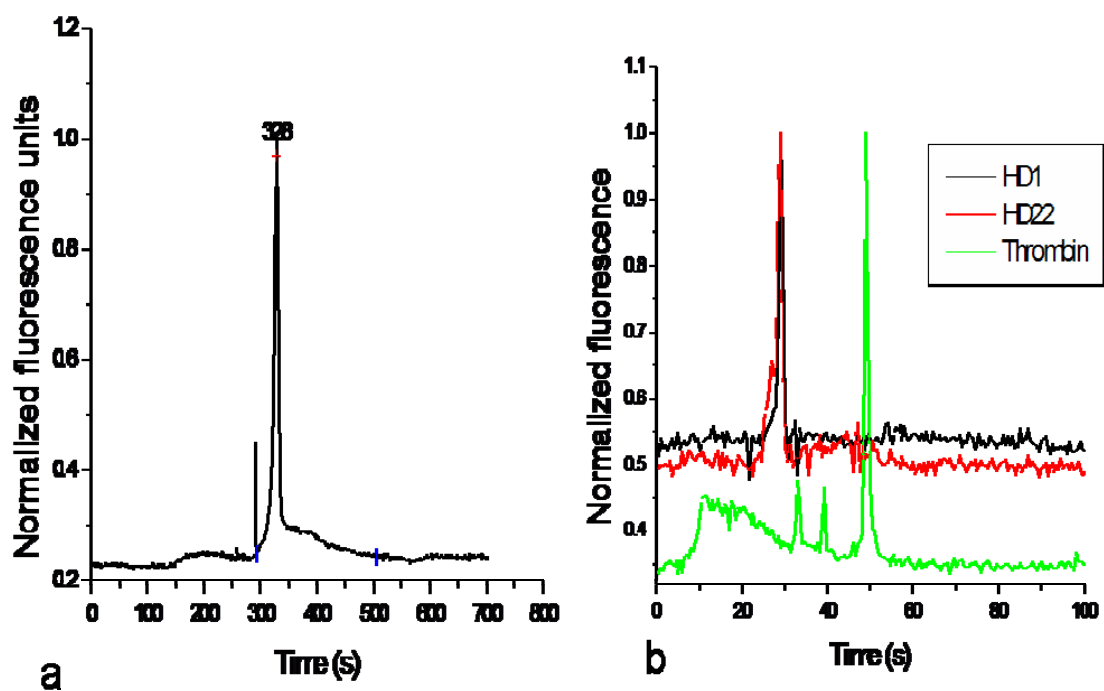


Figure 2. 1: Microchip CE traces of (A) Alexa Fluor 633-labeled thrombin run by microchip CZE in TG buffer at pH 8.4, $E = 300$ V/cm, and (B) HD1, HD22 and thrombin (all were labeled with Alexa Fluor 633) individually analyzed by microchip CGE in TG buffer (pH 8.8) with 2% LPA and $E = 300$ V/cm. Peaks appearing before the thrombin peak at less than 40 s in the CGE electropherogram were due to residual dye from purification of labeled thrombin. The detection was accomplished using laser induced fluorescence with a He-Neon laser (5 mW of laser power). For the microchip CGE case, the PMMA walls were conditioned with MHEC prior to the electrophoretic separation. All separations were performed in PMMA chips.

In order to provide better run-to-run reproducibility for the determination of thrombin, we investigated the use of microchip CGE since CGE analysis of proteins using low concentration sieving gels can provide high resolution and high migration time reproducibility.⁵³ Thus, microchip CGE conditions were employed to reduce the detrimental effects of the EOF by incorporating MHEC to be used as a dynamic coating for the channel walls and LPA added to the run buffer to serve as a sieving matrix for the affinity complexes and the uncomplexed components in the sample matrix. For the microchip CGE assays, LPA was prepared and diluted to about 2% total acrylamide.

Table 2.1: Microchip CGE and microchip CZE electrophoretic properties of thrombin, its aptamers and complexes formed in buffer or plasma. Symbols and abbreviations in this Table: Migration time, asymmetry factor (AF), resolution (Rs) and apparent electrophoretic mobility (μ_{app}) and electrophoretic mobility (μ_{ep}). The negative sign on μ_{app} , EOF or μ_{ep} represents directional movement from cathode to anode.

	Tm (s) (RSD)	AF	Plates (m ⁻¹)	Rs	Thrombin Concentration (nM) {SD}	μ_{app} (cm ² /V/s) (RSD)		μ_{ep} (cm ² /V/s) (RSD)
						CZE	CGE	CZE
Thrombin	49.2 (2.0)	1.4	4.57 x10 ⁵			-1.65 x10 ⁻⁵ (43)	-1.56 x10 ⁻⁴ (2.0)	-1.64 x 10 ⁻⁴ (4.2)
HD1	27.9 (7.5)	1.1	4.99 x10 ⁵				-2.67 x10 ⁻⁴ (3.6)	
HD22	29.1 (3.1)	1.0	4.20 x10 ⁵				-2.82 x10 ⁻⁴ (5.1)	
HD1/Thr	47.4 (6.9)	1.1	1.30 x10 ⁵	2.8			-1.59 x10 ⁻⁴ (2.1)	
HD22/Thr	46.1 (5.9)	1.3	2.52 x10 ⁵	2.7			-1.81 x10 ⁻⁴ (2.2)	
H. Plasma	52.1 (5.6)	1.8	1.20 x10 ⁵	1.8	543 {81.5}		-1.47 x10 ⁻⁴ (5.9)	
calibration plot equation					$y = 0.0038x + 0.0037$	$R^2 = 0.990$		
EOF (cm ² /V/s) (RSD)								1.81 x10 ⁻⁴ (7.2)

Figure 2.1b shows microchip CGE results of individually analyzed samples of fluorescently-labeled thrombin and the two dye-labeled aptamers. Addition of LPA to the buffer significantly enhanced the performance of the electrophoresis leading to highly reproducible migration times from repeated injections of the same sample loaded into the PMMA devices (RSD <10%, see Table 2.1). The aptamers exhibited faster migration rates with apparent mobilities (μ_{app}) of 2.67×10^{-4} and $2.82 \times 10^{-4} \text{ cm}^2 \text{ V}^{-1} \text{ s}^{-1}$ for HD1 and HD22, respectively, and higher plate numbers compared to thrombin (see Table 2.1). Thrombin displayed a 10-fold increase in μ_{app} for the microchip CGE format compared to microchip CZE due most likely to the diminished EOF value for the microchip CGE format. Peak asymmetry calculations⁵⁴ for individually analyzed thrombin and the aptamers showed peak tailing for thrombin and fronting for the

oligonucleotides, an indication that little interaction between aptamers and the channel walls occurred while thrombin adsorbed to some extent to the channels even after treatment with MHEC and addition of LPA to the run buffer.

Microchip CGE analysis of pre-incubated mixtures of the dye-labeled aptamers and unlabeled thrombin resulted in two well-resolved peaks, one for the free aptamer and the other for the thrombin/aptamer complex. Figure 2.2 shows electropherograms obtained for three different thrombin concentration (75, 250 and 500 nM) incubated with 500 nM HD1 (A) or HD22 (B). The resulting electrophoresis profiles differ from the reported traces observed in non-equilibrium CZE of aptamers and their targets, in which only a broad peak of the labeled aptamer was obtained due to complete dissociation of the complex during the electrophoresis.³⁸

The appearance of the complex peak for these non-equilibrium assays is a consequence of the presence of LPA in the electrophoresis run buffer, which provides a cage effect that can stabilize the protein/aptamer complexes during electrophoresis promoting re-association when in close proximity to dissociated aptamers and thrombin.⁵⁵⁻⁵⁸ Also, because of smaller diffusion constants in gels compared to free-solution,^{56, 57} dissociation may be greatly retarded during the short electrophoresis run times associated with the use of microchip CGE due to locally high relative concentrations of the ligands and target. The peaks obtained for the microchip CGE analysis were also reproducible from run-to-run and between devices (see Figure 2.3).

Resolution for the HD22 assay ranged from 3.0 to 1.6 with the resolution dependent upon the thrombin concentration with higher concentrations producing lower resolution between the complex peak and the free aptamer. However, the complex peak remained well-resolved from the free HD22 peak even at the highest thrombin concentration investigated (see Figure 2.2B).

The HD1-thrombin assays showed a similar trend as that of the HD22 assays. Resolution and plate numbers for both peaks decreased with increasing thrombin concentration. However, as the

thrombin concentration increased the free HD1 and complex peaks merged (Figure 2.2A) creating a region of dissociated complex as observed previously.³⁴

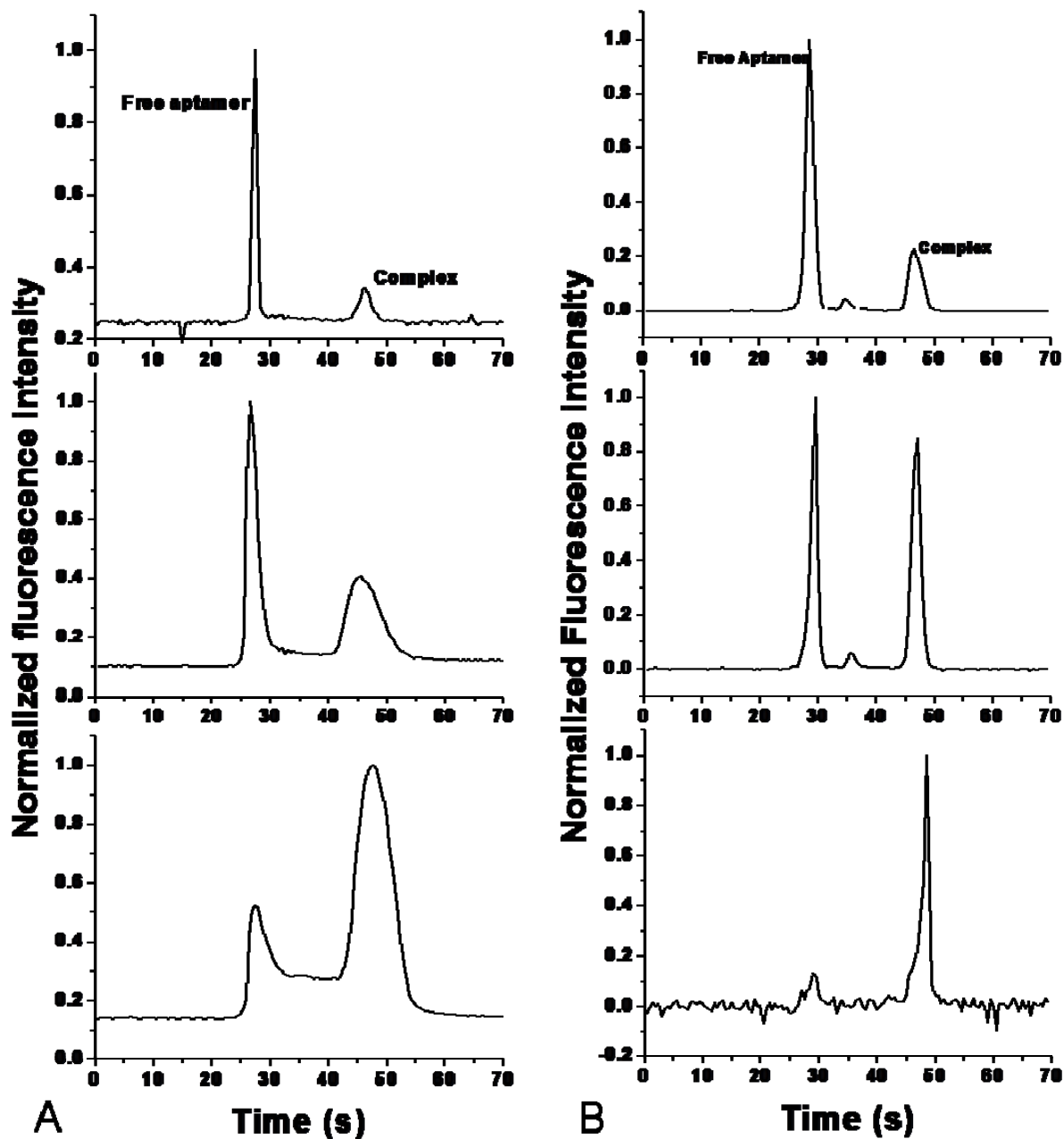


Figure 2.2: Electrophoresis traces of mixtures of 75, 250 and 500 nM unlabeled thrombin incubated with Alexa Fluor 647 labeled (A) HD1 and (B) HD22 showing the corresponding increases in complex peak areas with increasing thrombin concentrations (top to bottom). The electrophoresis run buffer consisted of TG buffer at pH 8.8 with 2% LPA gel with the microchip CGE performed using a field strength of 300 V/cm. Electrophoresis conditions were similar to those described in Figure 2.1B.

This region between the peaks would complicate peak area calculations for the complex for generating a standard curve for thrombin. Thus, HD22 was selected for determining the level of thrombin in real samples due to the fact that the free aptamer and complex peaks were well-resolved irrespective of thrombin concentration. The better resolution for the HD22 assays compared to HD1 is a direct result of the higher complex thermodynamic stability of the HD22 aptamer to thrombin compared to HD1.

To check the extent of variation in electrophoretic characteristics of aptamers and complex from run-to-run and device-to-device, three devices molded from the same batch of PMMA were compared. Migration times were reproducible with variation below 10% RSD from device-to-device and run-to-run (Table 2.1). It was also observed that the level of variation in the normalized peak area between runs and from device-to-device reduced with increasing thrombin concentration, especially above 150 nM for the HD22 assays.

2.3.4 Standard Curve Generation

To show the trend in amount of complex produced as the ratio of aptamer-to-thrombin was varied by increasing the thrombin concentration, normalized complex peak areas were plotted for different concentrations of unlabeled thrombin used in assays with HD1 and HD22 (see Figure 2.3). No complexes were observed for HD1 assays below 50 nM initial thrombin concentration, whereas complex peaks could be obtained for the HD22 assay down to 10 nM of thrombin. Results showed a linear increase in complex peak area formed with increasing thrombin concentration (see Figure 2.3) up to 150 nM for both the HD1 and HD22 assays ($R^2 = 0.990$). The limit of detection, taken as the lowest thrombin concentration for which a complex peak was produced following electrophoresis, for the HD1 assay was 50 nM while that for HD22 assay was 10 nM. The difference in detection limits reflects the difference in affinity constants of the aptamers for thrombin.

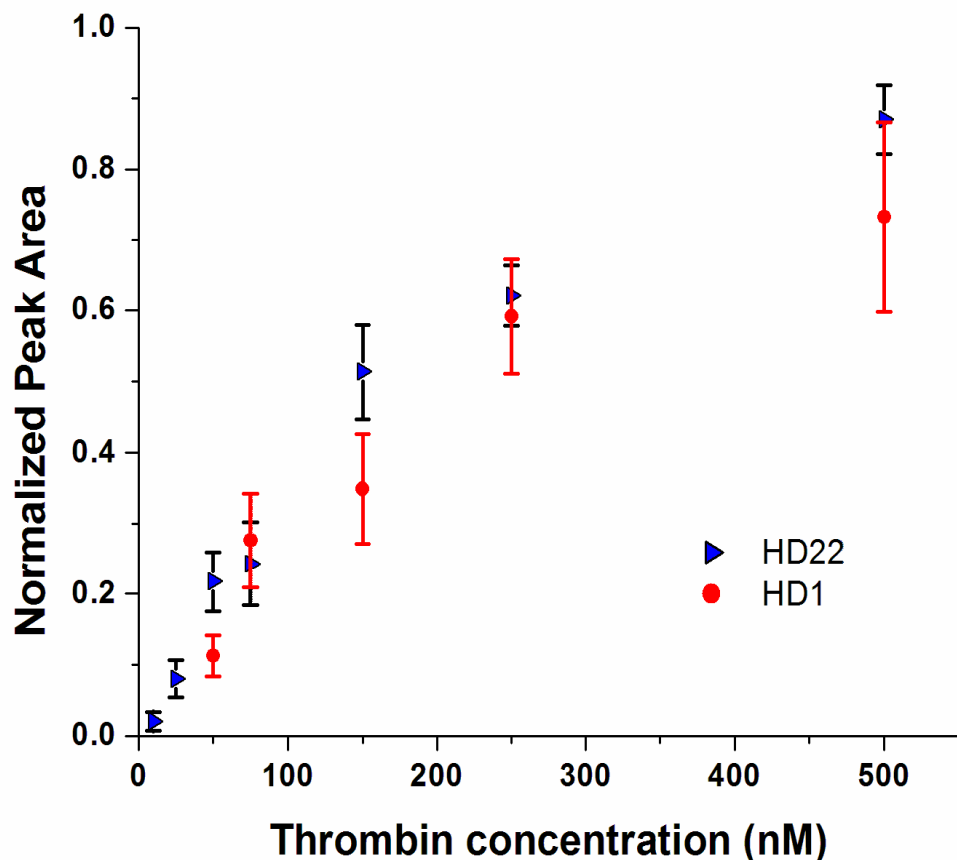


Figure 2.3: Variation of the amount of affinity complex produced with increasing unlabeled thrombin concentration for assays with HD1 (red circle plot) and HD22 (black square plot), both labeled with Alexa Fluor 647, in terms of average normalized complex peak areas obtained for the analyses carried out using three different PMMA microchips. The assays were performed using PMMA microchip CGE with LIF detection.

HD22 has a lower dissociation constant ($K_D = 0.5 \text{ nM}$) compared to HD1 with a reported dissociation constant (K_D) of 24 nM ⁴¹. Due to the higher stability of the HD22/thrombin complex and its more favorable electrophoretic performance compared to HD1, the remaining studies used HD22 as the affinity probe.

2.3.5 Analysis of Plasma Samples

Quantitation of analytes in real samples such as blood presents several problems, which are usually addressed with different sample preparation techniques. Whole blood consists of

different components with diverse solubility properties that can affect the analytical method of choice. The ionic strength of blood can increase Joule heating during electrophoresis, while the presence of cells, carrier proteins such as albumin, and lipoproteins lead to increased protein adsorption to the separation channel walls. To overcome some of these obstacles, plasma can be used for these assays. Prothrombin, the inactive form of thrombin, is present in circulating blood. To evaluate the potential of prothrombin interference in plasma giving rise to false positive results, 100 nM prothrombin was pre-incubated with HD22 in the electrophoresis run buffer and was analyzed by microchip CGE. We observed no complex peak using microchip CGE (see Figure 2.4A) indicating that the affinity probe would not bind to prothrombin. Assay conditions were optimized using plasma from citrate treated rabbit blood. The plasma samples were tested at 10, 25 and 50% v/v in the electrophoresis run buffer. After removal of excess salt by transferring the protein components into TG buffer using Microbio-Spin® 6 columns, microchip CGE analysis was carried out with LIF detection. Plasma treated only by diluting in the electrophoresis buffer produced an increase in current above 50 μ A even at 10% dilution due to a higher sample ionic strength. After exchanging the plasma into TG buffer, the main problem faced was adsorption of protein to the channel walls and association of the labeled aptamer with carrier proteins in the sample. This caused an increase in background fluorescence resulting in no electrophoretic peak for the thrombin/HD22 complex.

Studies carried out on aptamers have reported the use of excess non-specific oligonucleotides as competitors to enhance aptamer selectivity.⁵⁹ This technique was thus employed in an attempt to minimize non-specific interaction between plasma components and HD22. Unlabeled poly-dT at 3 μ M was added to the plasma prior to adding the HD22 reagent. This allowed formation of a free aptamer peak and a complex peak during electrophoresis (see Figures 2.4B, C and D). The plasma samples were again tested at 10, 25 and 50% levels. The

10% plasma dilution enabled repeated injections of the same sample load while 25% plasma dilution could only be injected once after which the microchip had to be thoroughly cleaned due to highly irreproducible electrophoretic results. Electropherograms could not be generated for a 50% plasma sample due to increased current and poor peak shape and in some cases, the absence of the target complex peak. A slight shift in the migration time of the HD22/thrombin complex occurred for the plasma samples compared to the control samples most likely due to interaction of thrombin with components of hemolyzed blood.

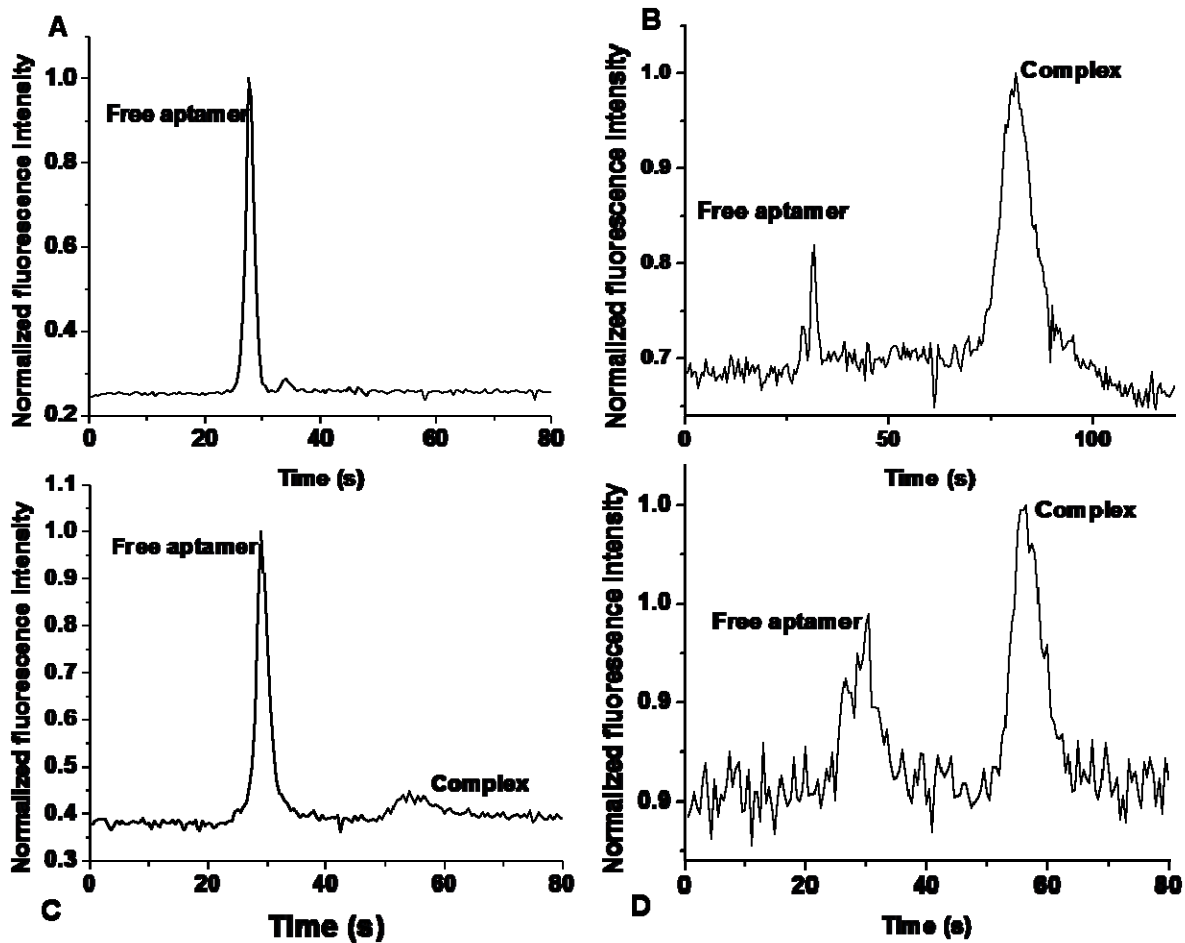


Figure 2. 4: Representative microchip CGE traces for HD22 assays in TG buffer (pH 8.8 E = 300V/ cm) for (A) 100 nM prothrombin analysis in buffer and (B) 25% rabbit plasma, (C) 10% and (D) 25% human plasma samples. Plasma samples were desalted and buffer exchanged into CGE buffer without LPA prior to dilution and microchip CGE analysis.

Based on the results obtained from rabbit plasma, human plasma was also analyzed for the presence of thrombin using affinity microchip CGE and the HD22 aptamer affinity probe. Ten and 25% dilutions of buffer exchanged plasma were analyzed with 500 nM HD22 (see Figures 4C and 4D). Microchip CGE results indicated the presence of thrombin at an average concentration of 543 ± 81.5 nM (see Table 2.1). This falls within the generated thrombin concentration range found in the literature.¹² The time required for sample preparation and analysis by this microchip CGE technique was relatively short (approximately 14 min for sample preparation and 2 min for microchip CGE).

2.4 Conclusion

We have demonstrated the use of PMMA microfluidic devices for conducting rapid affinity microchip CGE of a target protein using aptamers as the affinity probes with an electrophoresis development time of <2 min. For these microchip CGE assays, non-equilibrium conditions were used to allow for the sensitive LIF detection of thrombin without requiring fluorescence labeling of the target. Migration times were reproducible for thrombin complexes and free aptamers in CGE buffer with device-to-device RSD variations below 10%. By removing salts from plasma and adding an unlabeled random sequence oligonucleotide to the plasma, thrombin was detected in rabbit and human plasma. This method can be easily adapted for high throughput screening of plasma samples in a polymeric microchip device designed with multiple channels for analyzing several samples in parallel. Work is currently underway in our lab to develop detection systems for use with high throughput polymeric microchips for use with assays requiring high throughput screening capabilities.

2.5 References

- (1) Chen, Y. T., Weidong; Lu, Xiaofeng; Lu, Yanrong ; Qin, Shengfang ; Li, Shengfu ; Zeng, Yangzhi ; Bu, Hong ; Li, Youping ; Cheng, Jingqiu *Blood cells, Mol. Dis.* **2007**, *38*, 93-99.

- (2) Mann, K. G.; Brummel, K.; Butenas, S. *J.Thromb. Haemost.* **2003**, *1*, 1504-1514.
- (3) Matsumoto, T.; Shima, M.; Takeyama, M.; Yoshida, K.; Tanaka, I.; Sakurai, Y.; Giles, A. R.; Yoshioka, A. *J.Thromb. Haemost.* **2006**, *4*, 377-384.
- (4) Aria, T. M., Judith; Klegeris, Andis; McGeer, Patrick L. *J. Neuropathol Exp. Neurol.* **2006**, *65*, 19-25.
- (5) Serruys, P. W.; Vranckx, P.; Allikmets, K. *Int. J. Clin. Pract.* **2006**, *60*, 344-350.
- (6) Ireland, H.; Konstantoulas, C. J.; Cooper, J. A.; Hawe, E.; Humphries, S. E.; Mather, H.; Goodall, A. H.; Hogwood, J.; Juhan-Vague, I.; Yudkin, J. S.; di Minno, G.; Margaglione, M.; Hamsten, A.; Miller, G. J.; Bauer, K. A.; Kim, Y. T.; Stearns-Kurosawa, D. J.; Kurosawa, S. *Atherosclerosis* **2005**, *183*, 283-292.
- (7) Hemker, H. C.; Beguin, S. *Thromb. Haemost.* **1995**, *74*, 1388-1388.
- (8) Yngen, M.; Ostenson, C. G.; Li, N.; Hjemdahl, P.; Wallen, N. H. *Blood Coagul. Fibrinolysis* **2001**, *12*, 109-116.
- (9) Tripodi, A.; Primignani, M.; Chantarangkul, V.; Clerici, M.; Dell'Era, A.; Fabris, F.; Salerno, F.; Mannucci, P. M. *Hepatology* **2006**, *44*, 440-445.
- (10) Cohen, Z.; Gonzales, R. F.; Davis-Gorman, G. F.; Copeland, J. G.; McDonagh, P. F. *Thromb. Res.* **2002**, *107*, 217-221.
- (11) Hemker, H. C.; Al Dieri, R.; Beguin, S. *Curr. Opin. Hematol.* **2004**, *11*, 170-175.
- (12) Brummel-Ziedins, K. E.; Vossen, C. Y.; Butenas, S.; Mann, K. G.; Rosendaal, F. R. *J.Thromb. Haemost.* **2005**, *3*, 2497-2505.
- (13) Brummel-Ziedins, K. E.; Pouliot, R. L.; Mann, K. G. *J.Thromb. Haemost.* **2004**, *2*, 281-288.
- (14) Giansily-Blaizot, M.; Al Dieri, R.; Schved, J. F. *Pathophysiol. Haemost. Thromb.* **2003**, *33*, 36-42.
- (15) Varadi, K.; Turecek, P. L.; Schwarz, H. P. *Haemophilia* **2004**, *10*, 17-21.
- (16) Schwienhorst, A. *Cell. Mol. Life Sci.* **2006**, *63*, 2773-2791.
- (17) Paoli, G.; Merlini, P. A.; Ardissino, D. *Curr. Pharma. Design* **2005**, *11*, 3919-3929.
- (18) Brummel-Ziedins, K.; Vossen, C. Y.; Rosendaal, F. R.; Umezaki, K.; Mann, K. G. *J.Thromb. Haemost.* **2005**, *3*, 1472-1481.
- (19) Macfarlane, R. G.; Biggs, R. *J. Clin Pathol.* **1953**, *6*, 3-8.

- (20) Paulssen, M. M. P.; Kolhorn, A.; Rothuizen, J.; Planje, M. C. *Clin. Chim. Acta* **1979**, *92*, 465-468.
- (21) Pathak, A.; Zhao, R.; Monroe, D. M.; Roberts, H. R.; Sheridan, B. C.; Selzman, C. H.; Stouffer, G. A. *J.Thromb. Haemost.* **2006**, *4*, 60-67.
- (22) Luddington, R.; Baglin, T. *J.Thromb. Haemost.* **2004**, *2*, 1954-1959.
- (23) Wielders, S. J. H.; Beguin, S.; Hemker, H. C.; Lindhout, T. *Arterioscler. Thromb. Vasc. Biol.* **2004**, *24*, 1138-1142.
- (24) Kessels, H.; Willems, G.; Hemker, H. C. *Comput. Biol. Med.* **1994**, *24*, 277-288.
- (25) Rand, M. D.; Lock, J. B.; vantVeer, C.; Gaffney, D. P.; Mann, K. G. *Blood* **1996**, *88*, 3432-3445.
- (26) Shuman, M. A.; Majerus, P. W. *J. Clin. Invest.* **1976**, *58*, 1249-1258.
- (27) Profumo, A.; Cardinali, B.; Cuniberti, C.; Rocco, M. *Electrophoresis* **2005**, *26*, 600-609.
- (28) Hron, G.; Kollars, M.; Binder, B. R.; Eichinger, S.; Kyrle, P. A. *J. Am. Med. Assoc.* **2006**, *296*, 397-402.
- (29) Fliser, D.; Wittke, S.; Mischak, H. *Electrophoresis* **2005**, *26*, 2708-2716.
- (30) Shadpour, H.; Hupert, M. L.; Patterson, D.; Liu, C. G.; Galloway, M.; Stryjewski, W.; Goettert, J.; Soper, S. A. *Anal. Chem.* **2007**, *79*, 870-878.
- (31) Ravelet, C.; Grosset, C.; Peyrin, E. *J. Chromatogr. A* **2006**, *1117*, 1-10.
- (32) Fraga, M. F.; Ballestar, E.; Esteller, M. *J. Chromatogr. B: Anal. Technol. Biomed. Life Sci.* **2003**, *789*, 431-435.
- (33) Dwarki, V. J.; Belloni, P.; Nijjar, T.; Smith, J.; Couto, L.; Rabier, M.; Clift, S.; Berns, A.; Cohen, L. K. *Proc. Natl. Acad. Sci. U. S. A* **1995**, *92*, 1023-1027.
- (34) Buchanan, D. D.; Jameson, E. E.; Perlette, J.; Malik, A.; Kennedy, R. T. *Electrophoresis* **2003**, *24*, 1375-1382.
- (35) Schultz, N. M.; Kennedy, R. T. *Anal. Chem.* **1993**, *65*, 3161-3165.
- (36) Yang, W. C.; Schmerr, M. J.; Jackman, R.; Bodemer, W.; Yeung, E. S. *Anal. Chem.* **2005**, *77*, 4489-4494.
- (37) Krylov, S. N.; Berezovski, M. *Analyst* **2003**, *128*, 571-575.
- (38) Berezovski, M.; Nutiu, R.; Li, Y. F.; Krylov, S. N. *Anal. Chem.* **2003**, *75*, 1382-1386.

- (39) Jayasena, S. D. *Clin. Chem.* **1999**, *45*, 1628-1650.
- (40) Bock, L. C.; Griffin, L. C.; Latham, J. A.; Vermaas, E. H.; Toole, J. J. *Nature* **1992**, *355*, 564-566.
- (41) Tasset, D. M.; Kubik, M. F.; Steiner, W. *J. Mol. Biol.* **1997**, *272*, 688-698.
- (42) German, I.; Buchanan, D. D.; Kennedy, R. T. *Anal. Chem.* **1998**, *70*, 4540-4545.
- (43) Huang, C. C.; Cao, Z. H.; Chang, H. T.; Tan, W. H. *Anal. Chem.* **2004**, *76*, 6973-6981.
- (44) Soper, S. A.; Henry, A. C.; Vaidya, B.; Galloway, M.; Wabuyele, M.; McCarley, R. L. *Anal. Chim. Acta* **2002**, *470*, 87-99.
- (45) Shadpour, H.; Musyimi, H.; Chen, J. F.; Soper, S. A. *J. Chromatogr. A* **2006**, *1111*, 238-251.
- (46) Hupert, M. L.; Guy, W. J.; Llopis, S. D.; Shadpour, H.; Rani, S.; Nikitopoulos, D. E.; Soper, S. A. *Microfluid Nanofluid* **2007**, *3*, 1-11.
- (47) Smirnov, I.; Shafer, R. H. *Biochemistry* **2000**, *39*, 1462-1468.
- (48) Vairamani, M.; Gross, M. L. *J. Am. Chem. Soc.* **2003**, *125*, 42-43.
- (49) Kankia, B. I.; Marky, L. A. *J. Am. Chem. Soc.* **2001**, *123*, 10799-10804.
- (50) Wu, D.; Regnier, F. E. *Anal. Chem.* **1993**, *65*, 2029-2035.
- (51) Xian, J.; Harrington, M. G.; Davidson, E. H. *Proc. Natl. Acad. Sci. U. S. A* **1996**, *93*, 86-90.
- (52) Lausch, R.; Scheper, T.; Reif, O. W.; Schlosser, J.; Fleischer, J.; Freitag, R. *J. Chromatogr. A* **1993**, *654*, 190-195.
- (53) Nagata, H.; Tabuchi, M.; Hirano, K.; Baba, Y. *Electrophoresis* **2005**, *26*, 2687-2691.
- (54) Shadpour, H.; Soper, S. A. *Anal. Chem.* **2006**, *78*, 3519-3527.
- (55) Cann, J. R. *J. Biol. Chem.* **1989**, *264*, 17032-17040.
- (56) Svingen, R.; Takahashi, M.; Akerman, B. *J. Phys. Chem. B* **2001**, *105*, 12879-12893.
- (57) Cann, J. R. *Electrophoresis* **1998**, *19*, 127-141.
- (58) Fried, M. G.; Bromberg, J. L. *Electrophoresis* **1997**, *18*, 6-11.
- (59) Roulet, E.; Busso, S.; Camargo, A. A.; Simpson, A. J. G.; Mermoud, N.; Bucher, P. *Nat. Biotechnol.* **2002**, *20*, 831-835.

- (60) Shieh, P. C. H.; Hoang, D.; Guttman, A.; Cooke, N. *J. Chromatogr. A* **1994**, *676*, 219-226.

Chapter 3. Investigating the Expression of Recombinant EpCAM in Bacteria and Mammalian Cells and the Development of a Selective Tandem IMAC/ Electro Elution Purification Protocol for Histidine-Tagged Recombinant Proteins in Mammalian Cells

3.1 Introduction

Affinity-based bioanalytical techniques play a pivotal role in disease diagnosis and prognosis due to the high target specificity and selectivity afforded by the affinity agents used in these methods. Forty percent of eukaryotic cell proteins, which often times are used as biomarkers in diagnostic assays, are membrane-bound. These proteins can also serve as effective targets for drug development and antibody generation in disease treatment and diagnosis.¹ However, the need exists for obtaining the target proteins in a highly abundant and purified form in their native states to ensure recognition of the native target in complex environments by the affinity agent when used for affinity probe selection or designing and testing the biomolecular assay.

In many affinity-based techniques, the common and commercially available molecular recognition element used has been antibodies either monoclonal or polyclonal.² Recently, alternative recognition probes are becoming popular, such as aptamers or peptoids due to their ease of synthetic production, favorable chemical stabilities and good biochemical compatibilities.³⁻⁵ Unfortunately, few aptamer/peptoid probes are available for the large number of molecular/cellular targets used in many diagnostic assays.⁶ Therefore, to expand the library of aptamer/peptoid probes available for molecular recognition, large amounts of high purified target surrogates will be required for probe selection.

Recombinant DNA technology (RDT) allows for the production of protein targets through manipulation of the complementary deoxyribonucleic acid (cDNA) generated from the proteins

of interest through, for example, incorporation of fusion tags to meet protein production and purification requirements of researchers.^{7,8}

Recombinant protein expression consists of three components: a gene of interest, a vector for gene transfer into the appropriate host and the host for protein expression.⁹ Figure 3.1 shows a schematic of the cloning and expression process.

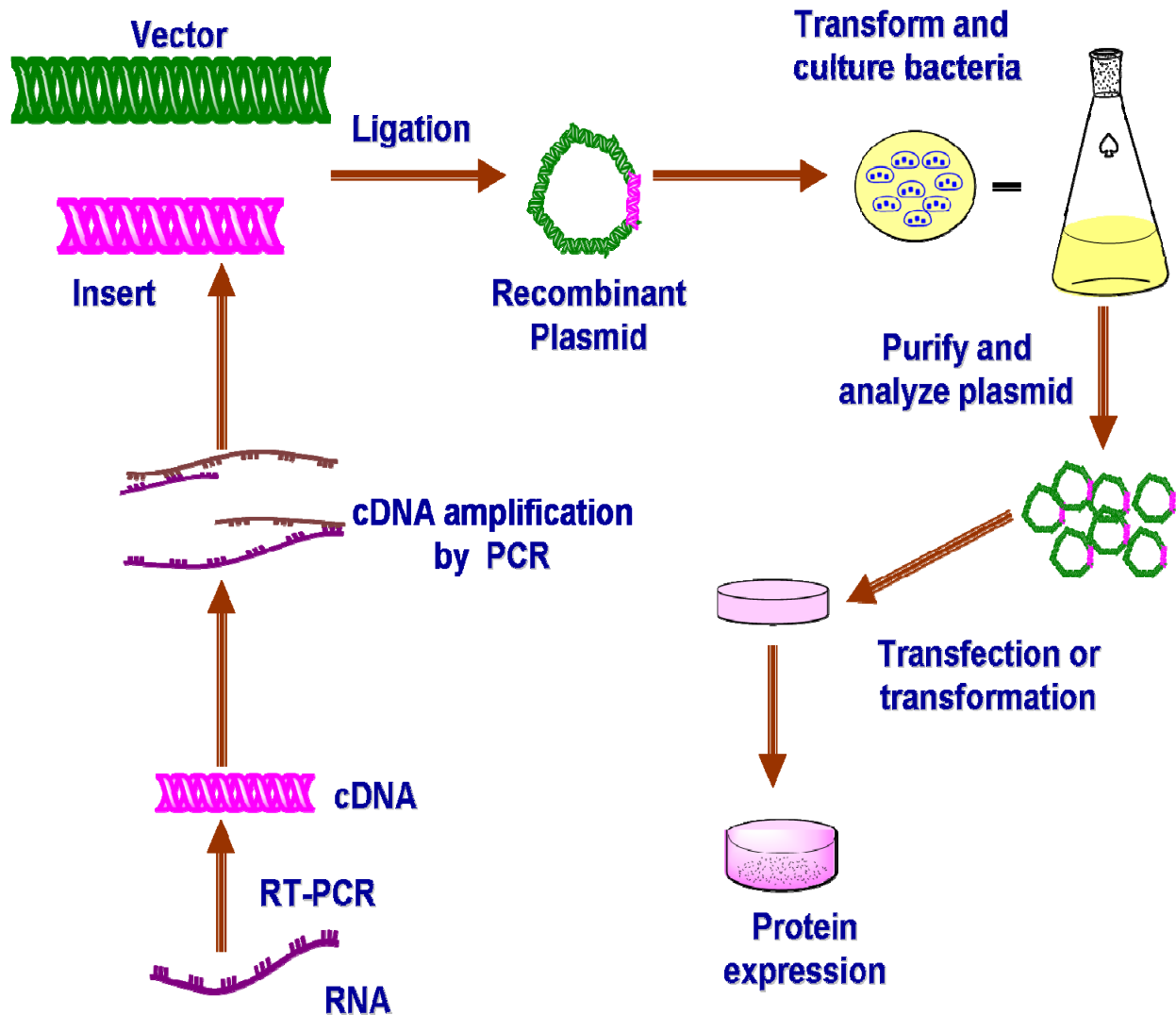


Figure 3.1 A schematic of the molecular cloning process. RNA extracted from an over-expressing source of the protein biomarker is reverse transcribed to the cDNA of the target. After PCR amplification the cDNA insert is enzymatically incorporated into the vector with subsequent transformation of bacteria with the recombinant vector. The recombinant vector containing the gene of interest is amplified by culturing the transformed bacteria in the presence of antibiotic and purified for transfection of eukaryotic hosts or transformation of bacteria for protein expression.

Starting with RNA extracted from a source that over-expresses the protein of interest, reverse-transcription is performed to obtain the cDNA. The cDNA thus obtained is amplified by polymerase chain reaction (PCR) and ligated into a vector, such as a plasmid. The recombinant plasmid is amplified in bacteria by inducing uptake of the plasmid by the bacteria strain of choice, a process referred to as transformation. The transformed bacteria is cultured in the presence of an antibiotic to which a resistance gene exists in the vector to enable selective growth of only bacterial cells containing the recombinant plasmid. The amplified plasmid is purified and used in the transfection of eukaryotic hosts or bacteria transformation for protein expression (see Figure 3.1).¹⁰

A wide variety of vectors are available for rapid and high throughput cloning of protein biomarkers in prokaryotic, eukaryotic and cell-free systems.¹¹ Integral membrane proteins (IMPs) are physiologically responsible for interfacing extracellular biochemical activities with intracellular ones.¹² They are implicated in various diseases and thus, approximately 50% of all drug targets are G-protein coupled receptors.¹²⁻¹⁴ However, a major setback to structural determination studies on eukaryotic IMPs is the expression and purification of sufficient amounts of homogeneous protein. The complexity of eukaryotic IMPs presents problems with their expression in prokaryotic systems.¹⁴ Thus, most eukaryotic IMP recombinants are expressed in eukaryotes, such as insect and mammalian hosts in spite of the lower yields.¹³ Currently, approximately 60-70% of all recombinant protein pharmaceuticals are produced in mammalian cells, the most commonly used being the Chinese hamster ovary cells, due to the possession of organelles that allow post translational modification of proteins to generate them in their native conformations.^{7, 15, 16}

An important aspect of recombinant protein production requiring detailed planning to ensure very high levels of yield and purity while maintaining the protein's structural properties is

the purification process. To this end affinity purification techniques involving the use of antibodies or other affinity agents play a very important role in recombinant protein production. A widely used affinity method is the immobilized metal affinity chromatographic (IMAC) technique for purification of histidine tagged recombinant proteins from cell lysates and growth media either in conjunction with other purification methods or as a one-step procedure with protein yields >95%.¹⁷⁻²¹

Unfortunately, eukaryotic cells have higher contents of cysteine and histidine compared to prokaryotes which bind to metal ions when exposed in clusters on protein surfaces under native conditions.^{22, 23} This leads to interference with IMAC purification of recombinant proteins from the expression hosts. Thus, to ensure high levels of protein purity, the IMAC technique can be used in conjunction with other purification techniques to remove co-eluting impurities. Electrophoresis has become an invaluable tool for protein analysis and purification.²⁴ An electrophoretic method commonly employed as an extraction technique for isolating protein bands from electrophoresis gels is electro elution. This purification and extraction method enables researchers to obtain highly purified biomolecules, such as proteins, in native form with yields ranging between 80 - 100%.²⁴ Electro elution, carried out either in static or continuous mode, has proven useful in the recovery of recombinant proteins from cell lysates. The technique has been employed in the continuous format for single-step purification of recombinant proteins from bacterial expression systems and inclusion bodies.²⁵⁻²⁷ Electro elution has also been used as a second purification step in, for example, the purification of tristetraprolin from an enzyme digest of an affinity purified recombinant fusion protein.²⁸

By coupling affinity chromatography with electro elution, electrophoretically pure histidine-tagged recombinant proteins expressed in eukaryotic systems may be obtained in native conformation for further downstream processes.²⁹ The technique is also adaptable to

microfluidic systems for simultaneous and high throughput processing of several protein biomarkers due to the ease of miniaturization of electrophoretic processes and chemical modification of polymeric substrates for immobilization purposes.¹

To study the cloning and expression characteristics in various expression systems and to develop a purification protocol for laboratory-scale production of integral membrane proteins, we chose the epithelial cell adhesion molecule (EpCAM), a 40 kilodalton transmembrane protein over expressed in breast cancer and other carcinomas, as our model.^{30,31} In this study we cloned EpCAM as a hexahistidine-tagged fusion protein in two different vectors for expression in mammalian and bacterial cells to optimize its expression for purification. A purification protocol based on tandem IMAC with electrophoresis and electro elution to obtain a pure and correctly folded protein as determined by western blot and sodium dodecyl sulphate polyacrylamide gel electrophoresis (SDS-PAGE) was developed.

3.2 Experimental

3.2.1 Cell Lines

Breast carcinoma cell lines MCF7 (HTB), Hs578T used for total RNA extraction and western blots of EpCAM, baby hamster kidney (BHK) cell line, cervical cancer cell line (Hep2), and Cos 7 cell line used in cloning and expression of recombinant EpCAM were obtained from the American Type Culture Collection (Manassas, VA). Cells were stored in liquid nitrogen and at – 80 °C until required.

3.2.2 Reagents and Materials

Cloning reagents and kits include Novagen UltraMobiuss plasmid kits (EMD Bioscience, San Diego, CA), Qiagen RNA/DNA mini kit (Hilden, Germany), lipofectamine and mammalian expression vectors obtained from Invitrogen Corp.(Carlsbad, CA) were pEF6/V5-His TOPO TA[®] and pcDNA 3.1 (+). EpCAM specific primers (Forward: 5'-AGC ATG GCT CCC CCG CAG

GTC C-3' (bases 176-197); Reverse : 5'- GGC GTT GAG TTC CCT ATG CAT CTC AC CAT-3' (bases 1091-1116)) flanking the region including the signaling peptide through part of the cytoplasmic region used for polymerase chain reaction (PCR) amplification of EpCAM cDNA were synthesized by Integrated DNA Technologies (Coralville, IA) based on the messenger RNA sequence of the tumor associated calcium signal transducer (TACSTD1: NM_002354) obtained from the National Center for Biotechnology Information (NCBI) website. Restriction endonucleases and Quick Ligation kit used in the cloning process were obtained from New England Biolabs Inc. (Ipswich, MA). Criterion Tris-HCl gels and electrophoresis and western blotting buffers were obtained from BioRad Laboratories (Hercules, CA).

Talon[®] metal affinity resin used in affinity purification of recombinant EpCAM was obtained from ClonTech Laboratories Inc. (Mountain View, CA). FluoStar Optima microtiter plate reader (BMG LabTech, Durham, NC) was used for total protein determination by Bicinchoninic assay (BCA) (Pierce, Rockford, IL) and DNA quantitation by Cyquant cell proliferation assay (Invitrogen, Carlsbad, CA). Western blot reagents and antibodies utilized included Full Range Rainbow Protein marker, ECL Plus western blotting reagent (GE Healthcare, Piscataway, NJ), MagicMark XP western protein marker, anti-V5 , C-terminus anti-Histidine monoclonal (Invitrogen, Carlsbad, CA), anti-hEpCAM (R&D, Systems, Minneapolis, MN) and anti-EpCAM VU D9 clone (EMD Biosciences, Inc., La Jolla, CA) primary antibodies. Detergents used in cell solubilization studies include dodecyl- β -D-maltoside (DDM) and sodium deoxycholate (DOC) from Sigma-Aldrich (St. Louis, MO), nonidet P40 (NP40) and n-octyl- β -D-glucopyranoside (O β DG) from EMD Biosciences (La Jolla, CA). Sodium molybdate used in NP40 buffer preparations and imidazole used in the purification studies were obtained from Sigma-Aldrich (St. Louis, MO).

3.2.3 Production of EpCAM cDNA from Total RNA of Breast Cancer Cells and Generation of EpCAM/Vector Constructs

MCF7 and Hs578T breast cancer cells were cultured in Dubelco minimum essential medium (DMEM) in p60 culture dishes under 6% CO₂ at 37°C until the cells reached approximately 90% confluency. The adhered cells were first washed with sterile phosphate buffered saline (PBS) and solubilized with 1% SDS solution. After shearing the DNA and centrifuging to remove debris, the total protein contents of the lysates were determined by bicinconninic acid assay (BCA). Aliquots of lysate containing 50 ug of total protein were analyzed by western blot to determine which cell line produced the highest level of EpCAM. MCF7 cells were cultured to 90% confluence and the cells harvested for total RNA extraction following the instructions for the Qiagen RNA/DNA kit. Total RNA was reverse transcribed using poly-dT primers to provide cDNA from which EpCAM cDNA was PCR amplified with EpCAM specific primers for cloning. The PCR amplification temperature cycle involved a 3 min initial denaturation at 95 °C followed by a 25 round thermal cycle of 30 s at 95 °C, 1 min at 58 °C and 1 min at 72 °C. A final extension at 72 °C for 7 min was carried out prior to cooling the PCR reaction to 4 °C.

To generate histidine tagged EpCAM cDNA containing vectors for transformation and transfection, EpCAM cDNA obtained from RNA of MCF7 cells was first cloned into the pEF6/V5-His TOPO TA[®] mammalian expression vector for bacteria transformation as follows; PCR amplified EpCAM cDNA was added to the TOPO vector without prior purification and allowed to incubate for 5 min at room temperature. Competent *E. coli* cells were transformed with the recombinant TOPO/EpCAM plasmid and cultured on Luria broth (LB) agar with 50 ug/mL ampicillin overnight at 37 °C following the TOPO kit protocol. The transformed *E. coli* cells were tested for the presence of EpCAM cDNA by PCR of heat lysed cells using EpCAM-specific primers. Colonies which tested positive for EpCAM cDNA were cultured in Luria broth

(LB) containing 50 µg/mL ampicillin at 37 °C for 16 h. Purified recombinant plasmid was obtained using the UltraMobiuss plasmid extraction kit and analyzed by restriction enzyme digest to determine the correct insertion of EpCAM cDNA into the vector based on the DNA fragment sizes obtained. Large scale plasmid preparation was carried out to obtain purified recombinant TOPO plasmid for extraction of EpCAM-V5-His₆ DNA sequence.

Transfer of EpCAM-V5-His₆ cDNA from the TOPO/EpCAM plasmid to pcDNA 3.1 (+) vector was achieved by digestion of the TOPO/EpCAM plasmid with Kpn1 and EcoRV restriction endonucleases and digestion of pcDNA 3.1 (+) with Kpn1 and Pme1 enzymes. The digested insert and vector DNA were agarose gel purified and extracted using the Novagen UltraMobiuss mini plasmid prep kit. The insert and plasmid DNA were then quantified and combined in a molar ratio of 3:1 insert to plasmid. Using the Quick ligase kit, a 5 min ligation of the EpCAM-V5-His₆ insert into pcDNA 3.1 (+) was carried out to generate the pcDNA/EpCAM-V5-His₆ recombinant plasmid. Transformed bacteria colonies containing this plasmid were selected on LB ampicillin (LB-amp) agar and determined to contain EpCAM cDNA by PCR. The transformed bacteria were cultured for plasmid preparation and storage at -80 °C in 10% glycerol. Recombinant plasmid for bacterial expression of recombinant EpCAM (rEpCAM) was prepared by digestion of pTriEX-4 Neo vector with Xho 1 and Eco RV and sequential digestion of pcDNA/EpCAM-V5-His₆ with Xho 1 followed by Pme 1. The purified cut vector and insert were ligated as previously described and transformed in bacteria for amplification.

All three recombinant plasmids were analyzed by restriction enzyme digest to determine the orientation of the insert in the vector. Fragments obtained were separated on 1% agarose and the sizes compared to the calculated fragment sizes. TOPO/EpCAM and pcDNA/EpCAM-V5-His₆ were sequenced using EpCAM, T7 and BGH primers to verify correct sequence orientation and the absence of mutations in the EpCAM cDNA.

3.2.4 Bacteria Expression of rEpCAM

pTriEx-4/EpCAM transformed Tuner (DE3) pLacI cells cultured in LB medium containing 75 µg/ mL carbenicillin, 34 µg/ mL chloramphenicol and 1% glucose overnight at 37 °C served as a starter culture for seeding fresh medium. The cells were allowed to grow for 3 h to an optical density (OD) between 0.5 and 1.0, measured at 600nm wavelength. Protein expression was induced with different IPTG concentrations ranging from 0 to 1 mM and the cultures incubated for 2.5 h. Aliquots of 1.5 mL cell suspension were centrifuges at 12, 0000 x g for 5 min and the cell pellets washed three times with phosphate buffered saline (PBS) before being lysed in reducing Laemli buffer and heat denatured for electrophoresis and western blot analysis. OD measurements were obtained at various time intervals for EpCAM transformed tuner cells and control tuner cells cultured without IPTG to determine the growth pattern of the cells and for cultures before and after IPTG induction.

3.2.5 Expression of C-Terminus Histidine-Tagged Recombinant EpCAM in Mammalian Cells

Three mammalian cell lines BHK, Hep 2 and Cos 7 were transfected with pcDNA/EpCAM for mammalian expression of rEpCAM. The cells were grown to approximately 90 % confluence, rinsed with PBS to remove growth medium and treated for 30 min with a suspension of lipofectamine emulsified recombinant vector in growth medium. The transfected cells were cultured in the presence of 400ug/ mL G418 selection agent over a two week time period to create a rEpCAM expressing stable cell line. Cells were harvested every five days after transfection to test for the presence of rEpCAM by western blot using anti-EpCAM, anti-histidine or anti-V5 primary antibodies.

3.2.6 Purification of Recombinant EpCAM

EpCAM expressing BHK cells were used in determining the best detergent for cell solubilization. Mild detergents DDM, DOC, NP40 and OβDG were selected and compared to

SDS to obtain the most effective non-denaturing detergent in terms of protein content. Cells in p10 plates were cultured under antibiotic selection until 90% confluency at 37 °C. The cells were rinsed with cold sterile tris buffered saline (TBS) and treated with 500 µL each of TBS containing different detergents and protease inhibitor cocktail. The cells were scraped and solubilized by several passes through 25 gauge syringes. The crude lysates were centrifuged for 10 min at maximum speed in a microcentrifuge to separate insoluble cell debris from the supernatant. Cell pellets were solubilized in 1% SDS in TBS and total protein contents of both fractions were determined spectrophotometrically using the BCA method for total protein. Lysate aliquots containing 50 µg total protein, were loaded on Criterion 10% tris-HCl gels and electrophoresed at 100 V for 2.5 h. The resolved proteins were electro-transferred to nitrocellulose membrane at 100 V for 60 min in tris-glycine buffer for western blot analysis. Nonidet P40 detergent was selected for cell solubilization and added to Tris saline buffer at 0.09% with 10 mM sodium molybdate.

3.2.7 Optimization of mMetal Affinity Purification Protocol for Recombinant EpCAM

Clarified cell lysate containing the recombinant protein was incubated with Talon® resin at a ratio of 1:5 resin-to-lysate volume for 2 h at room temperature or overnight at 4 °C on a shaker. Subsequent incubations were performed overnight at 4 °C, since this condition allowed maximum binding of protein to the resin. Bound protein was then washed with 10 column volumes of buffer containing different imidazole concentrations ranging from 1 mM to 50 mM to determine the most appropriate imidazole levels which would allow removal of non-specifically bound proteins while retaining the bulk of the recombinant protein on the resin. Other additives such as 5% glycerol, sodium chloride (500 mM) and beta mercapto-ethanol (BME) (10 mM) were introduced in the binding and washing stages for protein stability and to determine their effectiveness in reducing the level of non-specifically bound proteins. Each wash step was

carried out in triplicate with 3 min room temperature incubation periods on a shaker and the buffer removed by centrifugation for 2 min. The purified recombinant protein was eluted from the resin with one column volume of buffer containing imidazole at concentrations between 75-500 mM or EDTA (100 mM) and the eluted resin treated with 1% SDS solution to check the effectiveness of the elution buffer during the purification optimization process. Imidazole at 500 mM concentration was selected for elution of bound protein during the scale-up process. IMAC fractions were analyzed by SDS PAGE and western blot to ascertain which fractions contained the recombinant EpCAM and the level of its purity. Fractions collected were loaded on 10% polyacrylamide gel in volumetric ratios to allow comparison of the rEpCAM levels in each fraction.

3.2.8 Gel Electrophoresis and Western Blot Analysis

Samples of lysate and purification fractions were loaded on 10% polyacrylamide gels and electrophoresed at 100V for 2.5 h. The separated proteins were electro-transferred to nitrocellulose membrane (BioRad laboratories, Hercules, CA) after which the membrane was washed and blocked for 1 h with 5% skim milk in PBS buffer containing 0.05% Tween 20 (PBS-T). The membrane was incubated overnight at 4°C with anti-EpCAM antibody in 5% skim milk in PBS-T, washed 3 times with PBS-T for 5 min each and incubated 1 h at room temperature with horse radish peroxidase (HRP) linked secondary antibody. The membrane was washed 3 times with PBS-T and ECL Plus western blotting chemiluminescence detection reagent added for 5 min. Presence of rEpCAM was determined by exposure of the membrane to photographic film.

3.2.9 Electro Elution of rEpCAM from SDS-PAGE Gels

Pre-concentration of IMAC purified protein eluates was carried out by centrifugal ultrafiltration using centricon devices with molecular weight cut-offs (MWC) of 50, 30 and 10

kilodaltons (kD) and, in later experiments, by dialysis using MWC 20 kD slide-a-lyzer cassettes and concentrating solution. The rEpCAM concentrates were electrophoresed on 10 % Criterion Tris-HCl gels to separate the target protein from co-eluting proteins. The gels were stained with E-Zinc reversible stain (Pierce, Rockford, IL) and the rEpCAM bands excised and destained with tris/glycine buffer. The protein was electro eluted from the gel in a Model 422 Electro Eluter (BioRad Laboratories, Hercules, California) for 5 h in tris/glycine buffer with 0.05% SDS. The extracted protein was removed and concentrated by centrifugal ultrafiltration and analyzed by SDS-PAGE and western blotting.

3.3 Results and Discussion

In this study, two breast cancer cell lines (MCF 7 and Hs578T) were selected as sources for EpCAM due to over-expression of this biomarker in these cell types. The cells were cultured and the total protein content determined followed by western blot analysis to determine the relative EpCAM expression level in each cell type. Results showed a higher level of the target protein generated in the MCF 7 cells compared to the Hs578T cell line due to a faster growth rate. Thus the MCF 7 cell line was our source for total RNA extraction for the cloning process. Total RNA was converted to cDNA from which the EpCAM cDNA was obtained for further cloning steps.

3.3.1 Insertion of RT-PCR Amplified EpCAM cDNA into the Vectors

PCR amplification of EpCAM cDNA carried out with primers flanking regions of the EpCAM cDNA from bases 176 to 1116 yielded a sequence greater than 900 bp in size on 1% agarose gel, which corresponds to the expected 941 bp cDNA size calculated using the EpCAM mRNA sequence (Locus: NM_002354) obtained from the NCBI website. This portion of the EpCAM sequence encompasses the regions of the protein starting from the signaling peptide through most of the cytoplasmic domain. The amplified sequence was immediately inserted into

the pEF6/V5-His TOPO plasmid without the need for prior purification of the PCR product. Results of cloning and sub-cloning EpCAM cDNA into TOPO, pcDNA 3.1 (+) and pTriEx-4 Neo vectors are shown in figure 3.2. Recombinant plasmids generated for EpCAM expression were restriction enzyme digested and analyzed by agarose gel electrophoresis. Fragment sizes were compared to calculated fragments expected for correctly inserted cDNA fragments (Figure 3.2). PCR amplification of recombinant plasmids from transformed bacteria using EpCAM primers indicated the presence of a 941 bp EpCAM sequence.

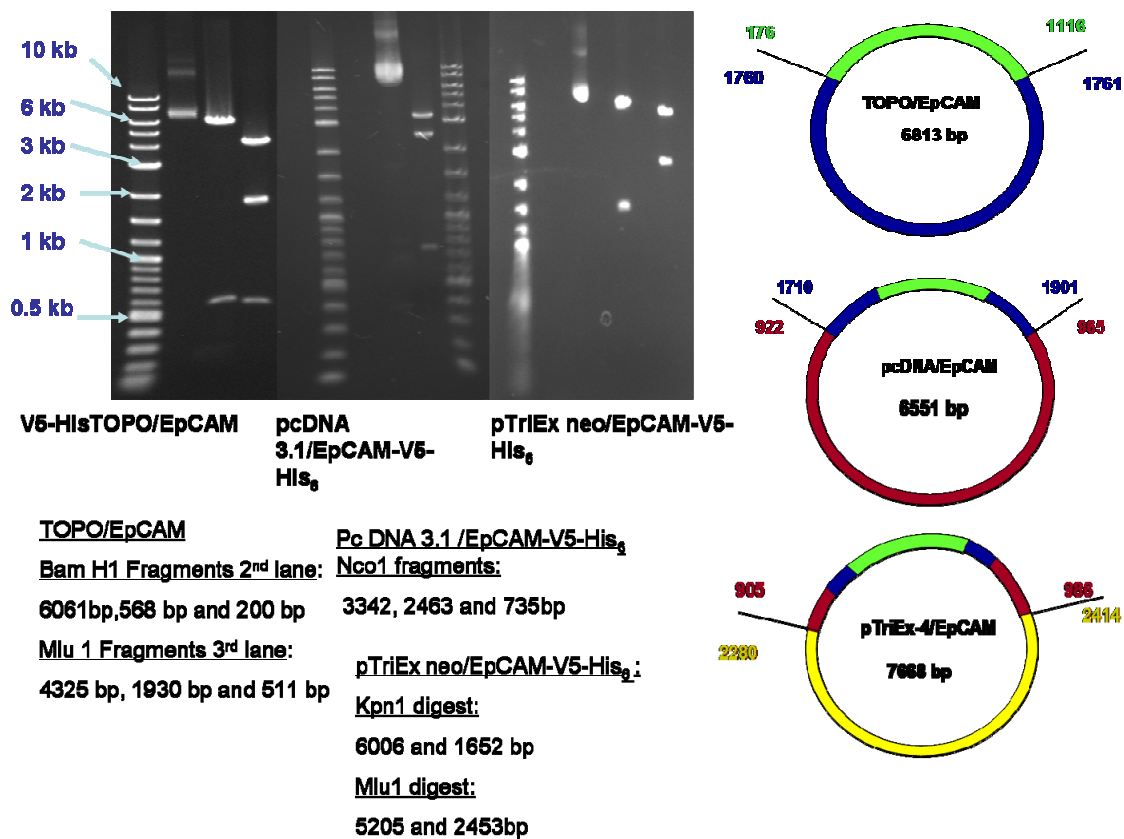


Figure 3. 2 Agarose gel electrophoresis of restriction enzyme digests of the three recombinant plasmids produced for rEpCAM expression. Given below the image are the calculated fragment sizes expected for each restriction enzyme digestion.

The TOPO TA cloning system was selected for cloning EpCAM cDNA due to the ease of cloning and the unidirectional TA cloning property of this technique, which prevented anti-sense orientation of the cDNA into the plasmid. Also, the technique allowed cloning of PCR amplified

cDNA without prior purification of the cDNA from the PCR mixture, thus reducing the number of steps involved in the cloning process while still providing high cloning efficiency. The pEF6/V5-His TOPO plasmid also attached carboxy-terminus (C-terminus) hexahistidine and V5 epitope tags on the recombinant protein, thus enabling purification of the protein by immobilized metal affinity chromatography and western blot detection of the recombinant protein using anti-histidine antibody or anti-V5 antibody. This property was exploited during transfer of the target cDNA into other plasmids.

Fifteen colonies of pEF6/V5-His TOPO/EpCAM (TOPO/EpCAM) transformed *E. coli* bacteria were positive for EpCAM when analyzed by PCR. Four colonies were selected, cultured and the recombinant plasmids purified and subjected to restriction endonuclease digestion using BamH1 and Mlu1 enzymes (see Figure 3.2). Each enzyme produced three fragments analyzed by agarose gel electrophoresis, the sizes of which were compared and corresponded to the calculated fragment sized expected for a correctly inserted EpCAM cDNA.

The pcDNA 3.1 (+) vector was selected for episomal expression studies based on its restriction enzyme map in order to allow transfer of the recombinant EpCAM-V5-His₆ (rEpCAM) cDNA from the TOPO/EpCAM plasmid. The plasmid contains a SV40 gene for episomal expression in cells expressing the SV40 large T antigen. The pTriEx-4 Neo vector was created for expression of target proteins in multiple systems including bacteria, insects and mammalian systems and was selected for bacterial expression of the rEpCAM protein.

To ensure unidirectional orientation of the histidine and V5 tagged rEpCAM cDNA sub-cloned into pcDNA 3.1 (+) and pTriEx-4 Neo vectors, restriction maps of the vectors and EpCAM cDNA were compared and restriction endonuclease enzymes selected to generate an overhang and a blunt end each on the insert and vectors. Thus, using Kpn1 and Pme1 on the TOPO recombinant and Kpn1 and EcoR V on pcDNA 3.1 (+), ligation of the excised histidine-tagged

EpCAM cDNA insert into the pcDNA episomal vector was carried out to generate the pcDNA/EpCAM-V5-His₆ recombinant plasmid. This procedure was repeated for the pTriEx 4 neo vector used for bacterial expression of recombinant EpCAM. The pcDNA/EpCAM-V5-His₆ plasmid was restriction enzyme double digested with Xho I and Pme I to obtain the histidine-tagged rEpCAM and ligated into pTriex 4 Neo treated with Xho I and EcoR V. The resulting recombinant vectors showed correct orientation of the insert as determined by restriction enzyme digestion (see Figure 3.2). To further confirm orientation without mutations the plasmids were sequenced with T7, BGH and EpCAM primers and compared to the GenBank sequence for EpCAM using the blast software. The sequence was at least 99% homologous to the EpCAM sequence and had no mutations. Thus, large-scale plasmid amplification and purification were carried out for mammalian cell transfection and transformation of bacteria Tuner cells for expression studies. Based on the DNA sequence for the recombinant, the molecular weight of the unglycosylated recombinant protein was determined to be approximately 37.033 kD.

3.3.2 Bacterial Expression Studies

Bacteria cells, Novagen Tuner(DE3)pLacI cells (EMD Bioscience, Inc., La Jolla, CA) transformed with pTriEx 4 Neo/EpCAM plasmid were cultured overnight and sub-cultured for 3 hr at 37 °C prior to induction with various IPTG concentrations. Induced cells were incubated at 37 °C for 2.5 h and cell density measurements were obtained at 600 nm absorbance. The results of bacterial expressions studies are shown in Figures 3.3-3.5. The OD measurements of the growth of control and pTriEx/EpCAM transformed and un-induced bacteria over time indicated slower growth for the pTriEx/EpCAM transformed bacteria compared to the same bacteria transformed with the control plasmid (see Figure 3.3). The recombinant plasmid transformed Tuner cells reached logarithmic growth phase after 3 h while the control cells were more than

half-way through the logarithmic phase at 3 h of growth with an optical density above 1.1. The recombinant plasmid transformed cells took almost 18 h to reach stationary phase.

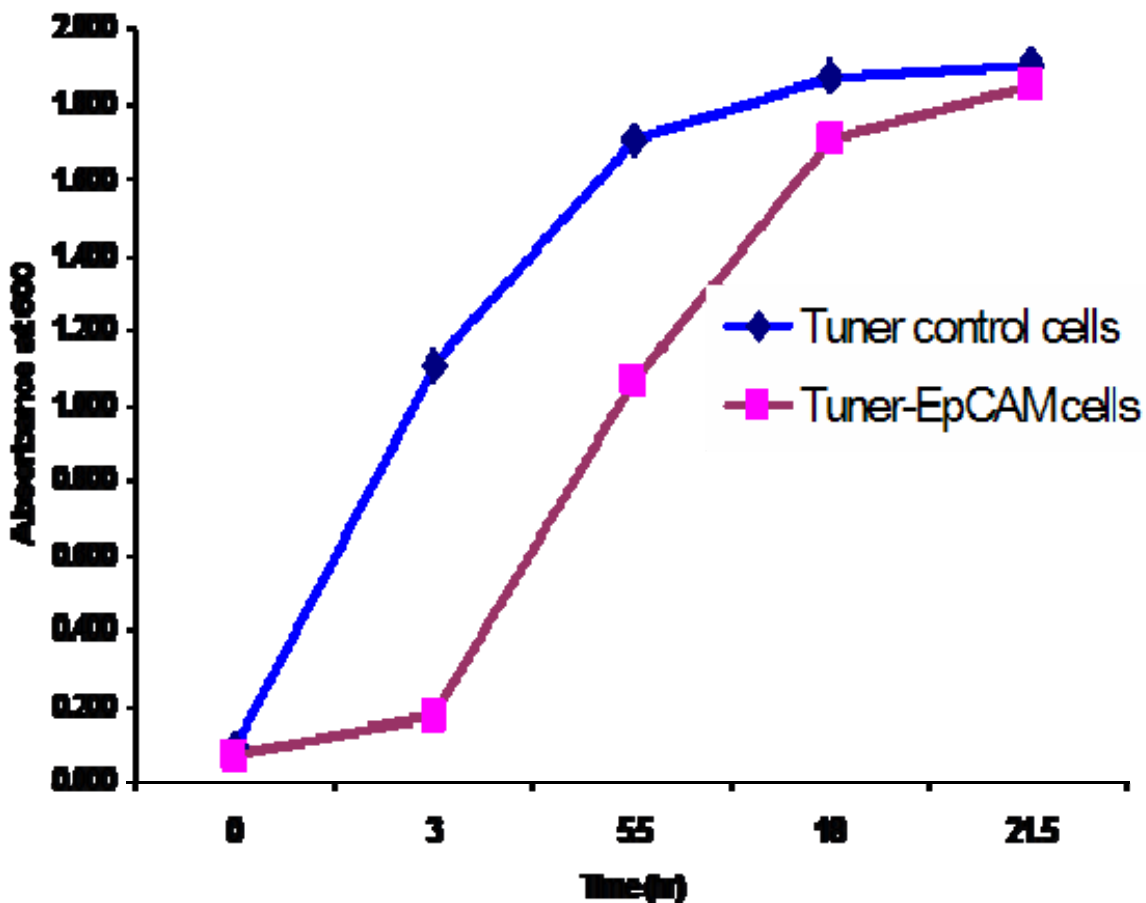


Figure 3. 3: Growth curves of Tuner (DE3)pLac bacteria transformed with pTriEx 4 Neo/EpCAM-V5-His6 and a control plasmid. The graphs show the rate of growth of the un-induced bacteria from initial media inoculation through the stationary phase.

The slower growth rate is an indication of inhibited growth due to the recombinant plasmid. The OD measurements of cells induced with different IPTG concentrations showed a decrease in intensity with increasing IPTG concentration after 2.5 h of induction (see Figure 3.4). At lower IPTG concentrations of 2.5 and 10 μ M cell growth occurred at almost the same rate as for un-induced cells cultured for the same time frame.

Above 100 μM IPTG the cell growth process was slower and at the maximum inducer concentration of 1 mM there was no change in optical density compared to the un-induced starting culture. In contrast however, control cells induced with 1 mM IPTG showed a slightly higher OD after 2.5 h of induction than the 0 mM IPTG control cells incubated for the same time period. The results thus indicate that induction of protein expression with IPTG exerted a growth-inhibiting effect on the cells leading to under-production of the recombinant protein by the bacteria as determined by western blot analysis.

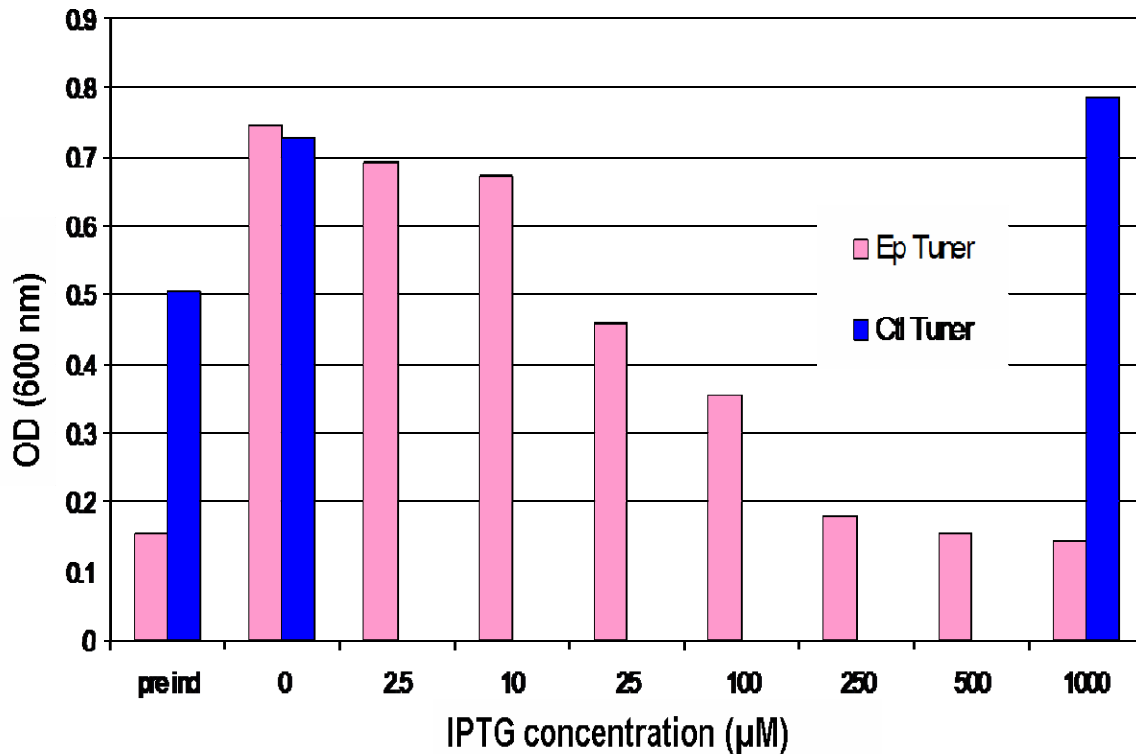


Figure 3. 4: Optical density measurements of un-induced and IPTG induced transformed bacteria cells, showing the effect of the recombinant pTriEx/ EpCAM plasmid on the growth of the cells (Ep Tuner) at various IPTG concentrations. Control cells (Ctl Tuner) were induced at 0 and 1000 μM IPTG levels to determine the effect of the inducer on cell growth.

To test the effect of temperature on the ability of the recombinant colonies to produce EpCAM, the cells were induced at IPTG concentrations of 500 μM and 1 mM and incubated at 10, 25 and 32 $^{\circ}\text{C}$. SDS-PAGE with gelcode blue staining showed no over-expression of proteins (see

Figure 3.5A). Results of OD measurements showed increased cell density with increasing temperature (see Figure 3.5B), however no protein over-expression was observed for the bacteria cultures.

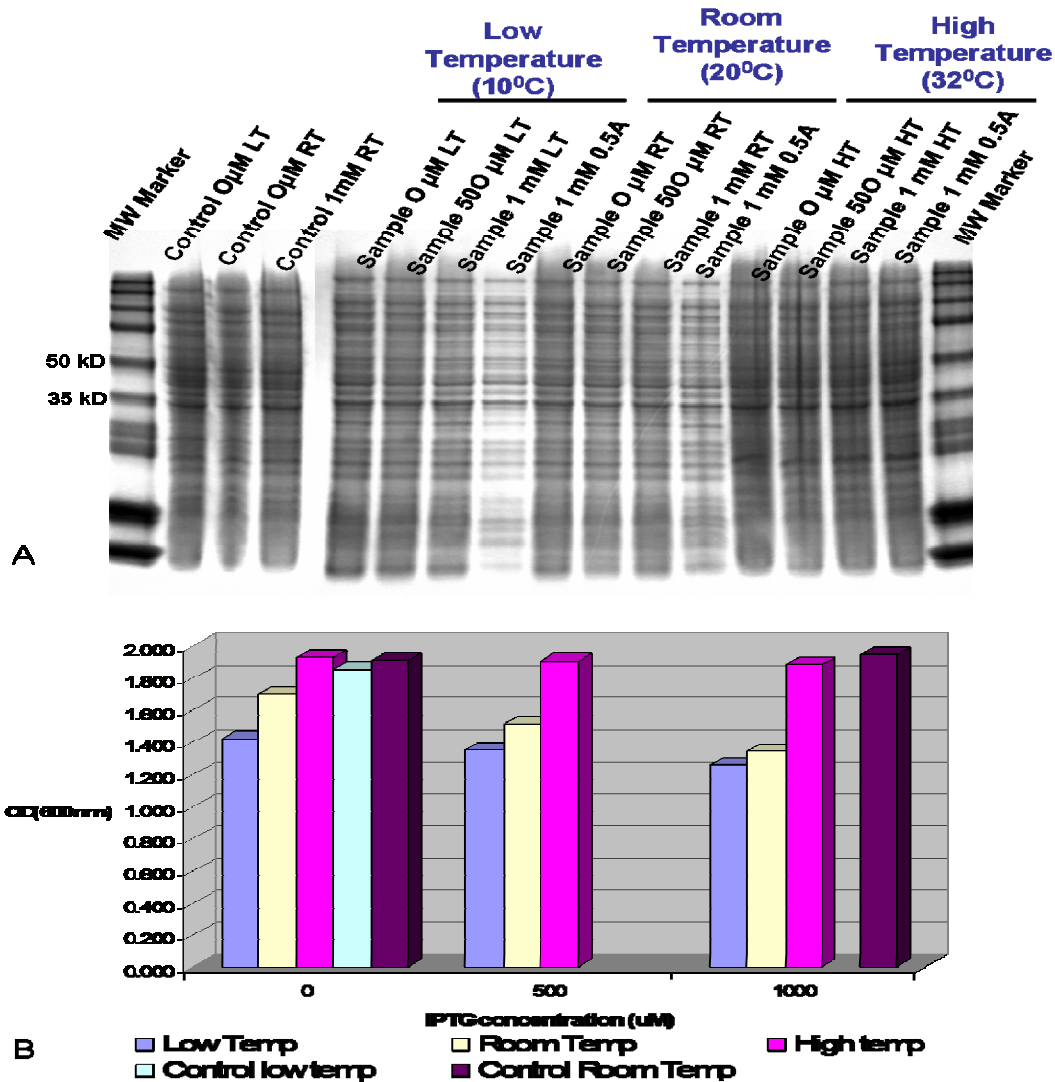


Figure 3. 5: The effect of temperature on A) protein over-expression in IPTG induce cells determined by electrophoresis with Gelcode Blue staining and B) the growth of the bacteria cells under different temperature conditions as determined by OD measurements.

Studies have shown that some mammalian membrane proteins exert a toxic effect on the bacterial expression hosts in addition to the lack of post translational modification mechanisms in bacteria. Thus, these proteins cannot be produced using bacterial expression systems.³² Western blot analysis performed on the bacteria cell lysates indicated the absence of rEpCAM in

the molecular weight range for this recombinant protein. Also, no degradation products were detected that would indicate possible synthesis and breakdown of the protein by the bacteria.

3.3.3 Mammalian Expression of rEpCAM

Mammalian expression of rEpCAM was next attempted using three different cell types. BHK cells were selected for transfection studies due to the robustness of this cell type and its widespread use in protein expression studies,^{7, 33} while Hep 2 cells were chosen for their epithelial cell property to test their ability to correctly fold and post-translationally modify and generate high yields of the rEpCAM. Cos 7 cells are used in episomal expression studies due to the SV40 large T antigen which allows episomal vectors to induce protein generation without genomic integration of the plasmid DNA.³⁴ Figure 3.6 shows the results of mammalian expression studies using these cell types. Western blots of lysates from the three cell types, SDS-PAGE separated under non-reducing conditions and without prior heat denaturation of the lysates, were performed with anti-EpCAM, anti-histidine and anti-V5 primary antibodies. The anti-histidine antibody was not effective for detecting the recombinant protein and was not used in subsequent analyses. Western blots performed with anti-V5 and anti-EpCAM antibodies produced better results. Anti-EpCAM was more effective at detecting the native form of the rEpCAM while the anti-V5 antibody was more appropriate for identification of the denatured form of rEpCAM.

Western blots indicated, as expected, that for equal total protein levels of lysate the Cos7 cells produced higher EpCAM levels compared to BHK or Hep 2 cells due to episomal expression of the protein in Cos 7 cells (see Figure 3.6). Anti-EpCAM western blots of lysate proteins electrophoresed under non-reducing conditions showed a band for EpCAM at the expected molecular weight of approximately 40 kD in the Hep 2 lysate and higher molecular weight band for the Cos 7 lysates while the BHK lysate showed no EpCAM band (see Figure

3.6A). The blots carried out using anti-V5 antibody showed multiple bands of monomeric and multimeric forms in the Cos 7 lysates of the recombinant protein while the Hep 2 and BHK lysates showed single bands of the monomeric recombinant protein at ~40 kD (see Figure 3.6A).

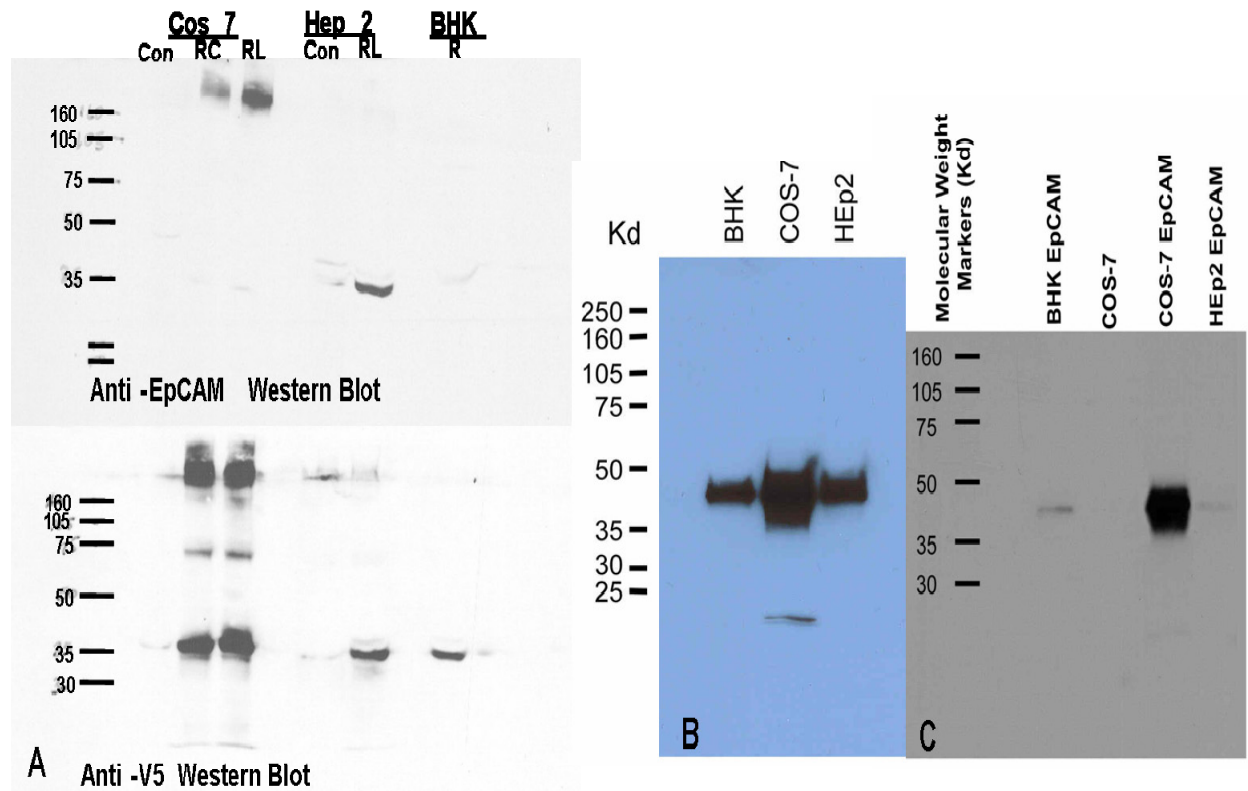


Figure 3. 6: Western blots of rEpCAM expression in three different mammalian cells. In A) lysates from Cos 7, BHK and Hep2 cells obtained 5 days after transfection were mixed in native sample buffer and immediately separated by SDS-PAGE on 10% tris-HCl gel prior to electrotransfer to nitrocellulose for western blotting using antiEpCAM and anti-V5 primary antibodies. In B and C, the lysates from stable transfectants were reduced with dithiothreitol and heat denatured prior to SDS-PAGE separation and western blot analysis using anti-V5 antibody. Image C also shows loss of rEpCAM expression by BHK and Hep2 cells after sub-culturing for between 4 to 5 passages.

A western blot carried out on dithiothreitol (DTT) reduce lysates showed higher levels of the recombinant protein in Cos 7 lysates compared to the Hep 2 and BHK lysates for the same total protein content loaded on the gels (Figure 3.6B). Over-expression of the protein in Cos 7 cells may have led to formation of the observed multimeric aggregates generated in the western blots. However, it was observed in subsequent western blots that multimeric bands observed for Cos 7

cell were lost in transfected daughter cell culture lysates due to a progressive decline in the protein expression levels through sub-culturing of the cells, until a steady level of monomeric rEpCAM remained.

Prolonged production of the recombinant protein in the transfected cells at a constant level of expression is important for the generation of adequate amounts of the protein for downstream processes. Thus, the ability of each cell type to sustain protein production over several weeks of culturing was determined by western blot of transfected and stabilized BHK, Hep2 and Cos 7 cells. The transfected cells were cultured under antibiotic selection for two weeks to produce stabilized transfectants. The cells were then split and the cultures expanded over several passages for storage and protein production. Results indicated that production of the recombinant protein in BHK and Hep2 cells declined and was completely inhibited after the fourth passage of cells although the cells continued to grow in the presence of the antibiotic (Figure 3.6C). This may be attributed to the effect of genomic integration of the recombinant DNA on protein production leading to strict regulation of recombinant protein production by the cells' transcriptional and translational mechanisms.¹⁶ Thus, rEpCAM expression was down regulated in daughter cells and with time the sequence may have been completely eliminated from the genome of BHK and Hep2 cells. On the contrary, in transfected Cos 7 cells a steady level of protein production was maintained up to about the eleventh passage before dropping off. The prolonged expression of rEpCAM in Cos 7 cells compared to the BHK and Hep2 transfectants is due to the episomal expression in these cells. However, it appeared that with time the plasmid copy numbers may have decreased in daughter cells until rEpCAM production was solely regulated by the Cos 7 cells transcriptional and translational mechanisms leading to loss of rEpCAM production over time. It has also been reported that BHK and Cos cells are generally more suited for transient expression of proteins. Because of the extended expression

time obtained with Cos7 cells transfected with pcDNA/EpCAM, this cell line was selected for production and purification of our recombinant protein.

3.3.4 Extraction and Affinity Purification of rEpCAM from Mammalian Cells

In order to maximize protein solubilization in non-denaturing detergent various detergents were tested for their ability to effectively solubilize proteins in the cells by comparing the total protein contents of supernatant and pellet fractions of lysed recombinant cells. The percentage of total protein obtained for the supernatant fractions solubilized using four mild detergents were compared to SDS lysed cells (see Table 3.1).

Table 3.1: The mammalian cell solubilizing efficiency of four mild detergents in comparison to SDS in terms of total protein content of lysate produced used in mammalian cell lysis.

Detergent	Detergent concentration (%)	Pellet fraction protein content (ug/ mL)	Supernatant fraction protein content (ug/ mL)	% protein in supernatant
DDM	1.0	352.3	4075.1	92.0
DOC	0.1	731.7	3170.0	81.2
NP40	0.1	214.6	4537.1	95.5
OBDG	1.0	585.4	3962.8	87.1
SDS	1.0	115.3	3461.9	96.8

NP40 had the highest percentage of supernatant total protein content (95.5%) of the four mild detergents with DOC having the lowest percentage of 81%. NP-40 was therefore the detergent of choice for cell lysis.

Utilizing a lysis buffer of Nonidet P40 detergent in Tris buffered saline (TBS-NP) with sodium molybdate, transfected Cos 7 cells were easily solubilized and subsequently centrifuged

to remove solid material. The supernatants obtained were analyzed by western blot analysis for rEpCAM and used in the protein purification studies. Affinity purification of solubilized rEpCAM from Cos 7 cells was accomplished using cobalt chelated resin. The incubation time and buffer composition were parameters optimized to selectively remove non-specifically adsorbed proteins while retaining the bound rEpCAM. Initial studies were carried out to determine the incubation time required for complete binding of the protein to the resin. Following the manufacturer's protocol for affinity binding of histidine tagged proteins to the Talon resin, clarified lysate was incubated with one fifth its volume of resin and incubated at room temperature for 2 h or overnight at 4 °C prior to washing with NP-40 buffer containing different imidazole concentrations. Results obtained indicated that longer incubation times at 4 °C were required to efficiently bind rEpCAM to the resin. At shorter incubation times up to 2 h approximately 93% of the rEpCAM was found in the unbound fraction. The longer incubation time requirement for protein binding may be a result of the hexahistidine tag being less accessible requiring a longer contact time for proteins to interact with the affinity resin. This, observation was based on western blot results of lysate and purified protein fractions detected using both anti-EpCAM and anti V5 monoclonal antibodies. It was observed in our studies that the anti-EpCAM antibody was more effective at detecting native rEpCAM in the lysate compared to the affinity purified protein while the anti-V5 antibody was more effective at detecting the affinity purified, denatured and reduced forms of the protein. This indicated that in the denatured and slightly unfolded state the V5 epitope tag was more accessible for binding to its antibody. Also as mentioned earlier in the protein expression section of this paper, western blots carried out on undenatured lysates using antibodies against EpCAM, V5 and C-terminus hexahistidine tag showed no rEpCAM band using the anti-histidine antibody probably due to inaccessibility of the histidine tag. Native EpCAM has been proposed to exist in epithelial cell

membranes with adjacent molecules interacting laterally through the EGF2-like domain of the protein molecules.^{35, 36} By expressing the bulk of the protein, the ability of the recombinant molecules to associate in this manner may to some extent have caused shielding of the hexahistidine tags, necessitating a longer incubation time with the IMAC resin in order to induce binding. Western blot results also showed that low levels of the protein were left in the unbound fraction even after overnight incubation of lysate with the resin although the loading capacity of the resin was not exceeded in the experiments (see Figure 3.7). Thus, purification steps were optimized to ensure optimum protein binding and maintenance of native structure of the protein. Buffer components play an important role during affinity purification of proteins. While some additives such as Tris can compete with the histidine tag for binding spots on the resin, other components such as detergents, reducing agents can denature the protein. Buffer components such as glycerol or ethylene glycol may be added to stabilize protein structure during the washing and elution stages of purification. Thus, in this study we varied buffer composition in terms of imidazole levels, addition or exclusion of BME in the wash buffer to provide the optimum conditions for removal of non-specifically bound proteins. Figure 3.7 shows a western blot of fractions from IMAC purification of Cos 7 lysate. Bound protein was treated with different levels of imidazole in solubilization buffer to wash and elute the recombinant protein. Results indicated that at the Tris concentration of 50 mM used in the cell lysis buffer, rEpCAM was eluted from the resin at imidazole concentrations as low as 25 mM due to interference of Tris with the binding interaction between the cobalt and rEpCAM. Imidazole concentrations between 1 and 75 mM were tested in wash buffers to remove weakly bound histidine containing proteins. From figure 3.7 it was observed that the bulk of bound protein was removed at imidazole concentrations below 100mM.

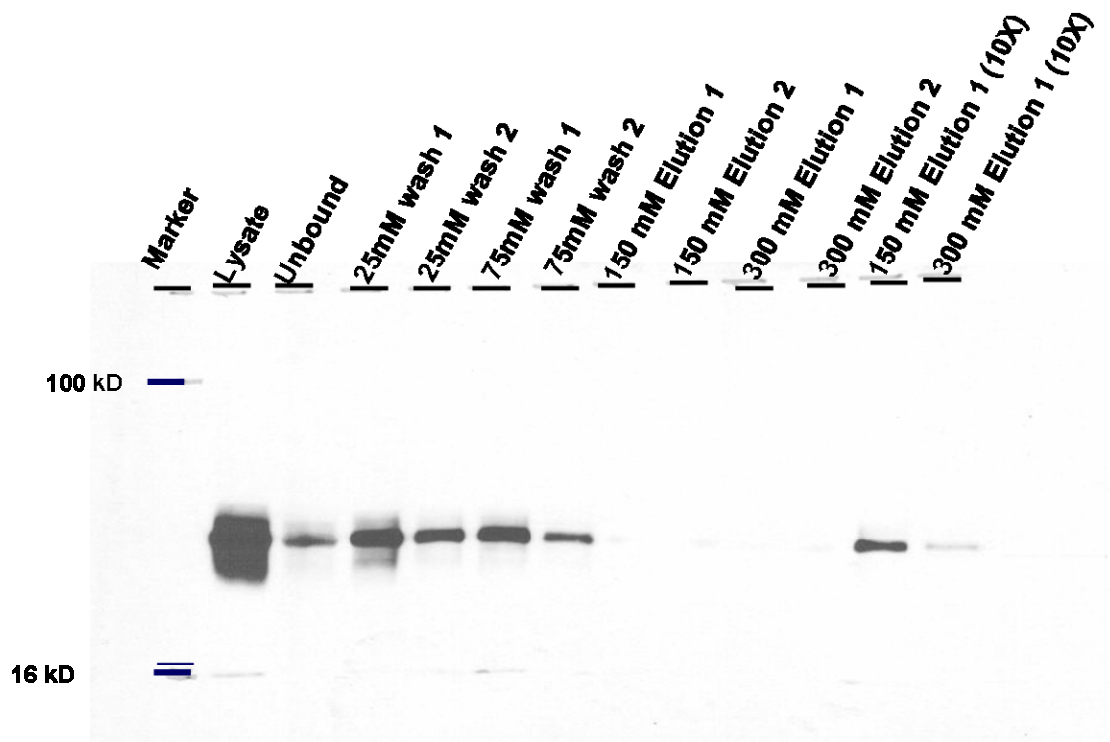


Figure 3. 7: Optimization of IMAC purification protocol for batch purification of rEpCAM from Cos 7 lysate using 0.09% NP40 in TBS. The Western blot image shows elution of rEpCAM at imidazole concentrations as low as 25 mM.

Analysis of SDS-PAGE gels of wash, elution and resin extract fractions by gelcode blue staining showed the presence of non-rEpCAM proteins in all the fractions indicating that the use of imidazole to selectively remove non-specifically bound proteins was ineffective (see Figure 3.8). To test the possibility that the non-specifically bound proteins were present due to strong interactions, such as disulphide bond formation, bound protein was treated with a 10 nM BME wash buffer for at least 20 min prior to washing with increasing imidazole concentrations. Results indicated that although some slight improvement was obtained with the use of BME the rEpCAM protein could not be detected with anti-EpCAM antibodies in a western blot due to disulfide bond reduction and unfolding of the protein. Increasing the NP-40 concentration to above 0.25% in wash buffers also led to loss of the rEpCAM in the wash buffers (results not shown). In subsequent experiments, reducing the Tris concentration to 25 mM in the wash and

elution buffers and diluting the lysate to half its initial concentration to decrease tris levels led to increased binding of rEpCAM to the resin during the overnight incubation period. At the 25 mM Tris concentration, imidazole levels up to 25 mM could be used to wash the resin bound rEpCAM without significant protein losses. However, gel staining of the eluted fractions still showed the presence of other proteins at significantly higher levels than the rEpCAM protein. Pre-concentrated eluate re-incubated with Talon resin in a second affinity purification step aimed at removing non-specifically interacting proteins resulted in re-binding of all proteins present in the starting fraction to the resin (see Figure 3.8). This indicated that the non-rEpCAM protein present in the eluate fractions contained surface exposed histidine clusters capable of very strong interactions with the IMAC resin. These protein contaminants were unfortunately expressed at much high levels compared to the target protein. Although the Talon resin was designed to selectively bind oligohistidine-tagged recombinants for one step purification of the desired protein, our recombinant proved to be difficult to purify in a one step process due to the requirement for well exposed histidine tags for enhanced binding to the IMAC resin. This finding necessitated the use of another technique in further purifying our protein target.

SDS-PAGE of lysate and purification fractions showed that after extensive washing of the bound protein with increasing imidazole concentrations up to 25 mM prior to elution with 500 mM imidazole, the bands of proteins in the the eluate fractions were well resolved to allow excision of the rEpCAM band without impurities. Thus, electrophoretic separation of the affinity purified protein could be carried out with extraction of the protein by electro elution. With this approach 100% electrophoretic purity of the target protein can be achieved. By combining this technique with affinity purification, the probability of co-eluting non-target proteins with the desired protein can be greatly reduced and the purification time decreased considerably.

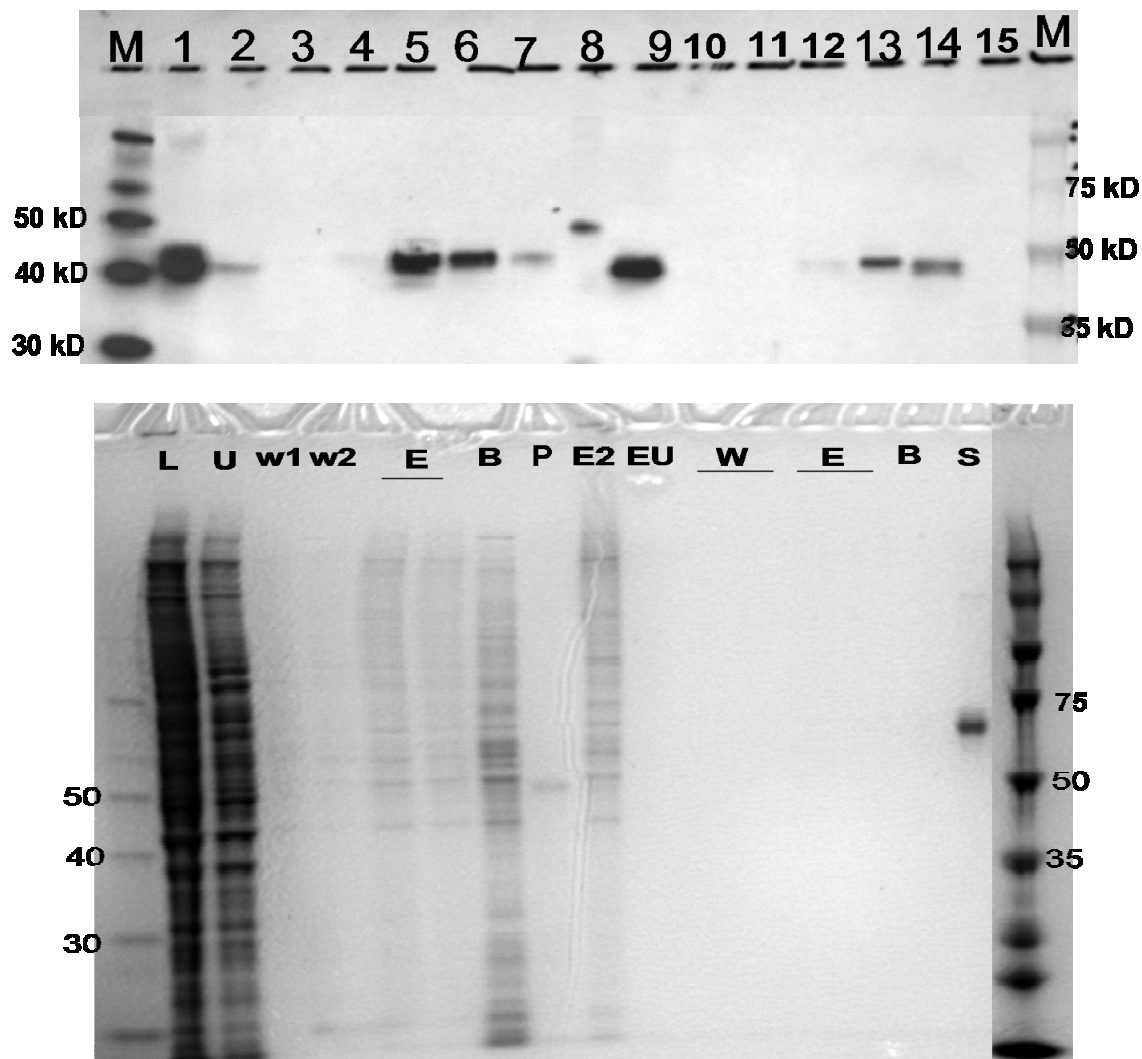


Figure 3. 8: A western blot (above) and gel images of fractions from a two-stage IMAC purification of rEpCAM from Cos 7 lysate showing the presence of rEpCAM in addition to non-EpCAM protein contaminants present in the elution fractions. Symbols used for the fractions collected are : L-lystae (1), U-unbound (2), w-wash (3, 4, 11, 12), E-eluates (5, 6,; 13, 14), B-resin (7, 15), S-EpCAM standard, P- positope (8), E2-ultrafiltered eluate (9), EU- unbound eluate (10), M-markers.

In our studies, eluates of affinity purified rEpCAM were pre-concentrated and electrophoresed on 10 % polyacrylamide gel using a 0.05% SDS Tris / glycine buffer. The gel was stained with E-zinc reversible stain and the bands in the molecular weight range 40 to < 50 kD were excised, destained and electro eluted. Two distinct bands were observed in this molecular weight range and were identified by western blot as rEpCAM (see Figure 3.9) using

both anti-EpCAM and anti-V5 primary antibodies. The two bands may be a result of different levels of glycosylation of the protein.

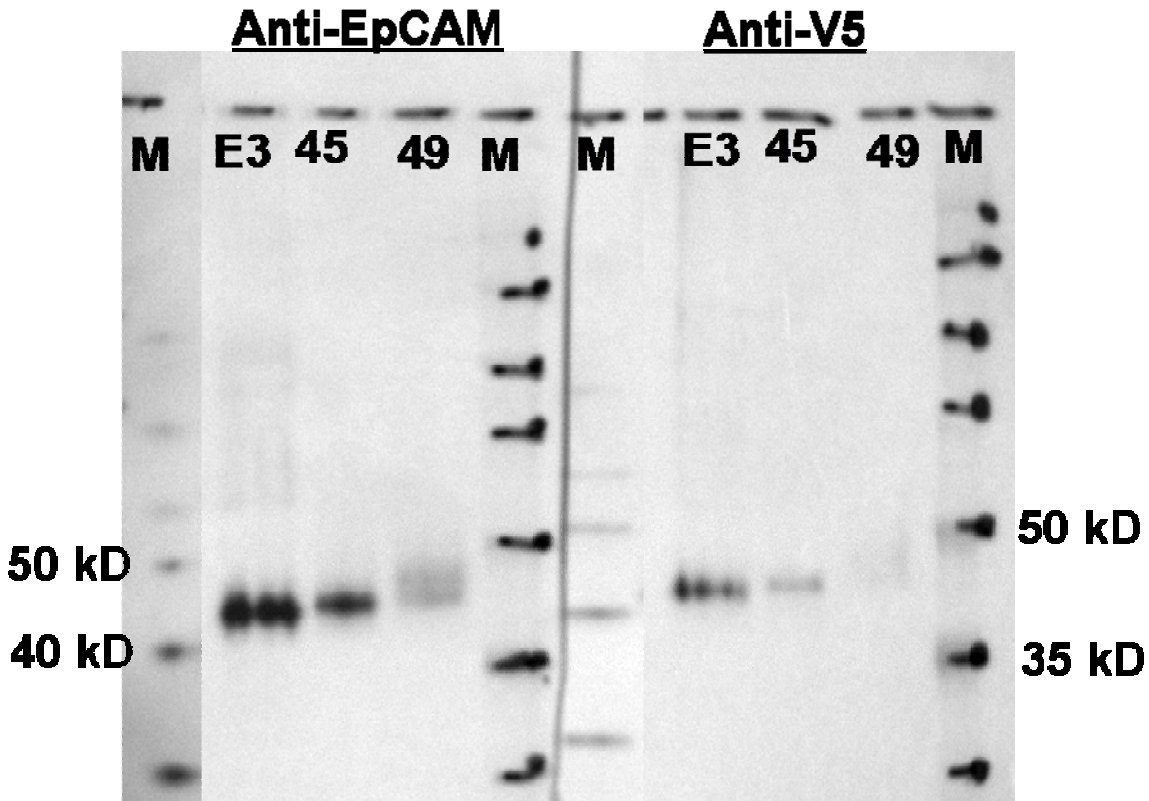


Figure 3. 9: Western blots of electro elution fractions of IMAC purified rEpCAM. Western blots were carried out with anti-EpCAM and anti-V5 primary antibodies to determine retention of native structure of the protein.

Also the anti-EpCAM western blot results confirmed retention of native structure after the purification process. Analysis of the band intensities for the rEpCAM protein on the western blot images using ImageQuant version 5.2 (Molecular Dynamics Sunnyvale, CA) indicated at least 75% recovery of the affinity purified protein after electro elution.

3.4 Conclusion

Thus, by combining a one-step IMAC procedure with electrophoresis and electro elution a more selective approach to obtaining a target protein in highly purified form and with the

required native conformation was achieved. With the demand for more rapid techniques for generating biomarkers for developing analytical techniques in disease management, the ability to integrate several biochemical processes efficiently would enable researches to achieve results in a more timely fashion. Microfluidic devices built on polymeric platforms provide the means to achieving this goal. The ability to incorporate several analytical processes such as the aptamer selection process, electrophoresis and other chromatographic processes in microfluidic devices makes it possible to combine protein target generation and purification with affinity agent selection on a scale that allows high throughput and rapid generation of analytical reagents for disease diagnostics without the use of large amounts of target. We have demonstrated the production of electrophoretically pure rEpCAM in its native folded state using IMAC and electrophoretic techniques. Further work will involve incorporation of the technique in microfluidic devices and coupling the process to aptamer selection to generate EpCAM specific aptamers.

3.5 References

- (1) Roobol-Boza, M.; Dolby, V.; Doverskog, M.; Barrefelt, A.; Lindqvist, F.; Oppermann, U. C.; Van Alstine, K. K.; Tjerneld, F. *J. Chromatogr. A* **2004**, *1043*, 217-223.
- (2) Jayasena, S. D. *Clin. Chem.* **1999**, *45*, 1628-1650.
- (3) Scott, J. K.; P., S. G. *Science* **1990**, *249*, 386-390.
- (4) Gold, L. *J. Biol. Chem.* **1995**, *270*, 13581-13584.
- (5) Luzi, E.; Minunni, M.; Tombelli, S.; Mascini, M. *TrAC, Trends Anal. Chem.* **2003**, *22*, 810-818.
- (6) Stoltenburg, R.; Reinemann, C.; Strehlitz, B. *Biomol. Eng* **2007**, *24*, 381-403.
- (7) Gupta, P.; Lee, K. H. *Trends Biotechnol.* **2007**, *25*, 324-330.
- (8) Knibbs, R. N.; Dame, M.; Allen, M. R.; Ding, Y. H.; Hillegas, W. J.; Varani, J.; Stoolman, L. M. *Biotechnol. Progr.* **2003**, *19*, 9-13.
- (9) Hartley, J. L. *Curr. Opin. Biotechnol.* **2006**, *17*, 359-366.

- (10) Sambrook, J.; MacCallum, P. *Molecular Cloning: A Laboratory Manual*, Third edition ed.; Cold Spring Harbor Laboratory Press: New York, 2001.
- (11) Marsischky, G.; LaBaer, J. *Genome Research* **2004**, *14*, 2020-2028.
- (12) Mus-Veteau, I. *Comp. Funct. Genom.* **2002**, *3*, 511-517.
- (13) Midgett, C. R.; Madden, D. R. *Journal of Structural Biology* **2007**, *160*, 265-274.
- (14) Grisshammer, R. *Current Opinion in Biotechnology* **2006**, *17*, 337-340.
- (15) Benting, J.; Lecat, S.; Zacchetti, D.; Simons, K. *Anal. Biochem.* **2000**, *278*, 59-68.
- (16) Barnes, L. M.; Bentley, C. M.; Dickson, A. J. *Biotechnol. Bioeng.* **2003**, *81*, 631-639.
- (17) Arnau, J.; Lauritzen, C.; Petersen, G. E.; Pedersen, J. *Prot. Express. Purif.* **2006**, *48*, 1-13.
- (18) Mohanty, A. K.; Wiener, M. C. *Prot. Express. Purif.* **2004**, *33*, 311-325.
- (19) Ueda, E. K. M.; Gout, P. W.; Morganti, L. *J. Chromatogr. A* **2003**, *988*, 1-23.
- (20) Porath, J.; Carlsson, J.; Olsson, I.; Belfrage, G. *Nature* **1975**, *258*, 598-599.
- (21) Gaberc-Porekar, V.; Menart, V. *Chem. Eng. Technol.* **2005**, *28*, 1306-1314.
- (22) Miseta, A.; Csutora, P. *Mol. Biol. Evol.* **2000**, *17*, 1232-1239.
- (23) Westra, D. F.; Welling, G. W.; Koedijk, D. G.; Scheffer, A. J.; The, T. T.; Welling-Wester, S. *J. Chromatogr. B* **2001**, *760*, 129-136.
- (24) Dyr, J. E.; Suttner, J. *J. Chromatogr. B* **1997**, *699*, 383-401.
- (25) Anjos, L.; Rotlant, J.; Guerreiro, P. M.; Hang, X.; Canario, A. V. M.; Balment, R.; Power, D. M. *Gen. Compar. Endocrinol.* **2005**, *143*, 57-65.
- (26) Reischl, U.; Gerdes, C.; Motz, M.; Wolf, H. *J. Virol. Methods* **1996**, *57*, 71-85.
- (27) Ubeidat, M.; Rutherford, C. L. *Prot. Express. Purif.* **2003**, *27*, 375-383.
- (28) Cao, H. P.; Dzineku, F.; Blackshear, P. J. *Arch. Biochem. Biophys.* **2003**, *412*, 106-120.
- (29) de Carlos, A.; Montenegro, D.; Alonso-Rodriguez, A.; de la Cadena, M. P.; Rodriguez-Berrocal, F. J.; Martinez-Zorzano, V. S. *J. Chromatogr., B* **2003**, *786*, 7-15.
- (30) Winter, M. J.; Nagtegaal, I. D.; van Krieken, J. H. J. M.; Litvinov, S. V. *Am. J. Pathol.* **2003**, *163*, 2139-2148.
- (31) Seligson, D. B.; Pantuck, A. J.; Liu, X. L.; Huang, Y. D.; Horvath, S.; Bui, M. H. T.; Han, K. R.; Correa, A. J. L.; Eeva, M.; Tze, S.; Belldegrun, A. S.; Figlin, R. A. *Clinical Cancer Research* **2004**, *10*, 2659-2669.

- (32) Lundstrom, K. *Biochim. Biophys. Acta* **2003**, *1610*, 90– 96.
- (33) Wurm, F. M. *Nat. Biotechnol.* **2004**, *22*, 1393-1398.
- (34) Van Craenenbroeck, K.; Vanhoenacker, P.; Haegeman, G. *Eur. J. Biochem.* **2000**, *267*, 5665-5678.
- (35) Szala, S.; Froehlich, M.; Scollon, M.; Kasai, Y.; Stepkowski, Z.; Koprowski, H.; Linnenbach, A. J. *Proc. Natl. Acad. Sci. U. S. A* **1990**, *87*, 3542-3546.
- (36) Trebak, M.; Begg, G. E.; Chong, J. M.; Kanazireva, E. V.; Herlyn, D.; Speicher, D. W. *J. Biol. Chem.* **2001**, *276*, 2299-2309.

Chapter 4 Immobilization of Aptamers onto Poly(Methyl Methacrylate) Polymer, PMMA, Substrates for Aptamer Sandwich Assay Development and Screening Low Levels of Protein Biomarkers

4.1 Introduction

The analysis of protein biomarkers in biological samples is of great importance in the area of proteomics, diagnostics and drug delivery. In many cases, a large panel of proteins must be analyzed simultaneously in a sample that contains a large number of potential contaminants and to complicate matters, these biomarkers must be quantified with the expression level of the targets spanning many orders of magnitude.¹ For example, tumor markers such as the glycosylated mucin protein MUC1 over-expressed and aberrantly glycosylated on the surfaces of cancer cells and the prostate specific antigen (PSA) are shed at low levels into the bloodstream of adenocarcinoma patients and serves as serum biomarkers in commercial serum tumor marker assays.^{2,3}

High throughput protein biomarker analysis techniques, such as immunoassays in microtitre plate format and protein microarray technologies, in many cases provide the ability to simultaneously screen for a large panel of these biomarkers and can produce the ability to deliver the quantitative information required, even when the targets are present in a large excess of interferences.^{1, 4, 5} Protein microarrays and biosensors utilize high affinity agents such as antibodies, peptides or nucleic acid aptamers, which confer specificity and selectivity in target identification without sample clean up procedures.^{1,6,7} Protein microarrays have been adapted to the current DNA microarray technology to make use of the commercially-available array equipment and confocal scanning systems in producing the arrays and reading their results, respectively.^{4,8,9} Three major immunoassay formats exist for protein arrays. These are the direct assay or reverse-phase immunoassay in which the protein of interest and the standards are

immobilized on a platform and probed with a labeled monoclonal antibody;^{3, 8} the antigen capture assay which utilizes an immobilized antibody for the capture of pre-labeled antigen; and the sandwich immunoassay which utilizes two antibodies to capture and detect the unlabeled antigen.⁸ The sandwich assay is the most effective and preferred means for target analyte identification in complex matrices due to its high sensitivity and stringency through the use of two antibodies.¹⁰

Despite advances made in refining immunoassays for microarrays and biosensors several problems exist which limit the application of antibody microarrays. These include antibody cross-reactivity with cellular proteins, difficulty in the development of sets of antibodies for different epitopes on a target, stability of the immobilized antibody and the difficulty in adapting current protein assay techniques to microarray format.^{4, 8} With the advent of nucleic acid aptamers some of these limitations may be reduced since, for example, the coupling chemistries utilized in DNA microarrays are applicable to aptamers and it has been reported that aptamers exhibit less cross reactivity compared to antibodies.¹

Aptamers are short single stranded oligonucleotide affinity elements which bind with high specificity and selectivity to their targets. They are generated for analytes of interest through systematic evolution of ligands by exponential enrichment (SELEX).¹¹ Aptamer targets range in size from as small as 100 daltons to very large targets such as cells.¹²⁻¹⁴ In addition, aptamers are capable of binding target molecules with specificity comparable to monoclonal antibodies through an induced-fit binding mechanism.¹⁵ Production methods for aptamers via solid phase synthesis make them relatively simple to produce compared to antibodies. They are chemically stable, less susceptible to irreversible denaturation, easily chemically modified and can thus be readily immobilized onto a variety of functional supports without affecting their recognition function.¹⁶ Their smaller size compared to antibodies provides a better chance of

generating aptamers to different epitopes on a protein target and also increasing the surface packing density of arrays and biosensors for increased assay sensitivity.^{16, 17}

The use of aptamers in protein array and biosensor development has been studied by various researchers using fluorescence or electrochemical detection methods for target identification by direct target labeling or sandwich assay. In these studies glass, silicon or polymeric substrates were employed as aptamer immobilization platforms.¹⁸⁻²⁰ For example, in a study by Collet *et al* (2005), functional RNA microarrays were developed on commercially available streptavidin coated microarray slides using an automated arrayer for spotting and a commercial microarray scanner for the readout. Test analytes were pre-labeled with fluorescent dye for their detection.⁷ In separate studies by the same authors, conditions were optimized for the production of aptamer microarrays in an attempt to determine the most suitable buffer and pH to use for simultaneous analysis of different protein biomarkers in a given sample.^{19, 21} In their studies aptamers selected under different buffer conditions during SELEX were immobilized on glass substrate via streptavidin-biotin interaction and assayed using various buffers and at different pHs to create optimum conditions for simultaneously identifying different pre-labeled protein biomarkers.

Sandwich assays using immobilized aptamers and labeled antibodies were developed for optical detection of biomarkers.^{2, 22} Ferreira *et al* (2008) developed a sandwich enzyme-linked immunosorbent assay (ELISA) using a biotinylated aptamer and monoclonal antibody for the detection of mucin protein, MUC1.² In a separate study by Kirby *et al.*, streptavidin-agarose bead with immobilized aptamers were used for the detection of protein targets using an electronic tongue sensor array.²² The sandwich assay format was demonstrated using anti-ricin aptamer as capture element and a fluorophore labeled antibody for detection of the target.

Although dual-aptamer sandwich assays have been demonstrated with electrochemical detection using enzymatic signal amplification, no reports are available on the direct fluorescence detection of target proteins using the sandwich assay method. Electrochemical detection of enzymatic signal amplification for biosensors based on aptamer sandwich assays was demonstrated in a study by Ikebukuro *et al.*²³ In this study the authors developed an electrochemical biosensor for thrombin using a glucose dehydrogenase (GDH) linked aptamer sandwich-type assay. A GDH-labeled anti-thrombin aptamer was used in conjunction with a thiolated capture aptamer immobilized on gold substrate in detecting the protein. The electrochemical signal was generated by the action of the GDH enzyme on its quinone substrate.²³

An important contributor to performance of nucleic acid arrays and biosensors in terms of reproducibility, probe density and availability is the immobilization of the capture element.²⁴ Various immobilization chemistries are available for aptamer attachment on different substrates in biosensor and microarray development. These include covalent, cross-linking and non-covalent binding interactions such as affinity binding, adsorption and absorption.^{4, 20, 25} One of the most widely used non covalent immobilization chemistries is the streptavidin-biotin interaction due to the high affinity of the biotin molecule for streptavidin.²⁴ Covalent attachment is the most common commercial method of nucleic acid immobilization on many supports due to its simplicity, higher packing density and the ease of derivatizing nucleic acids during synthesis depending on the immobilization surface and covalent linkage employed.^{24, 26, 27}

To provide flexibility and enhance binding interaction between the capture element and the target, long linkers can be incorporated at the end of the capture element to reduce steric hindrance after immobilization.¹⁷ Our group recently reported on the effect of linker length on the binding specificity of a thiol-terminated aptamer immobilized on gold slides to its target,

thrombin, in studies using Surface Plasmon Resonance. Results indicated that by utilizing a polyethylene glycol linker, a 4-fold increase in the binding capacity of the self-assembled monolayer created was achieved compared to the aptamer monolayer without the polyethylene glycol linker.²⁸ Thus, by designing the capture aptamer with a linker to further extend it from the surface of the support, enhanced binding interaction with the target can be achieved.

In an attempt to develop rapid, low cost, disposable single use components in diagnostic bioassays, plastic substrates are providing a viable alternative to glass-based supports. Several thermoplastic polymers have been used to fabricate bioanalytical devices including polystyrene, polycarbonate²⁹ and poly(methyl methacrylate), PMMA, all employing different immobilization chemistries.²⁰ Many polymers have good optical clarity for reading microarrays via optical techniques, with evolving chemical modification procedures appropriate for ligand attachment.²⁴ In addition, these materials are easily molded for generating complex microfluidic architectures in the development of integrated microdevices.³⁰ In our laboratory, PMMA and PC have been used for a variety of different devices and applications, including those that require immobilization of probes, such as oligonucleotides, for DNA microarray applications.^{31, 32}

Immobilization of nucleic acid ligands onto PMMA and PC surfaces has been achieved through ultraviolet³³ radiation activation of the polymers to generate carboxylic acid groups as scaffolds for carbodiimide coupling of amine terminated oligonucleotides to the polymer surface. Studies have been carried out to determine the optimum UV exposure time for polymer activation in order to generate a high density of functional groups and to determine which polymer provided the best signal-to-noise ratio (SNR) for optical readout and surface loading of the recognition element.³¹ These studies found PMMA to be particularly attractive for DNA microarray studies compared to PC due to its superior optical properties and also, it showed significantly lower levels of non-specific adsorption of targets.³¹ In another study by Fixe *et al*, a

one-step immobilization of aminated and thiolated DNA molecules onto unmodified methyl esters of PMMA was carried out.²⁰ Results showed immobilized probe densities greater or equivalent to those obtained by commercially available immobilization methods.

The focus of this study was to develop dual-aptamer sandwich assays on PMMA substrates using direct fluorescence detection without signal amplification techniques. As a model for these investigations, thrombin and PDGF-BB were used, because these proteins serve as biomarkers of different diseases and are present in serum. Thrombin has been widely studied for aptamer production and has two DNA aptamers that recognize different epitopes on the protein.³⁴ PDGF exists as a dimeric protein with three isoforms, PDGF-AA, PDGF-BB and PDGF-AB. An aptamer developed toward PDGF has high affinity for the B chain of the protein.³⁵ Using thrombin and its aptamers we first determined the most suitable aptamer for immobilization onto the PMMA substrate with subsequent capture of the target by considering the ease of G-quartet structure formation of the PMMA immobilized aptamer and also the effects of heat treatment on the adoption of the G-quartet structure. Dual-aptamer sandwich assays were then performed using a fluorophore-labeled aptamer for direct detection of thrombin. Conditions were optimized for a one-step covalent attachment of aptamers to UV-modified PMMA by carbodiimide coupling chemistry, to ensure optimal aptamer density and uniformity in immobilization for more efficient and enhanced target binding to the PMMA chip. Sandwich assays were developed for thrombin and PDGF-BB protein using different aptamers for thrombin and the same aptamer for PDGF protein with minimal assay performance steps and shorter assay time.

4.2 Experimental

4.2.1 Reagents and Materials

Aptamers used in this study were obtained from Integrated DNA Technologies (Coralville, IA) and are shown in Table 4.1. Nuclease-free water, 1-ethyl-3-(3-

dimethylaminopropyl) carbodiimide hydrochloride (EDC), N-hydroxy succinamide (NHS), Tris(hydroxyamino) methane (Tris), 4-(2-hydroxyethyl)-1-piperazine ethanesulfonic acid (HEPES), 2-(*N*-morpholino)- ethanesulfonic acid (MES), sodium chloride (NaCl), magnesium chloride (MgCl₂) and potassium chloride (KCl) were obtained from Sigma-Aldrich (St. Louis, MO). PMMA sheets of 0.5 mm thickness were purchased from GoodFellow (Berwyn, PA), N-methyl mesoporphyrin IX (NMM) was obtained from Frontier scientific (Logan, UT), Thrombin was purchased from Haematologic Technologies (Essex Junction, VT) and PDGF-BB and AB from R&D Systems (Minneapolis, MN).

4.2.2 Methylmesoporphyrin IX (NMM) Fluorescence Enhancement Test G-Quartet Structure Formation of Immobilized Thrombin Aptamers

PMMA sheets of 0.5 mm thickness were UV activated for 15 min (wavelength 260-300 nm) and then treated with 10 µg/ mL each of the thrombin aptamers, HD1 (sequence B1) and HD22 (sequence A) given in Table 4.1, in PBS buffer (pH 7.4) containing 40 mM NHS and 50 mM EDC for 4 h at room. The aptamer modified chips were rinsed with nuclease-free water and stored at 4 °C overnight. To determine the conformation adopted by the immobilized thrombin aptamers in solution, the NMM fluorescence enhancement test was performed.³⁶ Absorbance measurements were carried out on 40 µM NMM in Tris buffered saline (TBS) and phosphate buffered saline (PBS) to determine the appropriate excitation wavelength using an Ultrospec 4000 UV/visible spectrophotometer (Pharmacia Biotech, Cambridge, England). One centimeter wide strips of thrombin aptamer modified PMMA were either dipped in TBS containing 1 mM MgCl₂ and 5 mM KCl at room temperature, or dipped in the buffer at 80 °C and allowed to cool to room temperature. Each PMMA strip was transferred to a 1 µM solution of NMM in a fluorescence cuvette and aligned against one wall of the cuvette perpendicular to the fluorescence emission collection path. Fluorescence measurements were obtained on a Fluorolog

fluorimeter (Yvon Jobin Inc., Edison, NJ) between 550 and 750 nm at an excitation wavelength of 400 nm. UV-modified PMMA strips without immobilized aptamers served as control chips.

Table 4. 1: Sequences of DNA aptamers of thrombin (A-D), PDGF (E and F) used in sandwich assay development and the aptamer (G), a DNA variant of the prostate specific antigen aptamer, used for optimizing the EDC/NHS immobilization protocol on PMMA. Abbreviations used in the table are: AmMC6 = primary amine modification with a six carbon linker, iSp9 and iSp18 represent the internal spacers triethylene glycol and hexaethylene glycol respectively. The internal spacer, iSp18, was used to further extend immobilized aptamers from the surface to reduce steric effects and improve interaction of the aptamers with their targets.

	Aptamer	Aptamer sequence
A	HD22-NH2	5' /AmMC6/TT-AGT CCG TGG TAG GGC AGG TTG GGG TGA CT-3'
B1	HD1-NH2	5'/AmMC6/TTTT-GGT TGG TGT GGT TGG-3'
B2	Cy5-HD1	5'/Cy5/TTTT-GGT TGG TGT GGT TGG-3'
C	HD22-NH2	5'-/5NH ₂ -C ₆ /iSp18/-AGT CCG TGG TAG GGC AGG TTG GGG TGA CT-3'
D	Cy5.5-HD1	5'/5Cy5.5/iSp9/GGT TGG TGT GGT TGG-3'
E	PDGF aptamer 1	5'/AmMC6//iSp9/-CAG GCT ACG GCA CGT AGA GCA TCA CCA TGA TCC TG-3'
F	PDGF aptamer 2	5'/Cy5.5//iSp9/-CAG GCT ACG GCA CGT AGA GCA TCA CCA TGA TCC TG-3'
G		5'/AmMC6//iSp18/ACC GAA AAA GAC CTG ACT TCT ATA CTA AGT CTA CGT TCC/Cy5.5/3'

4.2.3 Aptamer Sandwich Assay for Thrombin by Laser Scanning Confocal Microscopy (LSCM)

PMMA sheets of 0.5 mm thickness were activated by UV light (260-300 nm for 15 minutes) through a 750 mesh Nickel TEM grid (SPI Supplies, west Chester ,PA) to generate a grid network of 25 μm^2 areas of activated surface separated by 8.6 μm wide unmodified regions that were not exposed to UV light. The UV-modified PMMA sheets were cleaned by sonication in MilliQ water for 2 min and air dried. A 1.18 μM concentration ($\sim 10 \mu\text{g}/\text{mL}$) of aptamer A (see Table 4.1), was immobilized on the UV modified PMMA sheets by carbodiimide coupling chemistry using 40 mM NHS and 50 mM EDC in phosphate buffer (pH 7.4). The reaction was

allowed to proceed for 4hr at room temperature and the HD22 immobilized chips were rinsed with deionized water and stored at -20 °C until required for further use.

Sandwich assays were performed in PBS buffer containing 10 mM KCl, 140 mM NaCl and 1 mM each MgCl₂ and CaCl₂. A 2.5 μM fixed concentration of aptamer B2 (table 1) was incubated for 10 min with various concentrations of thrombin ranging from 0 – 1 μM at room temperature. Twenty-five microliter aliquots of each HD1-thrombin sample was evenly distributed onto 1” x 0.2” chips of HD22-immobilized PMMA and the assays incubated overnight at 4 °C. The chips were then rinsed with PBS and deionized water and dried. Ten milligrams per milliliter BSA were similarly incubated with 2.5 μM aptamer B2 and an HD22 chip and prepared for analysis. The assay chips were mounted on microscope slides with cover slips prior to LSCM analysis.

The slides were imaged using a Leica TCS SP2 Spectral Confocal and Multiphoton Microscope (Leica Microsystems, Mannheim, Germany) equipped with a photomultiplier tube (PMT) detector. Images of the chips were obtained using a 63x oil immersion objective at 633 nm excitation, a scan rate of 200 Hz and the PMT set at 700 V. Images were analyzed using Image Quant V.5 software (Molecular Dynamics, Sunnyvale, CA).

4.2.4 Sandwich Assays for Thrombin and PDGF-BB Analyzed Using a Home-Built Near-IR Array Scanner

To generate dual aptamer sandwich assays for simultaneous detection of different concentrations of thrombin or PDGF-BB on a single chip, approximately 1 μM of aptamer C (for thrombin capture) and E (for PDGF-BB capture (see Table 4.1) were each immobilized onto UV-activated PMMA using 40 mM NHS and 50 mM EDC in MES (pH 6.7) buffer overnight. The lower pH was selected to ensure protonation of the carboxylic acid groups on the PMMA surface for enhanced formation of succinimidyl esters during the coupling reaction. Also, a polyethylene glycol linker was introduced at the 5’ end of the aptamers to increase

flexibility and reduce steric effects due to immobilization. The aptamer-modified chip was dipped in TBS-TPG buffer at 40 °C and cooled to room temperature. The chip was treated with 1 μ L volumes of different concentrations of protein pre-incubated with 3 μ M detection aptamer (see Table 4.1) in TBS-TPG for 5 min at 37 °C. The assays were incubated overnight at 4 °C, gently rinsed in buffer to remove unbound protein, dried and fixed on a microscope slide with a cover slip and scanned at 680 nm excitation on a home-built near-infrared (near-IR) fluorescence scanner that has been previously described.³¹ Briefly, the scanner consisted of a 670 nm 10 mW laser diode (Thorlabs, Newton, NJ) for sample excitation, a set of optical filters consisting of a neutral density filter (ND 0.6; Thorlabs) and a line filter (670DF20; Omega Optical, Brattleboro, VT), a beam splitter (690 DRLP; Omega Optical, Brattleboro, VT), a 40x high numerical aperture (NA 0.85) microscope objective (Nikon, Natick, MA) for focusing the laser beam on the array. The fluorescence was collected through the same objective and transmitted through a dichroic, 700 ALP longpass and 720 DF20 bandpass filters (Omega Optical) and a pinhole to a single-photon avalanche detector (SPAD). Samples were mounted on an X/Y translational stage and scanned at a 50.8 μ m step-size with a 0.1 s/ pixel integration time. Data acquisition was performed using software written in Visual Basic.

4.2.5 Optimization of Conditions for EDC/NHS Immobilization of Aptamers onto PMMA

To Optimize the EDC/NHS coupling protocol by shortening the immobilization time and increasing the immobilized aptamer density for aptamer immobilization onto PMMA surfaces for microarray development, aptamer G in Table 4.1 was used. Approximately 1 μ L volumes of various concentrations of G (5, 10, 15, 20 and 40 μ M) in 50 mM MES buffer (pH 6.7) with 2% glycerol, 50 mM EDC and 40 mM NHS were deposited on UV-modified 0.5 mm thick PMMA chips. One chip was incubated at 37 °C for 30 min and the other for 5 h, rinsed with deionized water and dried. The aptamer was similarly spotted in 50 mM HEPES buffer (pH 7.2)

containing 0.1% PEG 400, 2 % glycerol, 200 mM EDC and 40 mM NHS on UV activated PMMA. Incubation of the chips at 37 °C was for 30 and 80 min in a water bath prior to rinsing and drying. The chips were scanned at 680 nm excitation on the home-built near-IR fluorescence scanner at a 50 μ m step-size and an integration time of 0.1s per pixel.

4.2.6 Sandwich Assays for Thrombin and PDGF Using Optimized Immobilization Conditions

UV-modified PMMA chips were treated with 10 μ M each of amine terminated HD22 and PDGF aptamer (aptamers C and E in Table 4.1) in HEPES buffer with 200 mM EDC and 40 mM NHS, by inundating PMMA chips with a capture aptamer in HEPES buffer with EDC/NHS. The aptamer immobilized chips were treated as previously described for sandwich assays with minor changes. Instead of an overnight incubation of the sandwich assays, the assays were incubated for 1 h at 37 °C and processed for scanning on the near-IR scanner. Concentrations of Cy5.5-HD1 and Cy5.5-PDGF aptamers were fixed at 1 μ M and 500 nM respectively for detection of thrombin and PDGF.

4.3 Results and Discussion

4.3.1 NMM Fluorescence Test for Evaluating G-Quartet Structure Formation of Immobilized Thrombin Aptamers

Schematics of the UV modification and aptamer immobilization onto PMMA and the NMM fluorescence enhancement processes are depicted in Figure 4.1A and 4.1B. The immobilized capture element in an array or biosensor plays an important role in the sensitivity of the bioassay in terms of its ability to bind the target and its packing density.^{16,17} In developing a dual aptamer sandwich-type assay for thrombin using two aptamers that recognize different epitopes on the protein, an important consideration was the ability of the immobilized aptamer to maintain the necessary conformation required for binding the target protein with high affinity. The formation of an intramolecular G-quartet structure is essential to binding of thrombin by its

aptamers.³⁷ Thus the ability of the immobilized thrombin aptamers to form and maintain the G-quartet structure may enhance the performance of the sandwich assay. In order to select the more appropriate of the two aptamers for capturing thrombin in a sandwich-type assay, we considered the stability of G-quartet structure formation in addition to a higher binding affinity.

In a capillary electrochromatographic study by Joyce and McGown (2004), the adoption of the G-quartet structure by thrombin aptamers immobilized in a glass capillary was studied using NMM dye fluorescence enhancement.³⁶ This dye has been shown to selectively bind the three dimensional G-quartet structure of single-stranded DNA leading to fluorescence enhancement of the bound dye.³⁸ Results of the NMM fluorescence emission measurements at 610 nm performed on PMMA immobilized HD1 and HD22 aptamer chips are shown in Figure 4.1C. The absorbance maximum of NMM in Tris buffer was determined and an excitation wavelength of 400 nm was selected for these fluorescence measurements. Samples of PMMA immobilized aptamer dipped in 1 μ M NMM after heating to 80 °C and cooling in Tris buffered saline (TBS) showed an increase in fluorescence intensity compared to samples place directly in NMM solution without prior heat treatment. This is due to structural re-orientation of the heat treated aptamers to form the intra-molecular G-quartet conformation. The HD22 aptamer showed the highest fluorescence enhancement after heat treatment due to its higher structural stability produced by the formation of a four nucleotide DNA duplex through its 5' and 3' ends.³⁷ Even in the unheated samples the fluorescence intensity for the HD22 chip was slightly higher than that for the HD1 chip. The HD1_c sample showed the lowest fluorescence intensity of all four samples.

Because fluorescence enhancement of NMM occurs in the presence of the G-quartet structure, the lower fluorescence intensities obtained for the chips not subjected to heat treatment indicated potential DNA conformations other than the quadruplex. Thus, aptamers immobilized

on surfaces that require a G-quartet conformation for high target recognition capability may require heat treatment prior to performing the affinity assays to enable formation of the quadruplex structure for specific and stable target binding. Because HD22 showed the highest fluorescence enhancement and due to its higher binding affinity for thrombin, we selected HD22 as the capture element for the sandwich assay and used HD1 as the detection probe.

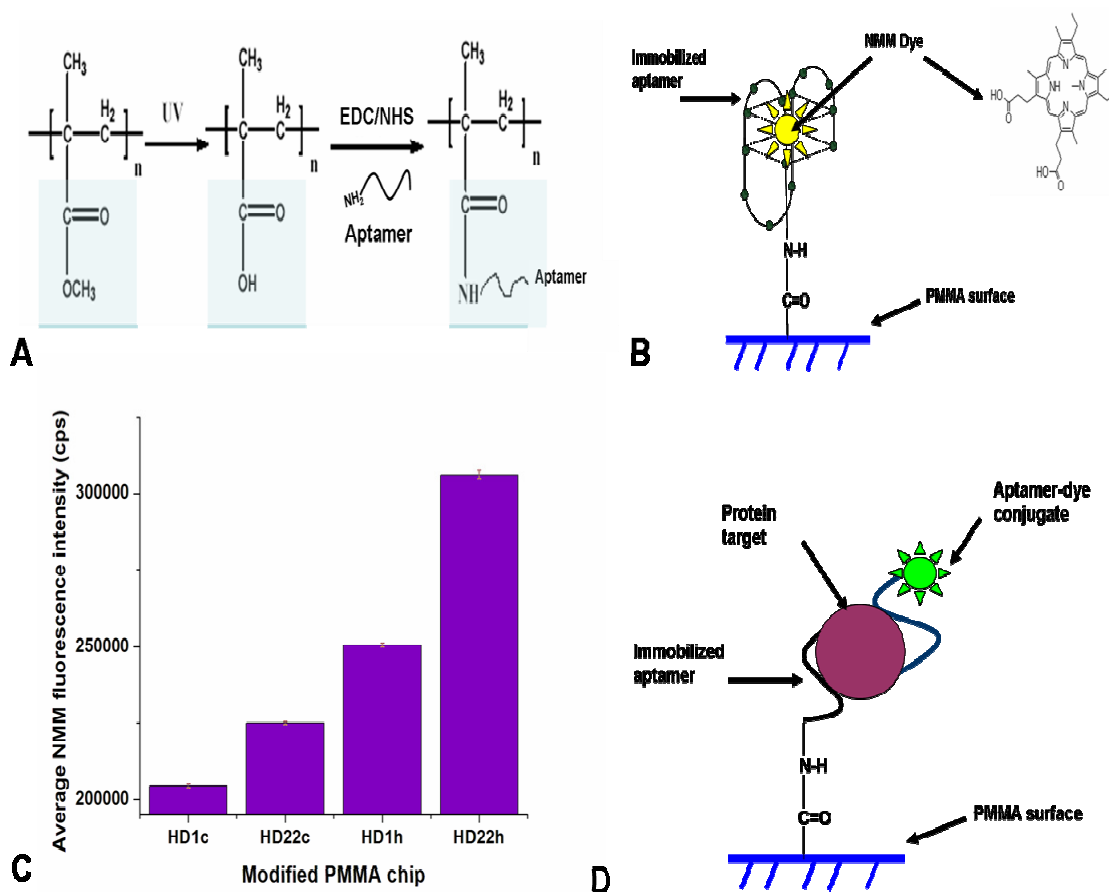


Figure 4. 1: A) Schematic of the UV-modification and EDC/NHS coupling process used in immobilizing aptamers onto PMMA, (B) Depiction of the NMM fluorescence enhancement assay showing intercalation of the dye to the G-quartet structure of the aptamer resulting in fluorescence enhancement. (C) The results of the fluorescence enhancement assays for HD1 and HD22 immobilized covalently onto PMMA chips. The aptamer chips were either heat treated at 80 °C in buffer and cooled prior to immersion in NMM solution (h) or placed in the solution without heat treatment (c) with un-functionalized PMMA as the control. Fluorescence emission was obtained at 610nm with excitation at 400 nm. (D) Schematic depicting the aptamer sandwich assay performed for thrombin and PDGF proteins on a PMMA substrate with immobilized aptamers.

4.3.2 HD1-HD22 Sandwich Assay for Thrombin Detection

One of the potential advantages of using aptamers in detection of protein targets in arrays is the ability to spot multiple aptamers capable of recognizing different proteins for doing spatial multiplexing and then, reading successful molecular association events by a second aptamer that binds to another epitope on the same target, which eliminates the need for labeling the target with a fluorophore or other reporting entity. Because thrombin and its aptamers HD1 and HD22, which bind to different epitopes, have been well studied, we used this system as a model for investigating the formation of aptamer recognition arrays onto PMMA solid support. Figure 4.1D shows a general schematic of the sandwich assay adopted for the protein targets studied herein. Because UV-irradiation of PMMA creates a functional scaffold of carboxylic acids that can be subsequently treated with EDC/NHS to covalently attach primary amines through amide bond formation,³⁰ initial studies were performed with the PMMA substrate UV-modified through a TEM grid to create regions of HD22 aptamer functionalized PMMA and areas essentially unmodified by UV radiation and thus, contained no immobilized aptamer. The HD22 functionalized chips were treated with target protein and a fixed concentration of 2.5 μ M Cy5-HD1 and imaged by LSCM after an overnight incubation at 4 °C (see Figures 4.2 and 4.3).

Figure 4.2A shows an image of a 10 nM thrombin sandwich assay chip acquired by LSCM showing areas of high fluorescence containing the sandwich assay and regions of low signal intensity indicating areas free of any discernible thrombin, which would indicate that only the UV-modified regions were able to support the covalent attachment of the recognition aptamer. In Figure 4.2B is shown the intensity plot taken from the image shown in Figure 4.2A in relative fluorescence units (rfu). As can be seen, the fluorescence intensity dropped to nearly 0 in those areas not exposed to the UV-radiation through the TEM grid shadow mask, indicating

the lack of any thrombin or reporter aptamer non-specifically adsorbing to the PMMA surface, consistent with our previous results using PMMA as supports for DNA microarrays.³¹

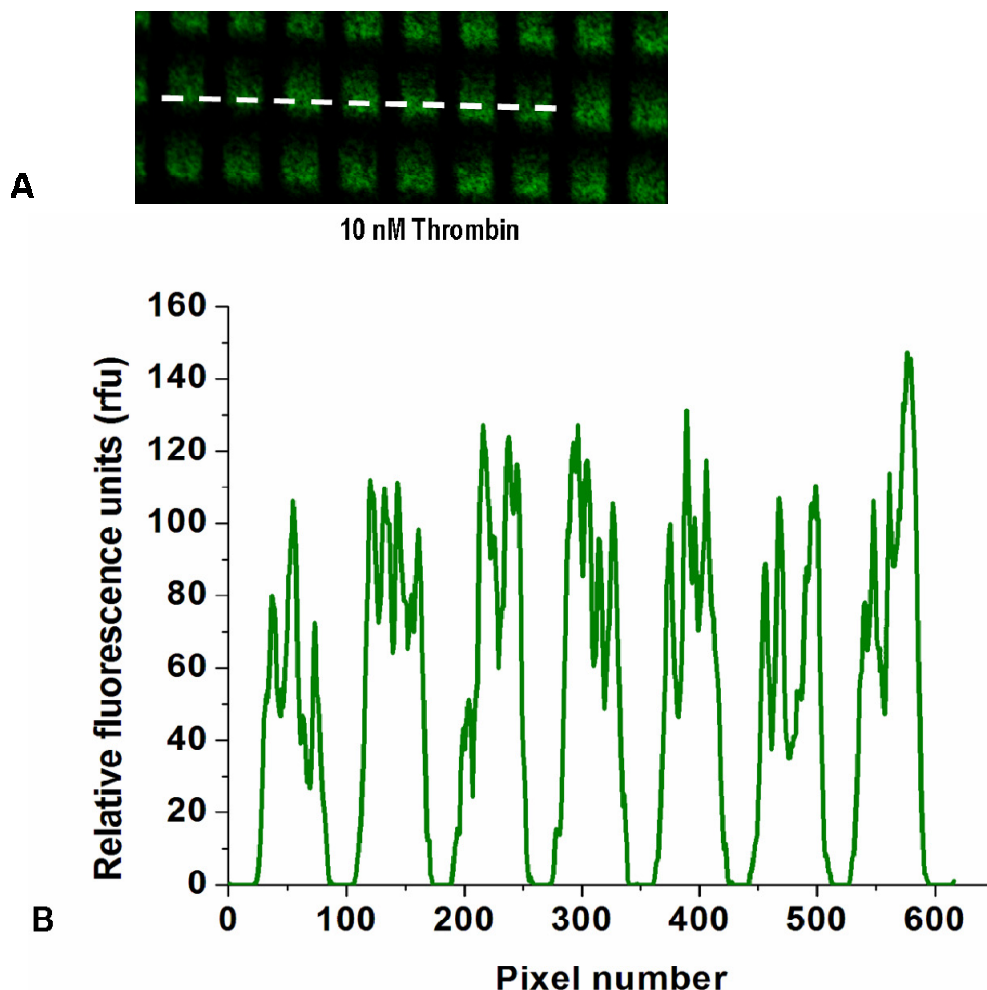


Figure 4. 2: LSCM analysis of thrombin aptamer sandwich assay on PMMA UV modified through a TEM grid showing A) an image of HD22 functionalized chip treated with 10 nM thrombin assayed with 2.5 μ M Cy5-HD1 with the detector set at PMT voltage of 700 V and B) a graphical representation of the chip obtained using ImageQuant analysis. The line drawn across the image in (A) represents the sampling section obtained for the profile shown in (B). Chips were incubated overnight at 4 $^{\circ}$ C prior to scanning.

Results of LSCM imaging of the aptamer chips showed specificity of the assay for thrombin compared to BSA (see Figure 4.3). A comparison of the average rfu values obtained for aptamer-functionalized areas and non-functionalized areas of each sandwich assay chip indicated a difference in intensities of the two regions for the thrombin treated chips. However,

no difference in intensity values was obtained for the HD22-chip treated with 10 mg/mL BSA and the HD1-Cy5 detection aptamer.

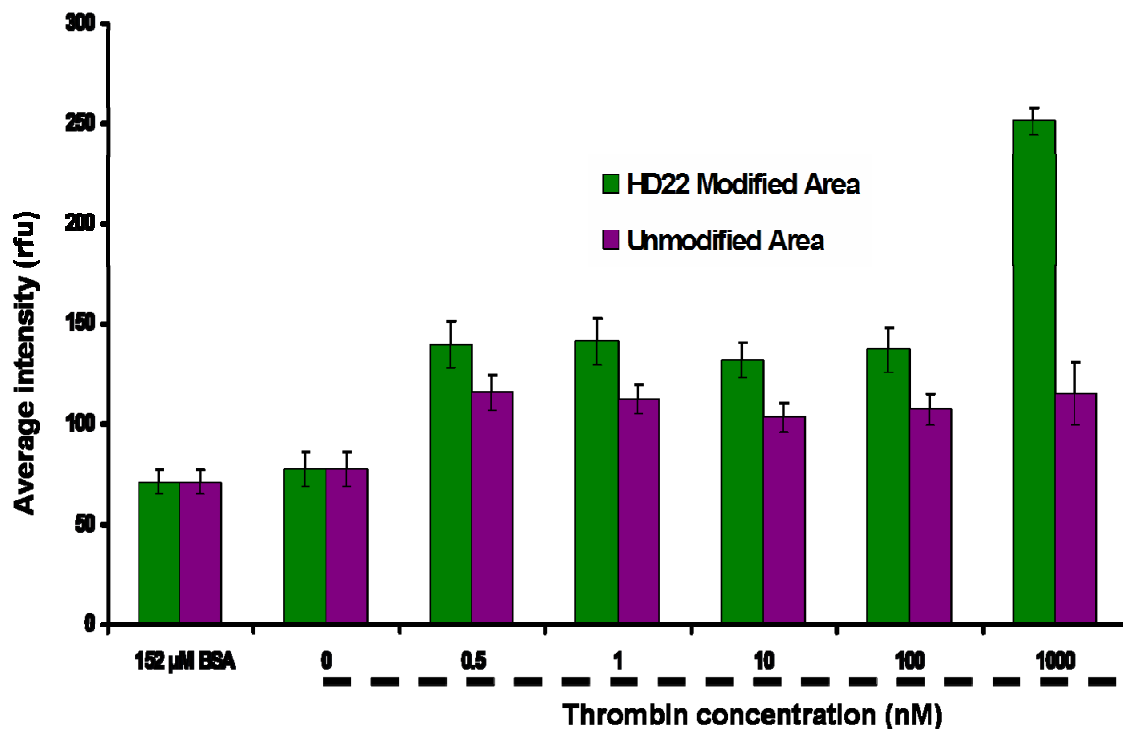


Figure 4. 3: ImageQuant analysis of LSCM images acquired for thrombin aptamer assays performed on PMMA that was UV-modified through a TEM grid. The bar graph shows intensity differences of the LSCM images of HD22 functionalized and unmodified regions of the PMMA chips generated for different thrombin concentrations, BSA and the control samples. The blank is an HD22 immobilized chip treated with Cy5-HD1. A chip treated with 10 mg/ mL BSA was used in testing specificity of the assay for thrombin. Images were obtained at a fixed PMT voltage of 700 V.

Also, the average intensity for the BSA chip was lower than values obtained for thrombin treated chips indicating specificity of the assay for thrombin. From Figure 4.3 the highest values were obtained for 1 μ M thrombin. Very little change in intensity of the assay was observed for thrombin concentrations of 100 nM and below. This may be due to the limiting effect of the surface coverage of immobilized aptamer on the PMMA surface. Two dimensional plots of the images, as shown in Figure 4.2, show non-uniformity in intensity of the assay regions. This is an indication of an increased PMMA surface roughness^{39, 40} which, may affect aptamer

immobilization. Also, the use of several pieces of PMMA in generating assays for different target concentrations introduced variability in results obtained due to differences in assay characteristics between the PMMA chips in terms of PMMA surface topography and the amount of aptamer immobilized on each chip.

Previous reports in our group on the amount of carboxylic acid groups generated on UV-modified PMMA show that between 0.8 to 1.3 nmoles/ cm² (8 to 13 picomoles/ mm²) of the functional group are generated for 10 to 30 min UV exposure times.⁴⁰ Thus, less than optimal immobilization conditions could affect the amount of aptamer immobilized, thereby affecting the performance of the assay in terms of the amount of protein bound and the time required for binding interactions between the target and immobilized aptamer to occur. In this experiment the carbodiimide coupling reaction was performed in phosphate buffer which has been reported to interfere with the EDC coupling of primary amines with carboxylic acid groups.⁴¹ Immobilizations were thus, carried out in MES buffer at pH 6.7 to prevent hydrolysis of EDC by phosphate buffer components.⁴¹

In order to generate sandwich assays for the detection of various concentrations of protein on a single chip, spots of thrombin and PDGF-BB sandwich assays were respectively generated on HD22 and PDGF aptamer-modified PMMA substrates and analyzed using a fluorescence scanner built in-house (see Figures 4.4A and 4.4B). Figure 4.4A shows spots of 50 % serial dilutions of each protein incubated with 3 μ M Cy5.5-labeled detection aptamer on aptamer-modified PMMA. Thrombin concentrations ranged from 0 to 4 μ M while PDGF-BB concentrations were varied from 0 to 1.85 μ M. Results for the thrombin sandwich assays (see Figure 4.4B) showed an increase in intensity of the spots with increasing thrombin concentration, an indication of the effectiveness of the sandwich assay in detecting thrombin. The assays for PDGF-BB were less effective compared to the thrombin assay. The plot of fluorescence intensity

versus protein concentration for the PDGF-BB assays showed an increase in signal intensity at the higher concentrations of 925 nM and above. Also, the assays required an overnight incubation for detection of the target, an indication that the immobilization conditions were still not optimal for performing the assays.

4.3.3 Optimization of the Aptamer Immobilization Protocol

We were interested in improving the rate of target binding and assay sensitivity by increasing the aptamer surface density through optimization of the immobilization conditions in terms of pH and EDC reagent concentration. Variations in the carbodiimide coupling chemistry for immobilizing DNA to UV modified PMMA surfaces exist.^{31, 39, 42, 43} For example, multiple-step immobilization processes has been reported in which the oxidized PMMA is first treated with EDC/NHS in MES buffer at pH 5 to enhance modification of the carboxylic acid groups. The amine functionalized DNA to be immobilized is then added in the same buffer to generate microarray spots.^{31, 42} The probe concentrations used for the immobilization processes in these studies ranged from 100 nM to 20 μ M with incubation times from 1 h to greater than 5 h.

Reports in literature indicate that although the addition of a succinimide to EDC stabilizes the reaction with carboxylic acid groups through the formation of a more stable succinimidyl ester intermediate, the reaction of succinimidyl esters with primary amines occurs more efficiently at basic pH values at which the primary amines are unprotonated.⁴⁴ Thus, immobilization of the amine terminated capture aptamer may still not be efficient at the acidic pH values necessary for EDC modification of carboxylic acid groups and longer incubation times may be required at the lower pH to ensure higher coupling efficiency. This may lead to excessive drying of the reaction mixture resulting in non-uniform immobilization of the aptamers. Non-uniformity in immobilized oligonucleotide densities have been reported as a condition that affects sensitivity of microarrays due to variation in the functional group densities on the

surfaces of the immobilization substrate.¹⁷ In addition, evaporation of the immobilization mixture after spotting leads to higher probe concentration at the outer edge of the spot compared to the center leading to non-uniform probe deposition on the support, which affects the performance of the assay.¹⁷

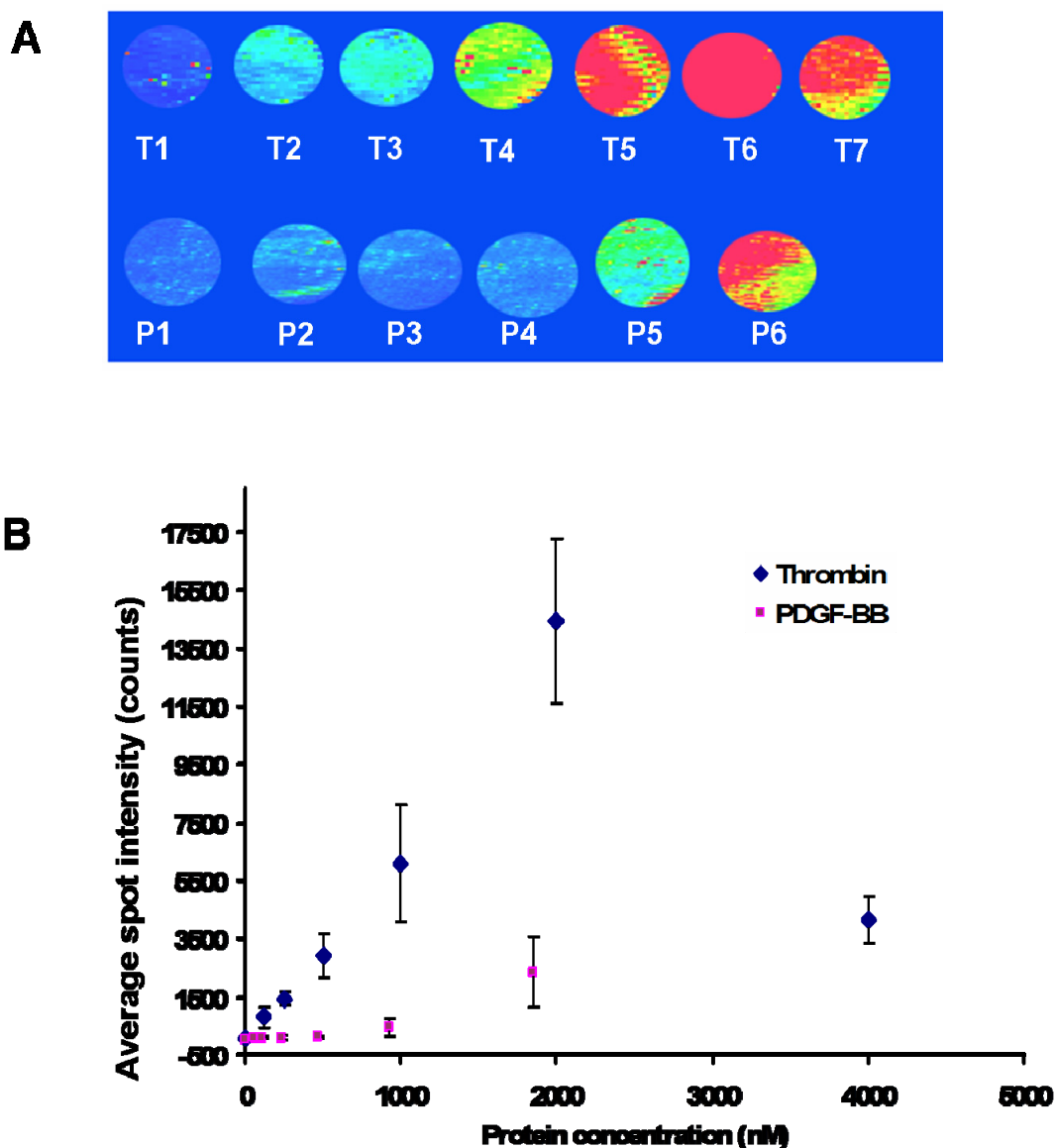


Figure 4. 4: Near-IR fluorescence images of 1:1 serial dilutions of thrombin (0, 0.125, 0.25, 0.5, 1.0, 2.0 and 4 μ M) and PDGF-BB (0, 0.058, 0.115, 0.231, 0.462, 0.925 and 1.85) were mixed with 3 μ M Cy5.5-labeled aptamer (aptamer D and F in table 1) and spotted on an HD22 and PDGF-functionalized PMMA slides respectively. The slides were incubated overnight at 4 $^{\circ}$ C prior to scanning. The scan rate was 500 μ m/s over a scan area of 18 x 20 mm. In (A) thrombin samples are represented as T1-T7 and PDGF-BB samples are represented as P1 – P6 in increasing order of protein concentration.

Thus, to optimize the coupling efficiency for higher aptamer density and uniformity and to shorten the time for immobilization of aptamers to PMMA surface, an aptamer amine-terminated at the 5' end and Cy5.5 dye labeled at the 3' end was used.

We first carried out immobilization studies on different dye labeled aptamer concentrations in MES buffer at pH 6.7 as previously performed for the sandwich assays to determine the probe density in terms of fluorescence intensity at shorter incubation times. In another set of experiments using HEPES buffer, we increased the EDC concentration to 200 mM to compensate for its rapid hydrolysis in the presence of amine nucleophiles⁴¹ and increased the pH to 7.2 to create a less acidic environment for better reaction of the succinimidyl ester intermediates with the primary amine moieties on the 5'-end of the aptamer. The amine-terminated oligonucleotide was added to the buffer containing EDC and NHS and spotted on UV activated PMMA. The incubation temperature was increased from room temperature to 37 °C and the incubation time shortened to between 30 min to 5 h for the reaction in MES buffer and 30 min and 80 min for the HEPES buffer reaction. A 2% glycerol concentration was used in the buffers to reduce dehydration of the reaction mixtures during the immobilization process.

Results indicated that in both buffer systems the average fluorescence intensity of the spots obtained across the width of each spot increased with increasing aptamer concentration especially at the higher concentrations of 20 and 40 μM (see Figure 4.5A and B). Variations in the uniformity of the spot intensities were higher at the shorter incubation time of 30 min (Figure 4.5A). By increasing the EDC concentration and increasing the pH to 7.2, the aptamer spot intensities increased above the values obtained in MES at the lower pH and lower EDC concentration, due to increased reaction rate at the higher EDC concentration and stability of the carbodiimide coupling reaction at neutral pH compared to the lower pH.⁴⁵ The 80 minutes incubation in HEPES buffer provided the highest coverage density of the oligonucleotide (see

Figure 4.5B). Based on the results obtained immobilization of aptamers for sandwich assay development was performed in HEPES buffer at pH 7.2 for 80 min.

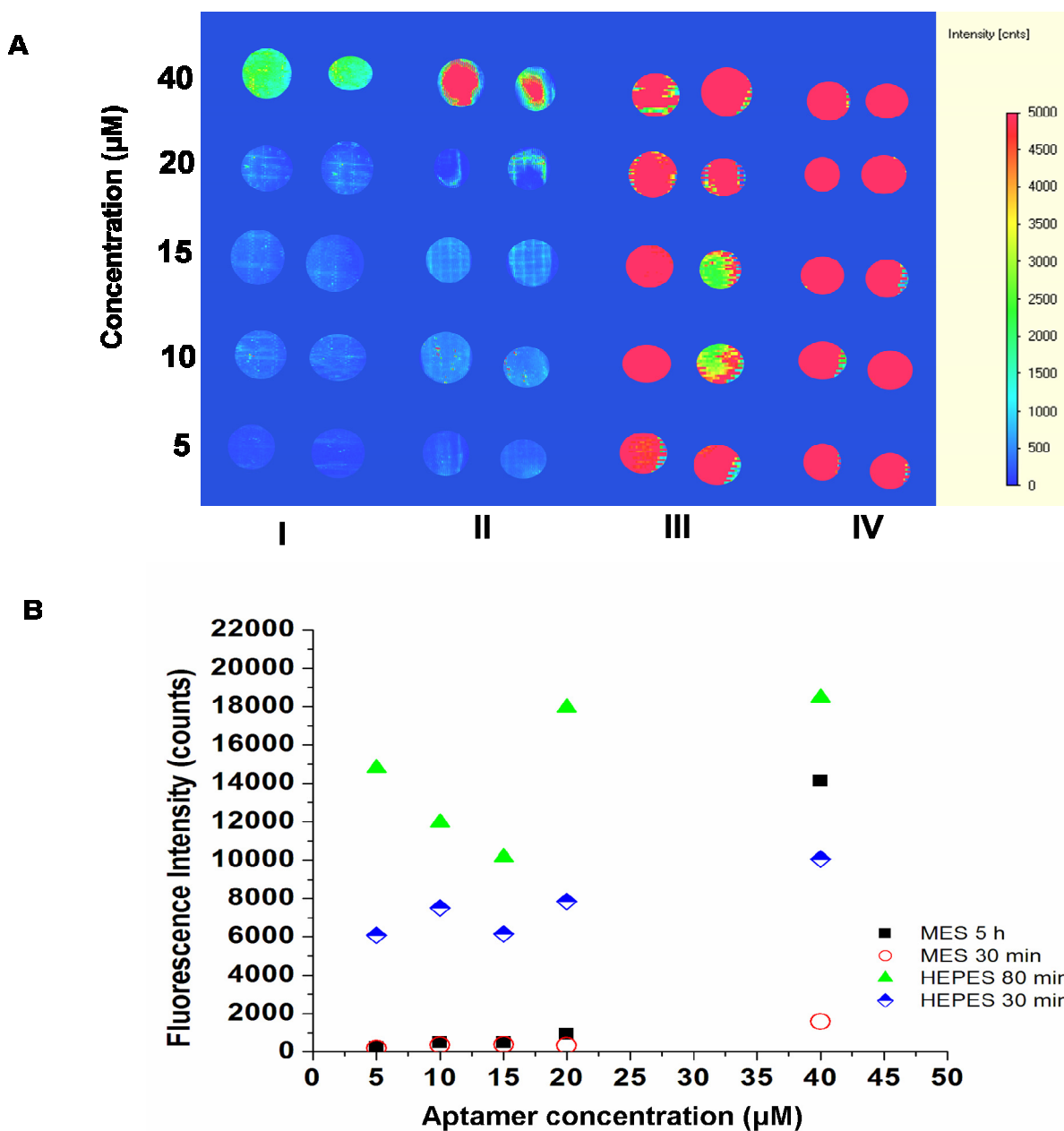


Figure 4.5: A) Images of a one-step EDC/NHS coupling reaction for various concentrations of immobilized Cy5.5 labeled aptamer (G) onto UV-modified PMMA with different incubation times of I) 30 min and II) 5 h in pH 6.7 MES buffer and III) 30 min and IV) 80 min in pH 7.2 HEPES buffer, and B) plots of fluorescence intensity of the spots showing the effect of pH and EDC concentration on the coverage density of the labeled aptamer. The MES buffer contained EDC at 50 mM while in the HEPES buffer EDC concentration was increased to 200 mM with a fixed 40 mM NHS concentration in both buffers. Imaging conditions are the same as those given in Figure 4.4.

4.3.4 Sandwich Assay Development Using Optimized EDC/NHS Immobilization Conditions

In order to further reduce the sandwich assay time, we investigated the effects of incubation time on the fluorescence response. Capture aptamers were immobilized at 10 μM concentrations in pH 7.2 HEPES buffer containing 200 mM EDC and 40 mM NHS for 80 min at 37 $^{\circ}\text{C}$. Results of the sandwich assays performed using 1 μM aptamer D for thrombin and 0.5 μM aptamer F for PDGF-BB detection are displayed in Figure 4.6.

Plots of sandwich assay fluorescence intensity versus protein concentration showed a general increase in intensity with increasing protein concentration. The slope of the curve for the PDGF assay (4.81 cnts/ nM) was sharper compared to that of the thrombin assay (1.42 cnts/ nM) within the linear region of each plot (see Figure 4.6 A and B). This implied higher sensitivity of the PDGF assay (see Figure 4.6A) as a result of the lower K_D value of the PDGF aptamer. The reported K_D value for the PDGF aptamer is 10^{-10} , whereas that for HD1 is between 10^{-8} and 4×10^{-7} , and 5×10^{-10} for HD22.^{35,37} Above a PDGF-BB concentration of 250 nM corresponding to an aptamer to protein ratio of 2:1 and below a PDGF concentration of 62.5 nM (4:1 aptamer to protein ratio), the fluorescence signal was no longer linear. This may be attributed to more aptamer binding sites being available on the homodimeric protein than there are detection aptamers at greater than 250 nM PDGF-BB concentration leading to lower fluorescence intensity at the 500 nM concentration. At 62.5 nM concentration of PDGF-BB and below the amount of available protein may have been so low as to cause competition between the capture and detection aptamers for the PDGF-BB target, since the same aptamer is used in the capture and detection of the protein. Thus, this limited the linear range of detection to less than an order of magnitude. This problem may be rectified in the development of dual aptamer sandwich assays for homodimeric protein targets using the same aptamer in capture and detection, through modification of the capture aptamer. For example, modified nucleotide bases can be

incorporated in the capture aptamer sequence to enable covalent attachment of the protein to the capture aptamer once bound to the chip surface.⁴⁶

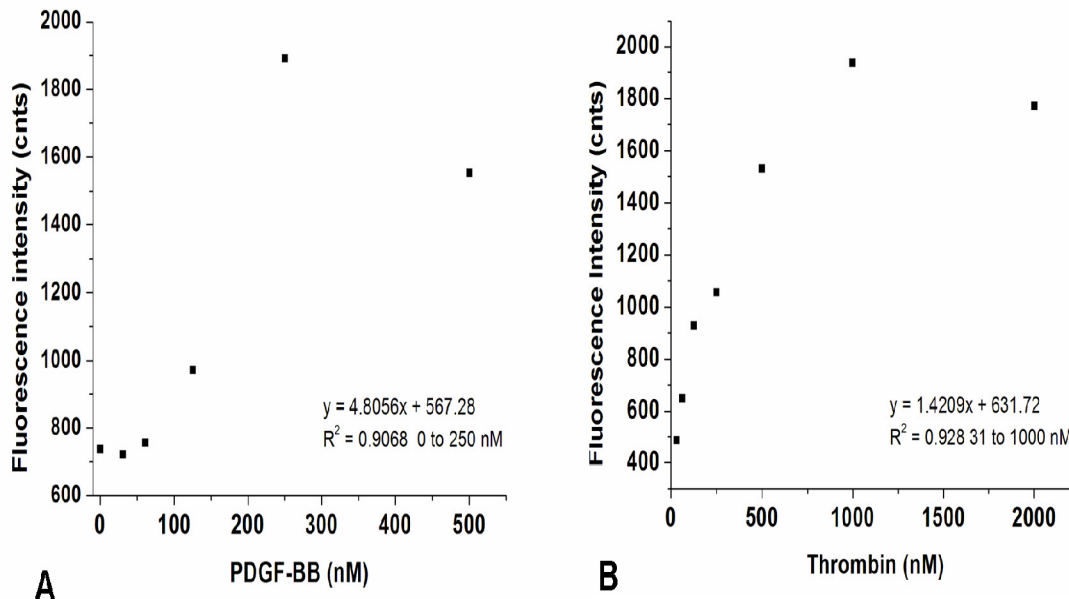


Figure 4.6: Sandwich assay intensity profiles of A) various PDGF-BB concentrations ranging from 0 - 500 nM combined with 500 nM Cy5.5-PDGF aptamer and B) thrombin at concentrations between 31 nM and 2000 nM with a fixed concentration of 1000 nM for the Cy5.5-HD1 reporting aptamer. The assays were incubated at 37 °C for approximately 1 h before scanning using the near-IR imager.

The use of different aptamers in the capture and detection of thrombin circumvented the problem of competition between the capture and detection elements for the target. For the 1 h assays performed for thrombin a linear response over one order of magnitude was achieved and HD1-Cy5.5 could be used at an excess of 1 μ M or more without affecting the assay performance (see Figure 4.6B). Thrombin could be detected down to 31.25 nM concentration in a 1 μ L sample volume. Also it was observed that by using the optimized immobilization conditions for HD22 aptamer, the assay performance time was drastically decreased to an hour due to enhance binding of thrombin to HD22 compared to the overnight incubations required in previous experiments in order to detect the protein.

4.4 Conclusion

Aptamers hold promise for the development of bioassays due to their selectivity and high specificity. We optimized a one-step EDC/NHS coupling procedure for aptamer immobilization onto UV-modified PMMA by using a higher pH of 7.2 and increasing the EDC concentration to 200 mM to provide increased surface density and uniform coverage of immobilized aptamers for enhanced target binding in dual-aptamer sandwich assay development. We demonstrated the use of thrombin aptamers in a sandwich assay with fluorescence detection without signal amplification techniques. The thrombin sandwich assay was specific for thrombin and showed very little interaction with BSA. Assays were performed for thrombin and PDGF-BB detection using the optimized immobilization protocol with a resultant decrease in the assay time and with fewer steps compared to the standard immunoassay protocols. Although an emerging class of affinity agents, more research on improving the binding affinities of some aptamers will eventually allow widespread use of aptamers in a variety of bioassays requiring immobilization of aptamers. Future work will involve incorporation of aptamers in PMMA devices for capture and detection of biomarkers or for capturing cells in disease diagnosis.

4.5 References

- (1) Brody, E. N.; Willis, M. C.; Smith, J. D.; Jayasena, S.; Zichi, D.; Gold, L. *Molecular Diagnosis* **1999**, *4*, 381-388.
- (2) Ferreira, C. S. M.; Papamichael, K.; Guilbault, G. G.; Schwarzacher, T.; Gariépy, J.; Missailidis, S. *Anal. Bioanal. Chem.* **2008**, *390*, 1039-1050.
- (3) Jaras, K.; Ressine, A.; Nilsson, E.; Malm, J.; Marko-Varga, G.; Lilja, H.; Laurell, T. *Anal. Chem.* **2007**, *79*, 5817-5825.
- (4) Bertone, P.; Snyder, M. *FEBS J.* **2005**, *272*, 5400-5411.
- (5) Henares, T. G.; Mizutani, F.; Hisamoto, H. *Anal. Chim. Acta* **2008**, *611*, 17-30.
- (6) James, W. *Curr. Opin. Pharmacol.* **2001**, *1*, 540-546.

- (7) Collett, J. R.; Cho, E. J.; Lee, J. F.; Levy, M.; Hood, A. J.; Wan, C.; Ellington, A. D. *Anal. Biochem.* **2005**, *338*, 113-123.
- (8) MacBeath, G. *Nat. Genet. Suppl.* **2002**, *32*, 526-532.
- (9) Kusnezow, W.; Hoheisel, J. D. *Biotech. Suppl.* **2002**, 14-23.
- (10) Gonzalez, R. M.; Seurnyck-Servoss, S. L.; Crowley, S. A.; Brown, M.; Omenn, G. S.; Hayes, D. F.; Zangar, R. C. *J. Proteome Res.* **2008**.
- (11) Ellington, A. D.; Szostak, J. W. *Nature* **1992**, *355*, 850– 852.
- (12) Mann, D.; Reinemann, C.; Stoltenburg, R.; Strehlitz, B. *Biochem. Biophys. Res. Commun.* **2005**, *338*, 1928-1934.
- (13) Lee, Y. J.; Lee, S. W. *J. Microbiol. Biotechnol.* **2006**, *16*, 1149-1153.
- (14) Homann, M.; Goringe, H. U. *Nucleic Acids Res.* **1999**, *27*, 2006-2014.
- (15) Stoltenburg, R.; Reinemann, C.; Strehlitz, B. *Biomol. Eng* **2007**, *24*, 381-403.
- (16) Luzzi, E.; Minunni, M.; Tombelli, S.; Mascini, M. *TrAC, Trends Anal. Chem.* **2003**, *22*, 810-818.
- (17) Pirrung, M. C. *Angew. Chem. Int. Ed.* **2002**, *41*, 1276-1289.
- (18) Wu, P.; Hoglebe, P.; Grainger, D. W. *Biosensors & Bioelectronics* **2006**, *21*, 1252-1263.
- (19) Cho, E. J.; Collett, J. R.; Szafranska, A. E.; Ellington, A. D. *Anal. Chim. Acta* **2006**, *564*, 82-90.
- (20) Fixe, F.; Dufva, M.; Telleman, P.; Christensen, C. B. V. *Lab on a Chip* **2004**, *4*, 191-195.
- (21) Collett, J. R.; Cho, E. J.; Ellington, A. D. *Methods* **2005**, *37*, 4-15.
- (22) Kirby, R.; Cho, E. J.; Gehrke, B.; Bayer, T.; Park, Y. S.; Neikirk, D. P.; McDevitt, J. T.; Ellington, A. D. *Anal. Chem.* **2004**, *76*, 4066-4075.
- (23) Ikebukuro, K.; Kiyohara, C.; Sode, K. *Biosensors & Bioelectronics* **2005**, *20*, 2168-2172.
- (24) Giusto, D. A.; King, G. C. *Top. Curr. Chem.* **2005**, *261*, 131-168.
- (25) Cavic, B. A.; McGovern, M. E.; Nisman, R.; Thompson, M. *Analyst* **2001**, *126*, 485-490.
- (26) Yang, M.; McGovern, M. E.; Thompson, M. *Anal. Chim. Acta* **1997**, 257-275.
- (27) Pividori, M. I.; Merkoci, A.; Alegret, S. *Biosensors & Bioelectronics* **2000**, *15*, 291-303.
- (28) Balamurugan, S.; Obubuafo, A.; Soper, S. A.; McCarley, R. L.; Spivak, D. A. *Langmuir* **2006**, *22*, 6446-6453.

- (29) Rupcich, N.; Nutiu, R.; Li, Y. F.; Brennan, J. D. *Anal. Chem.* **2005**, *77*, 4300-4307.
- (30) Soper, S. A.; Henry, A. C.; Vaidya, B.; Galloway, M.; Wabuye, M.; McCarley, R. L. *Anal. Chim. Acta* **2002**, *470*, 87-99.
- (31) Situma, C.; Wang, Y.; Hupert, M.; Barany, F.; McCarley, R. L.; Soper, S. A. *Anal. Biochem.* **2005**, *340*, 123-135.
- (32) Situma, C.; Moehring, A. J.; Noor, M. A. F.; Soper, S. A. *Anal. Biochem.* **2007**, *363*, 35-45.
- (33) Wiegand, T. W.; Williams, P. B.; Dreskin, S. C.; Jouvin, M. H.; Kinet, J. P.; Tasset, D. *J. Immunol.* **1996**, *157*, 221-230.
- (34) Verhamme, I.; Olsen, S.; Tollefsen, D.; Bock, P. E. *The Journal of Biological Chemistry* **2002**, *277*, 6788-6798.
- (35) Green, L. S.; Jellinek, D.; Jenison, R.; Ostman, A.; Heldin, C. H.; Janjic, N. *Biochemistry* **1996**, *35*, 14413-14424.
- (36) Joyce, M. V.; McGown, L. B. *Appl. Spectrosc.* **2004**, *58*, 831-835.
- (37) Tasset, D. M.; Kubik, M. F.; Steiner, W. *J. Mol. Biol.* **1997**, *272*, 688-698.
- (38) Arthanari, H.; Basu, S.; Kawano, T. L.; Bolton, P. H. *Nucleic Acids Res.* **1998**, *26*, 3724-3728.
- (39) Wei, S.; Vaidya, B.; Patel, A. B.; Soper, S. A.; McCarley, R. L. *J. Phys. Chem. B* **2005**, *109*, 16988-16996.
- (40) McCarley, R. L.; Vaidya, B.; Wei, S.; Smith, A. F.; Patel, A. B.; Feng, J.; Murphy, M. C.; Soper, S. A. *J. Am. Chem. Soc.* **2005**, *127*, 842-843.
- (41) Gilles, M.; Hudson, A.; Borders, C. L. *Anal. Biochem.* **1990**, *184*, 244-248.
- (42) Xu, F.; Datta, P.; Wang, H.; Gurung, S.; Hashimoto, M.; Wei, S.; Goettert, J.; McCarley, R. L.; Soper, S. A. *Anal. Chem.* **2007**, *79*, 9007-9013.
- (43) Wei, Y.; Ning, G.; Hai-Qian, Z.; Jian-Guo, W.; Yi-Hong, W.; Wesche, K.-D. *Sens. Actuators, B* **2004**, *98*, 83-91.
- (44) Staros, J. V.; Wright, R. W.; Swingle, D. M. *Anal. Biochem.* **1986**, *156*, 220-222.
- (45) Nakajima, N.; Ikada, Y. *Bioconjug. Chem.* **1995**, *6*, 123-130.
- (46) Jayasena, S. D. *Clin. Chem.* **1999**, *45*, 1628-1650.

Chapter 5 Utilization of an Aptamer Pair in Single Molecule FRET Determination of Low Levels of Thrombin

5.1 Introduction

Some diseases are characterized by the generation of low levels of biomarkers used in monitoring their progression and treatment effects. Hemophilia A and B, genetic disorders, which occur due to single point mutations result in prolonged bleeding of affected individuals.¹ Patients with the most common forms of this condition (hemophilia A and B) produce low levels of coagulation factors VIII (FVIII) and IX² respectively.³ The mean levels of FVIII and FIX determined for normal individuals in plasma are 0.7 nmol/L and 90 nmol/L respectively.^{1, 4} Individuals with the disorder produce lower levels of these factors which negatively affect hemostasis. Various methods have been developed to detect and monitor the effects and treatment of hemophilia. Analytical methods include, clotting time assays, enzyme linked immunosorbent assays (ELISA) for the coagulation factors and thrombin generation tests.⁵⁻⁷

Thrombin, the last coagulation protease in the blood clotting cascade, exists in blood in its zymogen form, prothrombin. When an imbalance in hemostasis occurs due, for example, to injury thrombin generation is triggered via a cascade process requiring a host of coagulation factors which include FVIII and FIX leading to clot formation.⁸ The time taken for thrombin generation to the level required for clot formation (usually 10 nM thrombin in the initiation phase) and the maximum level of thrombin produced during establishment of hemostatic control (between 200-800 nM thrombin in the propagation phase) are very important parameters used in identifying problems in hemostasis and for monitoring treatment regimes.⁹ In hemophilia, thrombin generation is very slow and thus, clotting based assays can only give qualitative information about the condition. Thus, more universal techniques for monitoring hemophilia and treatment therapies have been developed. The thrombin generation assay, first introduced in

1953 by MacFarlane and Biggs, is now widely used in monitoring hemophilia therapy.^{5,10} This technique measures the thrombin generation capacity of plasma by monitoring the enzymatic activity of thrombin using chromogenic or fluorogenic peptide substrates. This allows real-time monitoring of the thrombin generation process for detailed kinetic analysis of hemostasis.¹¹ The thrombin generation test allows thrombin generation in the nanomolar range to be measured using fluorogenic substrate.¹²

Because of the slower process of thrombin generation in hemophilia³ a method sensitive enough to allow direct measurement of thrombin at sub-nanomolar concentrations would allow studies to be carried out, which could provide more insight into the effects of hemophilia treatment options and individual variations in response to treatment regimes. Analytical techniques based on single molecule detection could provide solutions to problems not addressed by the current methods for monitoring hemophilia in patients.

Fluorescence resonance energy transfer at the single molecule level (smFRET) is a powerful spectroscopic technique for studying interactions of biomolecules at the molecular level with advantages of being able to reveal the population distribution more directly in heterogeneous systems and also provides the opportunity to determine the kinetics of unsynchronized complex biochemical processes.¹³ smFRET can be used to detect rare conformational transitions and for detection of transient reaction intermediates which are difficult to detect by ensemble FRET methods. In a real-time smFRET study by Sugawa *et al.*, conformational changes in the structure of immobilized Cy3-labeled H-Ras (1-171) protein arising from binding of the protein to its substrate labeled with Cy5 dye were determined by measuring smFRET intensity in the presence or absence of an effector capable of inducing protein denaturation.¹⁴ Quantum-dot (QD) FRET-based nanosensors were also used in a conformational dynamics study under capillary flow conditions to determine deformation of long

DNA strands.¹⁵ The smFRET signal was monitored with results indicating greater FRET efficiency observed for deformed DNA molecules under flow conditions .¹⁵ Thus, smFRET technique provides information on the state of individual molecules which would not be available under bulk FRET conditions.

Aptamers have emerged as a class of affinity agents capable of rivaling antibodies in bioassay development. These molecules recognize distinct epitopes on their targets and in some cases have affinities comparable to monoclonal antibodies.¹⁶ Their small size and ease of generation and production make it possible to generate aptamers that recognized different epitopes on the same target.¹⁷ Thrombin has been widely studied for aptamer selection and has two aptamers, HD1 and HD22,¹⁸ which bind to its exosites I and II respectively making it possible to develop assays for thrombin detection either using a single aptamer or both aptamers. Highly sensitive aptamer-based methods for protein detection at sub-nanomolar levels have been developed which, depend on DNA amplification for protein detection. These include the proximity ligation assays which consist of affinity agents linked to DNA primers and a connector DNA sequence. The DNA sequences are enzymatically ligated when in close proximity through binding of the affinity agents to the target. The DNA is then amplified by polymerase chain reaction for detection of the protein.¹⁹ This method was used in the detection of platelet derived growth factor and thrombin in complex biological fluids. An affinity-based detection system capable of detecting low levels of target without signal amplification in heterogeneous mixtures would be an invaluable diagnostic tool for disease detection.

Heyduk and Heyduk developed a FRET-based aptamer sensor for detection of thrombin in heterogeneous mixtures without sample manipulation.^{20, 21} The aptamers HD1 and HD22 were each linked at the 3' and 5' end respectively to one each of a complementary seven-base long oligonucleotide sequence via five hexaethylene glycol internal spacers. The complementary

oligonucleotide strands each had a donor or acceptor dye at the end of the short sequence opposite to the aptamer attachment end. Co-association of the aptamer beacons with thrombin led to enhanced annealing of the short oligo strands leading to increased FRET response. Thus, the sensor allowed selective detection of thrombin in heterogeneous assays.²⁰

In this study we sought to develop a smFRET-based assay for detection of low levels of thrombin in real-time using the aptamer sensors designed by Heyduk and Heyduk. Parameters considered included designing the complementary strand to ensure maximum FRET response through direct attachment of the dyes to the short complementary oligomers or attachment via a short internal linker; The ensemble FRET response of the aptamer sensor in the presence of different concentrations of thrombin or prothrombin was also determined to ensure its selectivity for thrombin; smFRET determinations were performed in the sub-nanomolar concentration range to determine the ability of the sensor to detect single molecule events.

5.2 Experimental

5.2.1 Reagents and Materials

Thrombin and prothrombin used in the determinations were obtained from Haematologic Technologies, Inc. (Essex Junction, VM). Short single stranded Cy3 or Cy5 labeled complementary oligonucleotide sequences were synthesized by Integrated DNA Technologies (Corallville, IA) with or without an ethylene glycol internal spacer between the dye and the oligonucleotide strand (sequences: CGC ATC T-/Cy3/-3 and 5'/Cy5/AGA TGC G). The aptamer beacons designed as described by Heyduk and Heyduk (sequences: 5'/Cy5//C7/AgA TgC g-(/hexaethylene glycol/)5-AgT CCg Tgg TAg ggC Agg TTg ggg TgA CT-3' ; 5' ggT Tgg TgT ggT Tgg-(/hexaethylene glycol/)5-CgC ATC T/C6/-/Cy3/-3') were synthesized by Midland Certified Reagent Company, Inc. (Midland, TX). Reagents for buffer preparation including

HPLC grade water, Tris, chlorides of sodium (NaCl), potassium (KCl) and magnesium (MgCl₂) were obtained from Sigma-Aldrich (St. Louis, MO).

5.2.2 Ensemble FRET Experiments

All bulk fluorescence measurements were carried out on a Fluorolog JY Jobin Yvon Horiba Spectrofluorometer (Jobin Yvon Inc., Edison, NJ) and absorbance measurements of dye labeled oligonucleotides and aptamer sensors were carried out on an Ultrospec 4000 UV/Visible Spectrophotometer (Pharmacia biotech, Cambridge, England) to determine the excitation wavelengths for the Cy3 and Cy5 labeled oligonucleotides.

Three prime and 5' Cy3 and Cy5 end-labeled complementary single stranded oligonucleotide sequences synthesized with or without an ethylene glycol internal spacer between the dye and each sequence were diluted in nuclease-free water from which 1 μ M stock solutions in Tris saline buffer (TBS) containing 1 mM MgCl₂ and 5 mM KCl at pH 7.7 were prepared. Each oligonucleotide sequence was then combined with its complementary strand in four different combinations depending on the presence or absence of the ethylene glycol internal spacer to a final concentration of 250 nM each. The oligonucleotide mixtures were incubated at 37 °C for 1 h and cooled to 4 °C in a thermocycler. Fluorescence determinations on the annealed strands were carried out at 532 nm excitation wavelength to determine the best internal spacer combination for maximum FRET response.

For ensemble FRET measurements carried out using the aptamer sensor, samples of thrombin and prothrombin at different concentrations ranging from 0 to 250 nM were gently agitated at room temperature with 250 nM each of aptamer 5'-HD1-3'-Oligo7-Cy3 and Cy5-oligo7-5'-HD22 in TBS (pH 8.5) containing 0.65mg/ mL polyethylene glycol, 1 mM MgCl₂ and 5 mM KCl for 1 h protected from light. The solutions were excited at 532 nm wavelength and

emission collected from 540 nm to 720 nm. The fluorescence intensity measurements obtained near the emission maximum for Cy5 were analyzed to determine the changes in FRET intensity.

5.2.3 smFRET Analysis of Thrombin/Aptamer Complexes

For smFRET studies 1 nM samples of each aptamer beacon, a combination of the two aptamer beacons and the beacons combined in 5 fold molar excess with thrombin were prepared in TBS buffer (pH 8.5) with buffer components as above for ensemble FRET measurements. The samples were incubated at room temperature with gentle shaking for 30 min and diluted to 30 pM aptamer concentration prior to analysis on a home –built single molecule detection system.

5.2.4 Instrumentation for smFRET Determinations

smFRET measurements were performed using a home-built epi-illumination fluorescence system with two detectors as depicted in Figure 5.1. The excitation source consisted of a 10 mW, 532 nm laser diode (model: GTEC-500-532-10, Lasiris, Inc., Quebec, Canada). The laser was directed via a dichroic mirror (Z532/780/RPC, Chroma Technologies, San Diego, CA) through a 40x, 0.75 NA focusing objective (Plan fluor, Nikon, Melville, NY) to a 5 μm spot size in a 50 μm internal diameter fused silica capillary (Polymicro technologies, Phoenix, AZ) through which the sample flowed at 4.2 cm/s linear velocity. The capillary was mounted on an XYZ translational stage. Greater than 90% of the fluorescence signal generated by Cy5 in the sample and collected by the same objective, was transmitted through the dichroic mirror to a second dichroic mirror (640DCSPXR, Chroma Technologies, San Diego, CA) which directed the Cy5 fluorescence emission through longpass and bandpass filters (FEL650/FB670-10 for Cy 5, Thorlabs, Newton, NJ). The beam was focused by a 20x objective onto the active area (175 μm) of a single-photon counting avalanche diode detector (SPCM-AQR-14, EG &G, Vandreuil, Canada). Photon counts were processed by a PCI-6602 data acquisition board (National

Instruments, Austin, TX) with a temporal resolution of 12.5 ns and analyzed using a custom-made Labview v.7 software (Dr. L. Davis, UT Space Institute, TN).

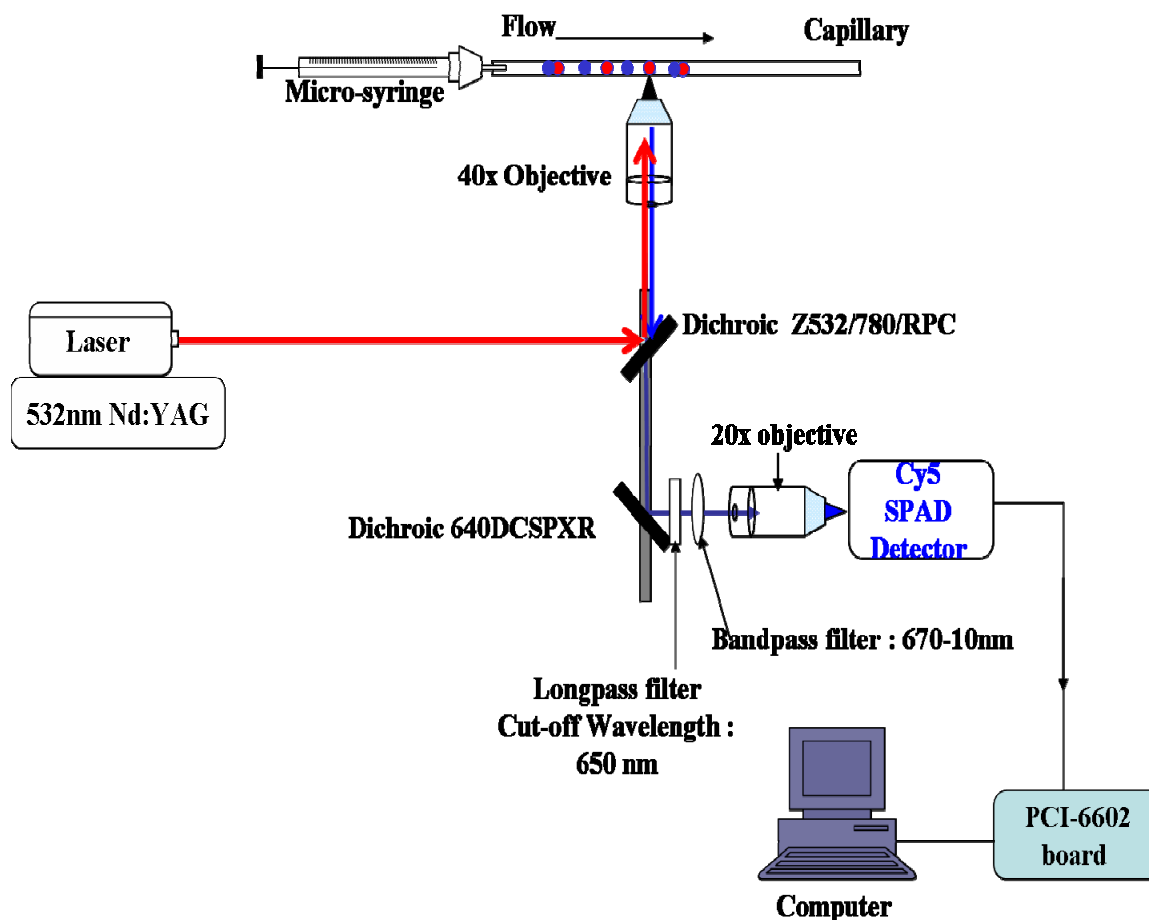


Figure 5.1: Diagram of the smFRET instrument set-up showing a 532 laser for excitation of the fluorophores and a system of dichroic mirrors and filters, and an avalanche diode detector for detection Cy5 fluorescence emission.

5.2.5 smFRET data analysis

To characterize the transit time and demonstrate the presence of non-random correlated single photon bursts, autocorrelation analysis was carried out using the Labview software over a data set of 50 s. To distinguish single-molecule events from the background the Microcal Origin software was used in determining the frequency of events and for setting a threshold for the background photons above which single molecule photon counts represented the occurrence of FRET.

5.3 Results

5.3.1 Effects of an Ethylene Glycol Spacer on the FRET Response of Annealed Cy3 and Cy5 Labeled Complementary Oligonucleotide

Results of the studies to determine the length of linker for maximum FRET response are shown in Figure 5.2. The aim of this research was to utilize the aptamer beacon under single molecule conditions. In this regard, factors that enhance FRET intensity, such as the distance between the dye molecules in the annealed strands, needed to be optimized to achieve this goal. Thus we investigated the effect of attaching the dyes via a short flexible spacer molecule to the complementary oligonucleotide sequences on the FRET response generated after the strands annealed. The emission spectra obtained for the different combinations of linker versus no linker yielded a higher FRET response for the oligonucleotide pair containing an ethylene glycol linker between each oligonucleotide sequence and the attached dye. Combinations of one linker and no linker or no linkers used produced relatively equal FRET responses for the annealed strands. Based on the information provided by Integrated DNA Technologies concerning the dyes used, the dye labeled oligonucleotide sequences were produced using Cy3 and Cy5 dyes synthesized with a three carbon linker for conjugation purposes. By introducing an ethylene glycol spacer molecule the effective linker length was increased further by 3 atoms. Thus, the results indicated that for maximum FRET to be generated by the oligonucleotide sequence used in this experiment a linker of approximately 6 atoms in length is required. This was taken into consideration in synthesizing the aptamer beacons.

5.3.2 Ensemble FRET Assays of the Aptamer Beacons for Analysis of Thrombin and Prothrombin

To determine the effectiveness of the aptamer beacons at selectively measuring thrombin in solution, samples of different thrombin or prothrombin concentrations were prepared and mixed with a fixed concentration of the two aptamers. Figure 5.3 shows results of variation of FRET

response with protein concentration. At 250 nM aptamer concentration an increase in FRET response was observed for thrombin from above 25 nM protein.

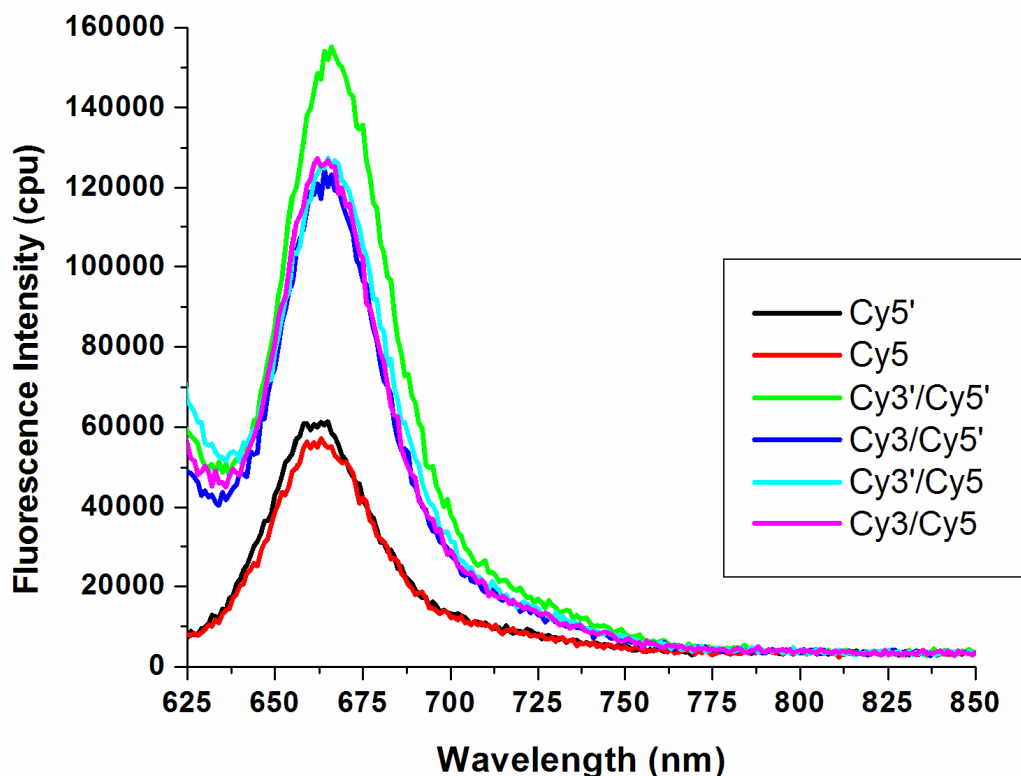


Figure 5.2: FRET and fluorescence emission spectra for annealed complementary seven-oligonucleotide sequences and the Cy5-labeled sequences in TBS buffer at pH 7.7. Excitation was carried out at 532 nm and the fluorescence emission spectra obtained for Cy5 emission. Both oligonucleotide sequences were synthesized with the FRET dyes attached with (represented by a prime (')) or without an ethylene glycol internal spacer between the dye and the sequence to determine the best linker combination for maximum FRET response.

No variation in FRET response was observed for prothrombin indicating specificity of the technique for thrombin. The assay required association of both aptamers with the protein molecule in order to enhance annealing of the signaling complementary oligonucleotide strands. Since exosite II is unavailable in prothrombin the co-association process was hindered leaving the FRET response unchanged in the presence of prothrombin.²² We were thus able to ascertain

proper functioning of the aptamer beacons for subsequent experiments at the single molecule level.

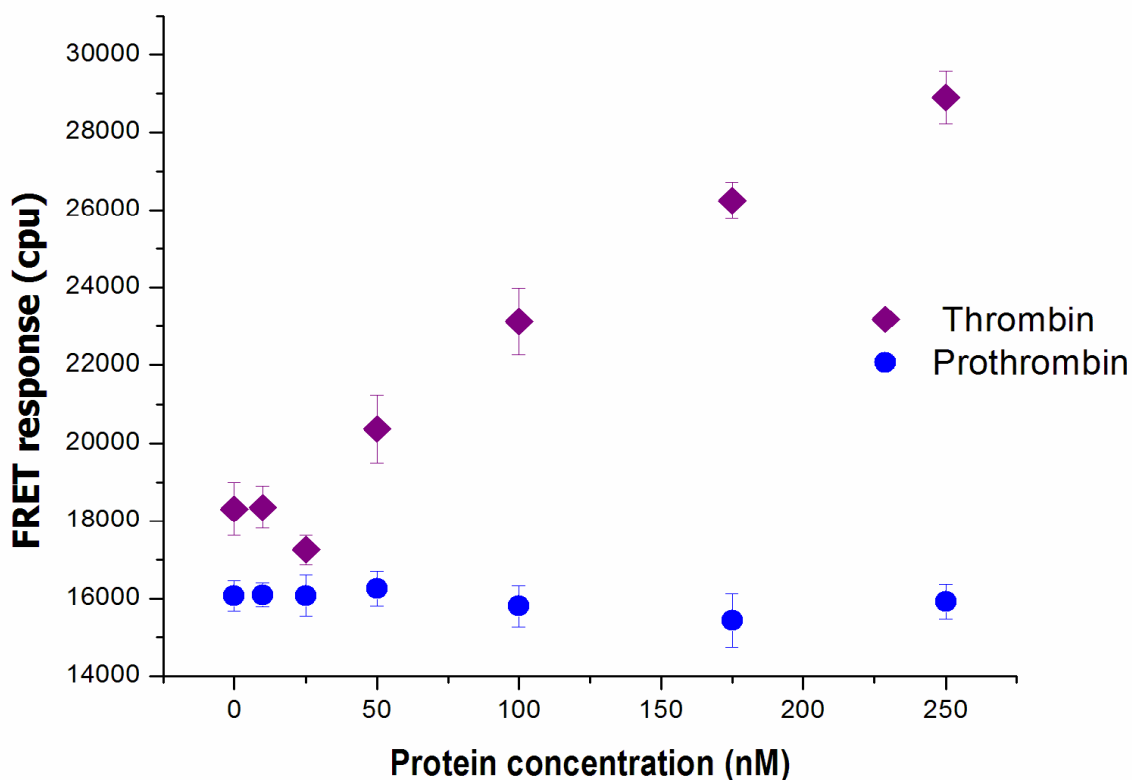


Figure 5.3: Variation in ensemble FRET response for aptamer beacon assays with increasing concentration of thrombin or prothrombin in TBS at pH 8.5. The HD1 and HD22 beacon concentrations were fixed at 250 nM.

5.3.3 smFRET Analysis of Thrombin-Aptamer Assays

The FRET beacons were used in single molecule studies for detection of picomolar levels of thrombin in solution. The home-built system was initially optimized for single molecule detection using fluorescent beads. To obtain the probe volume and concentration for probability of single molecule occupancy, the beam waist was determined experimentally at different sample flow rates using an autocorrelation function built into the Labview software. The beam diameter was determined to be 4 μm and used to estimate a probe volume between 133 and 222 fL. Based

on the results, the concentration of analyte required for single molecule occupancy of the probe volume was determined to be 6 pM at a sample linear velocity of 4.244 cm/s.

Pre-incubated samples of the aptamer beacons were analyzed after dilution to picomolar concentrations and the fluorescence generated by Cy5 was monitored for smFRET occurrence. Results of the smFRET analysis are shown in figures 5.4 and 5.5. Figure 5.4 shows photon burst data collected over 50 s time intervals for buffer, 30 pM Cy5-HD22, a mixture of the two aptamer beacons at 30 pM concentrations and both aptamers pre-incubated with thrombin in a 5 fold excess aptamer to thrombin ratio. The amplitude of photon bursts for the buffer and aptamer samples were below 4000 counts/s on the average. With the addition of thrombin to the sample the amplitude of photon bursts increased above 10^5 counts/s. To eliminate false positives due to excitation of Cy5 by the laser and formation of a FRET pair by the aptamer beacons in the absence of thrombin, the photon counting threshold was set at 4000 counts/s (see Figure 5.5) and the frequency of photon bursts above this threshold computed to determine the number of events for smFRET produced for the thrombin-aptamer complex. At 6 pM thrombin and a 5 fold excess of aptamer beacons the frequency of molecular events was 27 above the 4000 counts threshold. The expected number of events (N_{ev}) was calculated from the equation below.²³

$$N_{ev} = 2P_o \nu T / \pi \omega$$

Where P_o represents the probability of single molecule occupancy in the probe volume, ν is the linear flow velocity (4.2 cm/s), T is the duration of the experiment (50 s) and ω is the laser beam diameter (4 μ m). Based on a probability of 0.01, N_{ev} was calculated to be 3342 for the 50 s duration, which is far higher than the experimental results obtained.

Formation of a thrombin aptamer complex is governed by binding kinetics affected by the dissociation constant of the complex. HD22 has a higher affinity for thrombin with a dissociation constant (K_D) of 0.5 nM while that for HD1 is between 1.4 to 100 nM.¹⁸ Assuming

the K_D values remain unchanged for both aptamers during complex formation with thrombin, the 6 pM thrombin and 30 pM aptamer concentrations are well below the K_D of each aptamer and formation of the complex or retention of its structure after dilution during analysis would be affected.

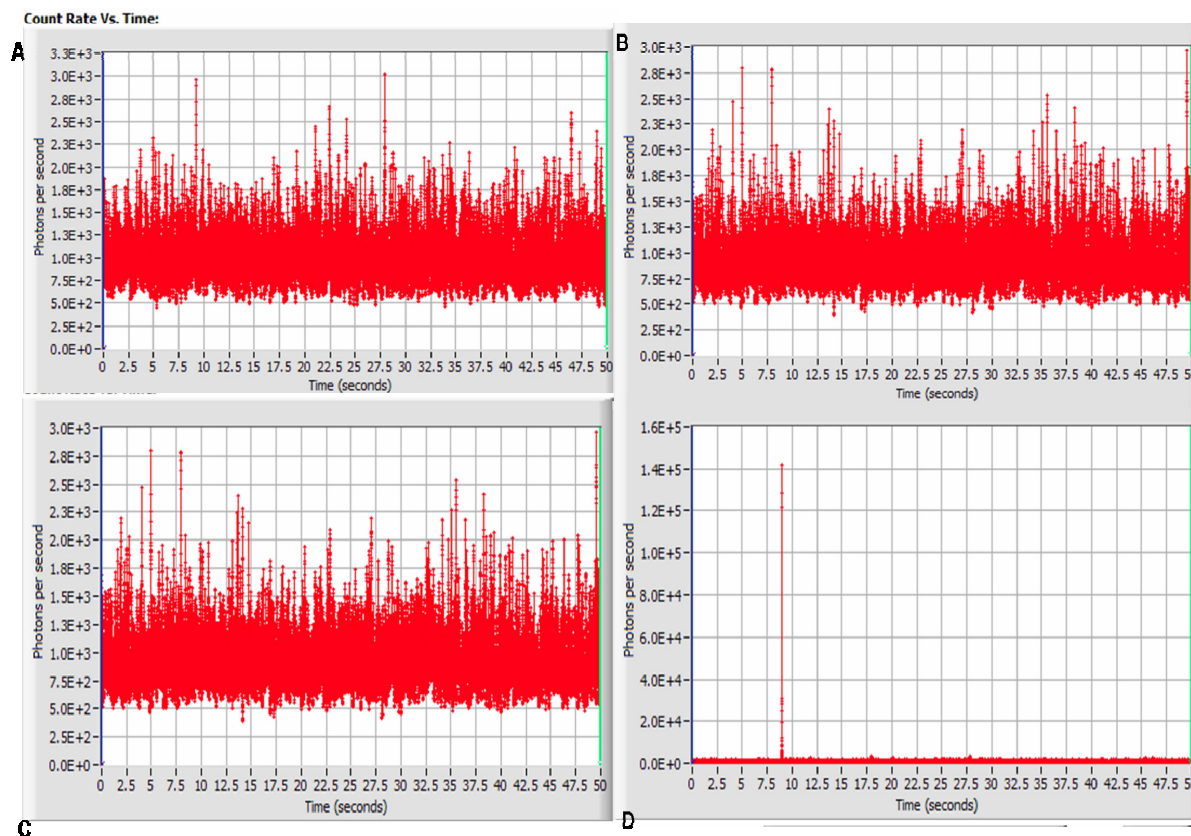


Figure 5.4: Computer generated readouts of the assays showing the rate of photon count with time obtained on the Cy5 fluorescence detector for A) buffer only, B) 30 pM Cy5-HD22 beacon in buffer, C) 30 pM HD1-Cy3/Cy5-HD22 mixture in buffer and D) 30 pM HD1-Cy3/Cy5-HD22 with 6 pM thrombin. Samples were prepared in buffer at pH 8.5, incubated at room temperature at a higher concentration and diluted to 30 pM aptamer beacon concentration prior to analysis on the smFRET system.

Thus, the lower molecular event counts obtained are a result of samples being analyzed at concentrations below the K_D of the aptamers. To enable single molecule detection of low thrombin concentrations the probe volume can be adjusted to allow higher sample concentrations to be used. By introducing a pinhole in front of the detector, the probe volume can be further

decreased. Alternatively, a higher magnification objective with high numerical aperture, such as a 100X oil immersion objective can be used to focus the beam to an even smaller diameter. By decreasing the probe volume, concentrations of aptamer and thrombin in the nanomolar range can be used for sample analysis.

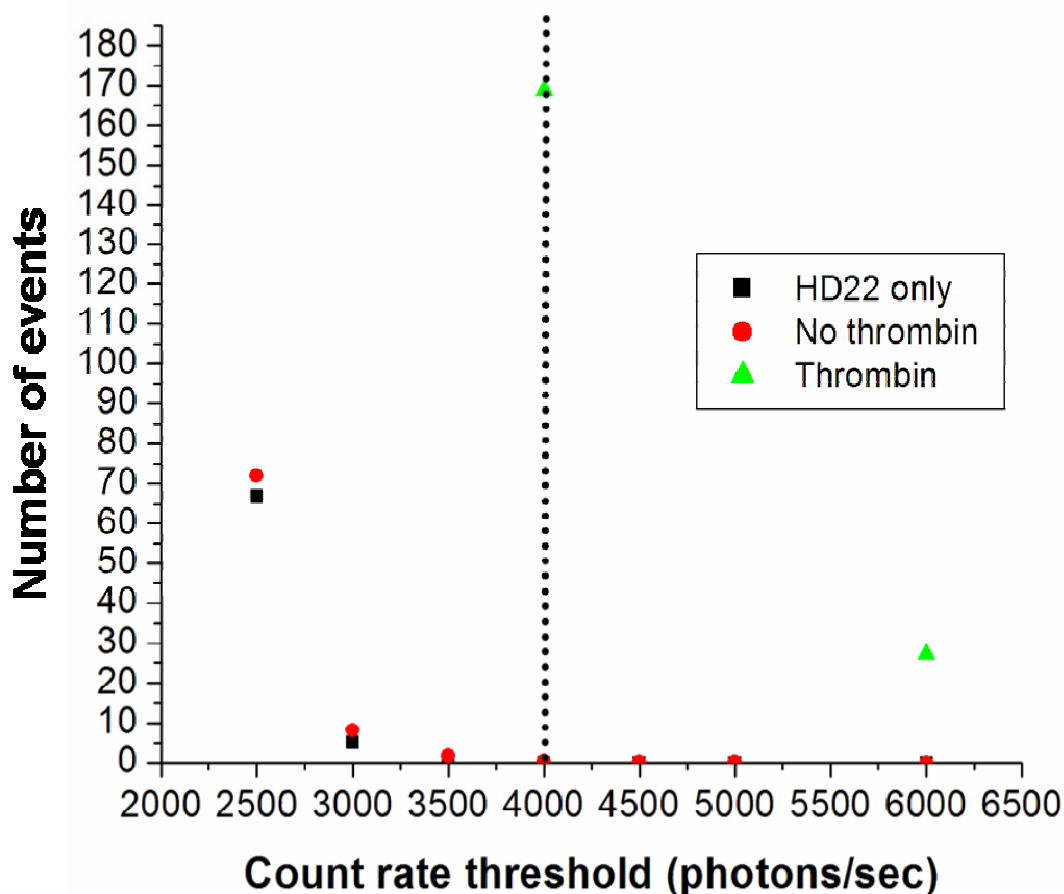


Figure 5. 5: Plots of photon burst data obtained for smFRET analysis of the aptamer assay showing the frequency of molecular events obtained at different count rate thresholds for Cy5-HD22, both aptamer beacons without thrombin and the assay with thrombin at 6 pM concentration

5.4 Conclusion

Aptamers have emerged as potential affinity agents that rival or complement antibodies in developing diagnostic assays for disease detection. Single molecule detection methods also

provide high sensitivity techniques in which aptamers can find use. We have demonstrated the use of two aptamers in a FRET-based assay for the detection of low levels of thrombin. Sensitivity and reliability of the smFRET assay depends on formation of the complex and its stability. Due to the dissociation constants of the aptamers, low levels of molecular events were detected for a 6 pM concentration of thrombin. Future work will involve adjusting the single molecule system by either the use of a higher magnification lens or use of pinholes to enable analysis of higher concentrations of samples.

5.5 References

- (1) vantVeer, C.; Golden, N. J.; Kalafatis, M.; Simioni, P.; Bertina, R. M.; Mann, K. G. *Blood* **1997**, *90*, 3067-3072.
- (2) Fixe, F.; Dufva, M.; Telleman, P.; Christensen, C. B. V. *Lab on a Chip* **2004**, *4*, 191-195.
- (3) Matsumoto, T.; Shima, M.; Takeyama, M.; Yoshida, K.; Tanaka, I.; Sakurai, Y.; Giles, A. R.; Yoshioka, A. *J Thromb Haemost* **2006**, *4*, 377-384.
- (4) Lawson, J. H.; Kalafatis, M.; Stram, S.; Mann, K. G. *J. Biol. Chem.* **1994**, *269*, 23357-23366.
- (5) Macfarlane, R. G.; Biggs, R. *J. Clin. Pathol.* **1953**, *6*, 3-8.
- (6) Luddington, R.; Baglin, T. *J Thromb Haemost* **2004**, *2*, 1954-1959.
- (7) Rand, M. D.; Lock, J. B.; vantVeer, C.; Gaffney, D. P.; Mann, K. G. *Blood* **1996**, *88*, 3432-3445.
- (8) Mann, K. G.; Brummel, K.; Butenas, S. *J Thromb Haemost* **2003**, *1*, 1504-1514.
- (9) Brummel-Ziedins, K.; Vossen, C. Y.; Rosendaal, F. R.; Umezaki, K.; Mann, K. G. *J Thromb Haemost* **2005**, *3*, 1472-1481.
- (10) Varadi, K.; Turecek, P. L.; Schwarz, H. P. *Haemophilia* **2004**, *10*, 17-21.
- (11) Hemker, H. C.; Al Dieri, R.; Beguin, S. *Curr. Opin. Hematol.* **2004**, *11*, 170-175.
- (12) Butenas, S.; Brummel, K. E.; Paradis, S. G.; Mann, K. G. *Arterioscler. Thromb. Vasc. Biol.* **2003**, *23*, 123-129.
- (13) Ha, T. *Methods* **2001**, *25*, 78-86.
- (14) Sugawa, M.; Arai, Y.; Iwane, A. H.; Ishii, Y.; Yanagida, T. *Biosystems* **2007**, *88*, 243-250.

- (15) Zhang, C. Y.; Johnson, L. W. *Anal. Chem.* **2006**, *78*, 5532-5537.
- (16) Jayasena, S. D. *Clin. Chem.* **1999**, *45*, 1628-1650.
- (17) Luzi, E.; Minunni, M.; Tombelli, S.; Mascini, M. *TrAC, Trends Anal. Chem.* **2003**, *22*, 810-818.
- (18) Tasset, D. M.; Kubik, M. F.; Steiner, W. *J. Mol. Biol.* **1997**, *272*, 688-698.
- (19) Fredriksson, S.; Gullberg, M.; Jarvius, J.; Olsson, C.; Pietras, K.; Gustafsdottir, S. M.; Ostman, A.; Landegren, U. *Nat. Biotechnol.* **2002**, *20*, 473 - 477.
- (20) Heyduk, E.; Heyduk, T. *Anal. Chem.* **2005**, *77*, 1147-1156.
- (21) Heyduk, T.; Heyduk, E. *Nat. Biotechnol.* **2002**, *20*, 171-176.
- (22) Han, J.-H.; Côté, H. C. F.; Tollefsen, D. M. *J. Biol. Chem.* **1997**, *272*, 28660-28665
- (23) Soper, S. A.; Mattingly, Q. L.; Vegunta, P. *Anal. Chem.* **1993**, *65*, 740-747.

Chapter 6 Conclusions, Current and Future Developments

6.1 Conclusions

We have demonstrated the use of aptamers in analytical applications including microchip affinity CGE, aptamer sandwich assays on PMMA substrate and smFRET analysis and expressed and purified a membrane protein biomarker as a possible target for aptamer selection. In the microchip CGE assay aptamers derived towards thrombin were compared to determine the one most suited for thrombin quantification in plasma. The HD22 aptamer with a higher binding affinity than HD1 aptamer was able to form well resolved aptamer-thrombin complexes during microchip CGE separation. Concentrations as low as 10 nM thrombin could be detected by this method. De-salted plasma samples diluted to 10% in running buffer were successfully analyzed for thrombin with microchip CGE separations performed in less than one minute.

We also expressed a histidine-tagged rEpCAM in bacteria and mammalian cells to determine the system best suited for large-scaled production of the protein. The episomal expression method in Cos 7 cells was selected, due to higher protein yield, for production of rEpCAM. To ensure high purity of protein in its native state a selective purification technique based on a tandem IMAC with electro elution was developed. Using this purification method electrophoretically pure protein was obtained and detected by western blot using an anti-EpCAM antibody specific for the native form of EpCAM. This technique may be effective in the purification of histidine-tagged proteins expressed in eukaryotic systems in which histidine-rich contaminating proteins affect purity of the target protein.

Aptamers have an advantage over antibodies due to their chemical and thermal stability, ease of chemical modification and resistance to denaturation when immobilized on surfaces. The use of an aptamer pair in a sandwich assay format was developed on PMMA substrate using thrombin and PDGF aptamers. To increase the capture element density and enhance target

binding the immobilization conditions were optimized by using neutral pH and 200 mM EDC concentration in the immobilization process. In the thrombin aptamer assay, HD22 served as the capture element due to its higher binding affinity and ability of its immobilized form to maintain the G-quartet structure as determined by NMM fluorescence enhancement. The HD1 aptamer was dye labeled and served as the detection aptamer. In the PDGF-BB sandwich assay, the aptamer served both as the capture and detection elements due to the homo-dimeric nature of the protein. Results indicated higher sensitivity for the PDGF-BB assay compared to the thrombin assay due to the higher binding affinity ($K_D=100$ pM) of the PDGF aptamer. However, its linear dynamic range was smaller due to competition between the immobilized aptamer and the detection aptamer for the protein target. The thrombin sandwich assay had a larger dynamic range and since both aptamers recognize different epitopes the binding kinetics was unaffected by competition for similar binding sites on the protein.

Initial results in the development of an aptamer-based smFRET technique for detection of low levels of thrombin indicated that aptamers can be effectively utilized for single molecule detection of biomolecules. However, detection of the aptamer-protein complex at low picomolar concentrations was greatly affected by the dissociation constant of the aptamers. The single molecule detection system needs to be optimized to allow utilization of analyte and reagents at concentrations above the K_D of the aptamers.

6.2 Current Work

Detection of analytes in the single molecule realm lends sensitivity to analytical techniques in the analysis of biomolecules. By decreasing the detection volume, background interference is drastically reduced thus increasing the signal-to-noise ratio. In the aptamer-based smFRET studies samples of pre-incubated aptamer beacon and thrombin were diluted to low picomolar concentrations prior to analysis. With the lowest aptamer beacon K_D value of 500 pM

the concentrations required for single molecule detection were far below concentrations required for complex stability or formation. Detection of the aptamer-thrombin complexes formed in the aptamer smFRET assay can be achieved by maintaining the concentrations of the target and aptamer beacons in the nanomolar range. This can be achieved by controlling the probe volume through focusing the laser beam into a tighter spot. To achieve this, a high magnification objective such as an oil-immersion objective with high numerical aperture (NA ~ 1.3) can be used to increase resolution. Alternatively a pinhole can be used to decrease the probe volume to about 1 femtoliter. With this probe volume size analytes in nanomolar concentration range can be used for single molecule detection.

Current modifications are underway to decrease the laser beam diameter for the home-built single molecule system by the use of a pinhole or replacing the 40x objective with a 100x oil-immersion objective lens. With these modifications smFRET detection of aptamer-thrombin complexes will be easily accomplished thereby increasing the scope of analytical applications of aptamers.

6.3 Future Developments

The need for generating more aptamers with high specificity for targets has given rise to automation of the SELEX process and utilization of microfluidic devices for the aptamer generation process.^{1, 2} A high throughput process for SELEX of protein targets involving integrated purification and selection methods on polymeric microfluidic platform would further enhance aptamer generation for multiple targets. A simple microfluidic device for IMAC purification and aptamer selection containing nanoposts functionalized with tetradenate chelating groups for immobilizing nickel or cobalt ions can be designed for purification and immobilization of polyhistidine tagged proteins (see Figure 6.1).

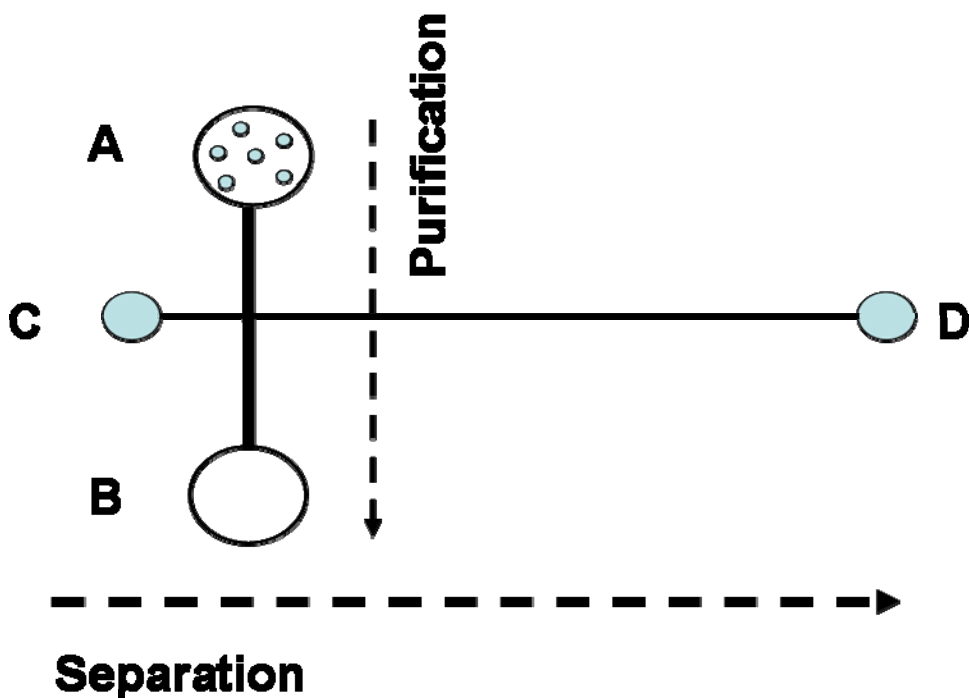


Figure 6. 1: Diagrammatic representation of the layout of a simple polymeric microdevice for immobilization and purification of histidine-tagged proteins with subsequent electrophoretic separation of complexes formed with nucleic acid strands in a degenerate library for aptamer selection. Reservoir A contains nanoposts functionalized with tetradentate chelating groups for immobilized metal affinity purification in channel AB with channel CD as the separation channel.

Histidine-tagged protein targets can be captured on the IMAC nanoposts and purified by washing with the appropriate buffers in the purification channel (AB in Figure 6.1). The purified target is then incubated with a random library and the washing steps performed to remove unbound target as is performed in the SELEX process. Alternatively, the mixture of oligonucleotides and protein target can be directly injected, after the incubation period, into the cross-section of the device and separated in the separation channel (CD in figure 6.1) by non-equilibrium capillary electrophoresis.³ For simultaneously processing several targets a multichannel version of the microdevice could be designed. The microfluidic format for aptamer selection enables utilization

of less reagent and would provide an inexpensive means of generating aptamers toward protein targets.²

6.4 References

- (1) Cox, J. C.; Ellington, A. D. *Biorg. Med. Chem.* **2001**, *9*, 2525-2531.
- (2) Hybarger, G.; Bynum, J.; Williams, R. F.; Valdes, J. J.; Chambers, J. P. *Anal. Bioanal. Chem.* **2005**, *384*, 191-198.
- (3) Berezovski, M.; Musheev, M.; Drabovich, A.; Krylov, S. N. *J. Am. Chem. Soc.* **2006**, *128*, 1410-1411.

Appendix: Letter of Permission

From: "VCH-RIGHTS-and-LICENCES" <RIGHTS-and-LICENCES@wiley-vch.de>
To: "Anne Obubuafo" <aobubu1@lsu.edu>
CC:
Subject: Antwort: Re: Antwort: Copyright permission request
Date: Thursday, July 10, 2008 7:23:43 AM

Dear Customer,

Thank you for your email.

We hereby grant permission for the requested use expected that due credit is given to the original source.

Please note that we only grant rights for a printed version, but not the rights for an electronic/ online/ web/ microfiche publication, but you are free to create a link to the article in question which is posted on our website (<http://www3.interscience.wiley.com>)

If material appears within our work with credit to another source, authorisation from that source must be obtained.

Credit must include the following components:

- Books: Author(s)/ Editor(s) Name(s): Title of the Book. Page(s). Publication year. Copyright Wiley-VCH Verlag GmbH & Co. KGaA. Reproduced with permission.

- Journals: Author(s) Name(s): Title of the Article. Name of the Journal. Publication year. Volume. Page(s). Copyright Wiley-VCH Verlag GmbH & Co. KGaA. Reproduced with permission.

With kind regards

Bettina Loycke

Bettina Loycke
Copyright & Licensing Manager
Wiley-VCH Verlag GmbH & Co. KGaA
Boschstr. 12
69469 Weinheim
Germany

Phone: +49 (0) 62 01- 606 - 280
Fax: +49 (0) 62 01 - 606 - 332
Email: rights@wiley-vch.de

Wiley-VCH Verlag GmbH & Co. KGaA
Location of the Company: Weinheim
Chairman of the Supervisory Board: Stephen Michael Smith
Trade Register: Mannheim, HRB 432833
General Partner: John Wiley & Sons GmbH, Location: Weinheim
Trade Register Mannheim, HRB 432296
Managing Directors : Christopher J. Dicks, Bijan Ghawami, William Pesce

"Anne Obubuafo"
<aobubu1@lsu.edu>

10.07.2008 14:13

VCH-RIGHTS-and-LICENCES
<RIGHTS-and-LICENCES@wiley-vch.de>

"Dr.Soper

An

Kopie

"Anne Obubuafo"

An
09.07.2008 21:19 rights@wiley-vch.de
Kopie

Thema
Copyright permission request

Dear Bettina Loycke,

Copyright permission request

I am the first author of the following electrophoresis journal research article entitled : Poly(methyl methacrylate) microchip affinity capillary gel electrophoresis of aptamer-protein complexes for the analysis of thrombin in plasma, by Anne Obubuafo, Subramanian Balamurugan, Hamed Shadpour, David Spivak, Robin L. McCarley, Steven A. Soper and would like to request permission to incorporate it as part of my dissertation. Thank you.

Sincerely,
Anne Obubuafo
Graduate Student
Dept. of Chemistry
Louisiana State University
Baton Rouge, LA 70803
Phone 225 578 7709

Vita

Anne Kabukwor Obubuafo was born in March 1967, in Tema, Ghana, to Mr. David Doe Obubuafo and Mrs. Diana Claudine Obubuafo. She has two sisters and two brothers, Elizabeth, Joyce, David and Jonathan. Upon completion of her secondary school education, she enrolled at the Kwame Nkrumah University of Science and Technology (KNUST), Kumasi, Ghana, in 1990 where she obtained a Bachelor of Science degree in biochemistry graduating with honors in 1995. She was accepted in 1998 to undertake graduate studies in environmental chemistry at Wright State University, Dayton, Ohio, and was awarded a Master of Science degree in chemistry in 2001. In the fall of 2002, Anne enrolled in the chemistry graduate program at Louisiana State University, Baton Rouge, Louisiana. She is currently a candidate for the degree of Doctor of Philosophy in analytical chemistry to be awarded in August 2008.